Disruption of Epigenetic Regulatory Elements and Chromosomal Alterations in Patients with Beckwith-Wiedemann Syndrome

Adam C. Smith

A thesis submitted in conformity with the requirements for the degree of Doctor of Philosophy

Institute of Medical Science

University of Toronto

Your file Votre référence
ISBN: 978-0-494-61096-1
Our file Notre référence
ISBN: 978-0-494-61096-1

Disruption of Epigenetic Regulatory Elements and Chromosomal Alterations in Patients with Beckwith-Wiedemann Syndrome

Adam C. Smith

Doctor of Philosophy

Institute of Medical Science

University of Toronto

2009

Abstract

Genomic imprinting refers to the parent-of-origin specific monoallelic expression of a gene. Imprinted genes are often clustered in the genome and their expression is regulated by an imprinting centre (IC). ICs are regions of DNA that propagate the parental specific regulation of gene expression, which are usually characterized by differential DNA methylation, histone marks and the presence of non-coding RNAs. Beckwith-Wiedemann syndrome (BWS) is an overgrowth syndrome associated with the dysregulation of imprinted gene expression on human chromosome band 11p15.5. The 11p15.5 imprinted region has two imprinting centres, IC1 and IC2. IC1 is telomeric and regulates the imprinted expression of the genes *H19* and *IGF2*. IC2 is ~700kb centromeric and is associated with a cluster of nine imprinted genes including *CDKN1C*, *KCNQ1* and an imprinted non-coding RNA associated with IC2, *KCNQ1OT1*.

Loss of differential DNA methylation at IC2 is seen in 50% of patients with BWS with loss of imprint of the non-coding RNA *KCNQ1OT1* and associated with a decreased expression of the

putative tumour suppressor *CDKN1C*. Patients with BWS also have a thousand-fold increased risk of pediatric cancer. The focus of this thesis involves investigation of dysregulation of imprinting in three groups of BWS patients. Firstly, I show that BWS patients with alveolar rhabdomyosarcoma have constitutional loss of methylation at IC2 and biallelic expression of *KCNQ1OT1*. Secondly, loss of methylation at IC2 has been previously associated with female monozygotic twins discordant for BWS. In male monozygotic twins with BWS, however, the molecular lesions reflect the molecular heterogeneity seen in BWS singletons. Thirdly, BWS patients associated with translocations and inversions that have breakpoints within the *KCNQ1* gene near IC2 show regional gain of DNA methylation around the breakpoint and decreased expression of *CDKN1C*. Therefore, using a rare collection of BWS patients, I have attempted to determine the various roles of the imprinting centres IC1 and IC2 and their involvement in tumourigenesis, monozygotic twinning and structural chromosomal rearrangements causing BWS.

Acknowledgments

I would like to thank all of the patients and families who participate in scientific research. It is their contributions that make our discoveries possible. It is also important to acknowledge the funding organizations that have awarded me scholarships that have enabled my work. Therefore, I would like to thank the Natural Sciences and Engineering Research Council of Canada, the Molecular Medicine Collaborative Program at the University of Toronto and the Research Training Centre at the Hospital for Sick Children.

I would like to thank all the past and present members of the laboratory of Dr. Rosanna Weksberg. I would especially like to thank Yanling Fei, Chunhua Zhao, Youliang Lou and Idy Chiu. Each of you gave of your time and energy to help push all the projects in the lab forward and your dedication is greatly appreciated.

Working on my Ph.D. has afforded me great learning opportunities and it is important to recognize Dr. Rosanna Weksberg. For not only supervising and supporting my project but in also realizing that succeeding in a Ph.D. is more than simply the project itself and encouraging my participation in a diverse range of experiences that are important to developing the skills necessary to be a successful scientist.

I would like to thank all the members of my thesis supervisory committee: Dr. Paul Sadowski, Dr. Jeremy Squire and Dr. Philip Marsden. Your thoughtful guidance and support throughout

my work has helped to guide the projects I have worked on and develop my knowledge and scientific skills.

I am thankful for all of the friendship, advice and knowledge that were shared with me by my colleagues. To John Cleary, Ray Oh, Dave Sinasac, Paul Bradshaw and Jim Stavroupoulos for distraction, advice and support whenever I needed it. A special thanks must go to David Ng, Cynthia Jung and Dan Stevens. For David and Cynthia who invited me to play GSU volleyball with the 'Genetic Spikers', and went on our many biking trips - piling all of our bikes into my 1987 Oldsmobile '98 for off-road and on-road adventures – we met through our shared experience being Ph.D. students in Genetics and Genome Biology and have become great friends. For Dan Stevens, who has been a constant friend throughout my Ph.D. and convinced me that triathlon was a really excellent way to spend my free time.

I would like to thank my family for their continued support of my career goals. And finally I need to thank my wife, Andrea. Her support of my work and career goals have helped me to focus my energy and work towards my goals even when times were difficult.

Table of Contents

List of Tables

List of Figures

Abbreviations

BWS	Beckwith-Wiedemann Syndrome
CGH	Complete Genomic Hybridization
DMR	Differentially Methylated Region
DNA	Deoxyribonucleic Acid
DNMT	DNA Methyltransferase
GOM	Gain of Methylation (DNA)
HELP	HpaII tiny fragment Enrichment by Ligation-mediated PCR
IC	Imprinting Centre
ICR	Imprinting Control Region
LOM	Loss of Methylation
mRNA	Messenger RNA
miRNA	Micro RNA
PCR	Polymerase Chain Reaction
RMS	Rhabdomyosarcoma
RNA	Ribonucleic Acid
snoRNA	Small nucleolar RNA
UPD	Uniparental Disomy

Disambiguation of Terms

Several genes and regions in the human 11p15.5 chromosome band imprinted domain have changed names over the past several years under the direction of the Human Gene Nomenclature Committee of the Human Genome Organization. This section provides a reference for some of the major name changes and use of terms to help minimize any confusion that may result.

Imprinting Centre (IC) A region of DNA that can regulate the imprinted expression of neighbouring imprinted genes over large distances. ICs are usually characterized by differential DNA methylation and differential histone modifications. Sometimes referred to as Imprinting Control Regions (ICRs) or occasionally simply called differentially methylated regions (DMRs).

IC1 On chromosome 11p15.5 the telomeric imprinting centre that regulates the genes *H19* and *IGF2*. Also called ICR1, DMR1 or H19DMR.

IC2 On chromosome 11p15.5, the centromeric imprinting centre that regulates the genes *KCNQ1OT1, KCNQ1, CDKN1C* and others. Also called ICR2, DMR2, and KvDMR1.

Gain of Methylation Increased levels of DNA methylation compared to control samples.

Loss of Methylation	Decreased levels of DNA methylation compared to control samples.
Hypermethylation	Gain of methylation, usually at an IC on the normally unmethylated allele.
Hypomethyation	Loss of methylation, usually at an IC on the normally methylated allele.
KCNQ1	Previous name, *KvLQT1*.
KCNQ1OT1	Also called *LIT1* or *KvLQT1*-AS. The non-coding RNA transcribed from intron 10 of *KCNQ1*.
PHLDA2	Also called *IPL*.
CDKN1C	Codes for the protein $p57^{KIP2}$.

Chapter 1: Introduction

1.1 Monoallelic Gene Expression

1.1.1 Concepts

In diploid eurkaryotic organisms, the sexual reproduction process functions to transmit one copy of genetic material from each parent to the next generation. It is generally assumed that both alleles, if expressed, are expressed at similar levels. In reality, many genetic factors can cause the two parental alleles to be differentially expressed. *Cis*-acting inherited variations have been shown to bias the expression of one allele over another (Pant et al., 2006; Yan et al., 2002). There are, however, three additional mechanisms that are known to silence the expression of one of the two parental alleles using a variety of mechanisms. Examples of monoallelic expression patterns present in the mammalian genome are: 1) autosomal genes subject to random monoallelic expression, 2) genes of the X chromosome that are subject to random inactivation of one of the X chromosomes in females and finally 3) autosomal genes subject to parent-of-origin specific expression or genomic imprinting.

1.1.2 Random Monoallelic Expression

Until recently, random monoallelic expression has been documented only for odorant receptors, some of the interleukins and T-cells (Bix and Locksley, 1998; Hollander et al., 1998). The selection of which allele was to be expressed was seemingly a random cellular process giving rise to a variety of odours and antigens detectable by our sensory and immune systems, respectively, this process maximizes the sensitivity of a specific response to external stimuli. However, several recent studies have shown that the frequency of random monoallelic expression in subsets of human genes is surprisingly common. Allelic variation, the difference

in expression between two alleles, was studied in a small sample of human white blood cells by Pant and colleagues and they found 60 genes out of 1389 genes were differentially expressed in 3 or more individuals. They divided these genes into 3 categories: those that were imprinted, those that were in strong linkage disequilibrium with the assayed exonic single nucleotide polymorphism (SNP) and finally those that did not show a correlation in expression with a particular genotype (Pant et al., 2006). This suggested that allelic variation, at least for a small number of genes, was regulated by several different mechanisms. Further, Gimelbrant and colleagues studied the expression of over 4000 genes in lymphoblastoid cell lines by microarray analysis of coding single nucleotide polymorphisms and demonstrated that up to 10% of genes were subject to random monoallelic expression (Gimelbrant et al., 2007; Pant et al., 2006). They used monoclonal cultures of lymphoblastoid cell lines that demonstrated that expression of either allele could occur randomly in different clones and was maintained in each clonal cell population.

From an evolutionary perspective the benefit of expressing two alleles should provide important protection from expressing a deleterious mutation. So it seems counterintuitive that random monoallelic expression should be so widespread. Perhaps then, in the context of the whole organism the relative contribution of a single monoallelically expressed allele is minimized due to the mixing of cells that might be expressing either allele or both alleles. Further, similar to skewing of X-inactivation, where one X chromosome in a female may be preferentially silenced if it harbours a deleterious mutation expression of the wild type allele of a monoallelically expressed gene could occur by positively selecting the cells expressing those alleles. In an evolutionary context, it may even have positive ramifications by increasing the ability of an

organism to respond to changes in the environment. A similar concept for the evolution of genomic imprinting is proposed by Beaudet and Jiang called the "Evolvability Model" discussed in section 1.3, The Evolution of Genomic Imprinting.

The range of mechanisms that may be controlling random monoallelic expression still needs to be fully elucidated. For CD4+ T-cells the maturation to Th1 and Th2 cells is a process that has been demonstrated to be epigenetic (Sanders, 2006). Recent studies looking at larger numbers of genes in the human genome further support the epigenetic basis of monoallelism. For example, Milani and colleagues (Milani et al., 2008) showed that 16% of 2529 genes analyzed in blood and bone marrow from patients with acute lymphoblastic leukemia showed monoallelic expression. Of that 16%, those genes that were monoallelically expressed from either allele irrespective of genotype had higher levels of DNA methylation (however, the authors speculated but did not determine if the silenced allele was also the methylated one). Another study of lymphoblastoid cell lines on over 80 individuals, demonstrated that 130 of the 643 (~20%) genes analyzed showed differential allelic expression (Serre et al., 2008). Furthermore, 23 of the 130 that showed differential allelic expression were statistically associated with a common haplotype, potentially representing a regulatory haplotype, which could be causing differential *cis*-regulation. Therefore, several mechanisms are likely involved in the regulation of random monoallelic expression and it is an exciting area of on-going research.

1.1.3 **X-Inactivation**

Sex determination in mammals is specified by the presence of two X chromosomes for females and one X and one Y chromosomes for males. Dosage compensation for genes on the X

chromosome in males and females is achieved by random inactivation of one of the X chromosomes in females. This is observed cytologically as the Barr body (the condensed and inactive X chromosome located on the nuclear periphery). This heterochromatinization of one of the X chromosomes in females is associated with silencing of numerous genes on the inactive X chromosome. Although the exact mechanism whereby X inactivation completes the random selection and repression of one X chromosome in each cell has not been completely elucidated, this much studied area illustrates the importance of epigenetic mechanisms and shares many similarities with genomic imprinting. Briefly, the inactivation of one of the two X chromosomes in females is mediated by the expression of a non-coding RNA called *XIST* (X-inactive-specific transcript). *XIST* RNA accumulates *in cis* on the future inactive X chromosome through a poorly understood process called 'RNA coating'. This RNA coating phenomenon is an important event in triggering a complex cascade of epigenetic events, including recruitment of chromatin-modifying enzymes and nuclear compartmentalization that results in the *cis*-silencing of thousands of genes on the chromosome (Masui and Heard, 2006). Therefore, for many X-linked genes they are expressed monoallelically.

Despite the dramatic changes in chromatin structure that characterize the inactive X chromosome a surprising number of genes on the X chromosome escape inactivation (Brown and Greally, 2003; Carrel and Willard, 2005). Estimates from fibroblast-based assays suggest that about 15% of the 471 transcripts studied on the X-chromosome escape inactivation to some degree (Carrel and Willard, 2005). An additional 10% of genes showed escape from inactivation in some but not all fibroblasts tested.

1.1.4 **Genomic Imprinting**

Genomic imprinting is the final mechanism of monoallelic gene expression to be discussed in this Introduction. Unlike random monoallelic expression and X-inactivation, the expression of imprinted genes is not random and depends on the parent of origin for each allele. Thus, imprinted genes are expressed from either the maternal or paternal allele in each generation in a pre-determined expression pattern in each species. During gametogenesis the imprinted loci are differentially marked and these marks are not erased during the wave of demethylation that occurs after fertilization (Reik et al., 2001). In humans, 59 imprinted genes have been identified, although more likely remain to be discovered (Figure 1-1) (Morison et al., 2005). Genomic imprinting in mammals is essential for viability (Kono et al., 2004). This absolute requirement for both a maternal and a paternal genome in mammalian development became evident from experiments done in the early 1980's, in which attempts to reconstitute a viable mouse embryo entirely from either the maternal germline (gynogenetic conceptus derived from the fusion of two female pronuclei) or the paternal germline (androgenetic conceptus from two male pronuclei) were unsuccessful. Only rudimentary embryos were formed by these manipulations, with extremely poor placental growth followed by death *in utero* of the gynogenetic embryos, and with a different but equally non-viable phenotype - substantial outgrowth of placental tissues but almost no embryonic growth - seen in the androgenetic conceptuses (McGrath and Solter, 1984; Surani et al., 1984).

Figure 1-1: Idiogram of Imprinted Genes.

Representation of the location of imprinted genes in the genome. Only chromosomes with a verified imprinted gene are shown. Genes with red text are maternally expressed, genes with blue text are paternally expressed. As suggested by the UPD phenotypes, and from a review of data from knockout mice and human syndromes involving imprinted genes, there does appear to be a disproportionate involvement of such genes with two processes: growth and behavior. Genes with a demonstrated function in growth regulation have a green circle preceeding their name, with behaviour, a yellow circle and with both growth and behaviour, a purple circle. Indents represent genes that are present in the same functional component. It should be noted that information about the status of human imprinted genes may change as more studies are performed on a variety of tissues. Evidence for a role in growth and behaviour function for some genes may not yet be demonstrated. *GRB10 has alternate transcripts that are maternally or paternally expressed.

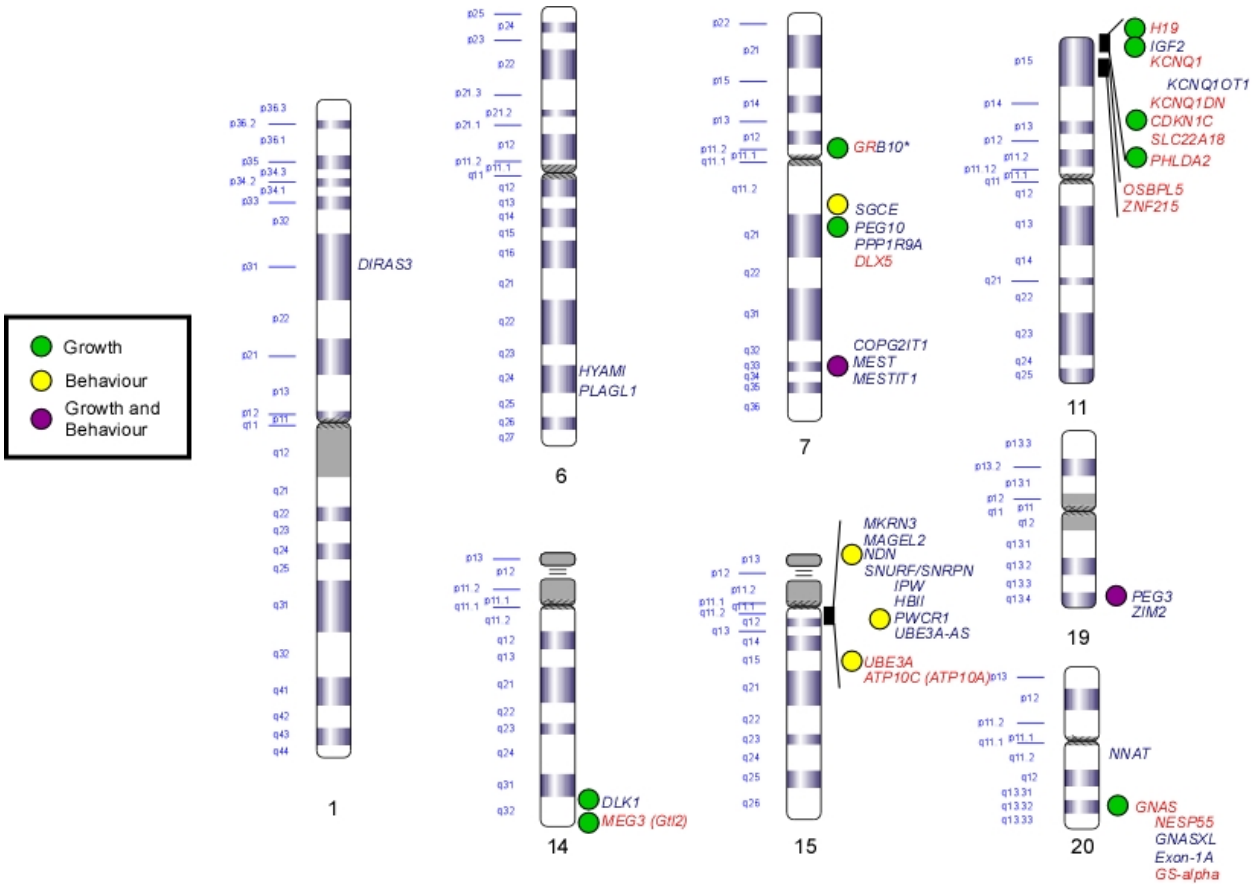

Figure 1-1. Idiogram of Imprinted Genes

1.2 Regulation of Genomic Imprinting - Epigenetics

Epigenetics refers to transmissible changes in gene expression that are not accompanied by changes in primary nucleotide sequence (Wolffe and Matzke, 1999). Epigenetic marks include alterations in DNA methylation and chromatin conformation specified in part by the covalent modifications of histone proteins. Epigenetic marks are essential for normal developmental gene regulation, in particular the correct expression of imprinted genes. Recent evidence has also revealed the existence of transcriptional and epigenetic gene networks that may coordinate the expression of imprinted gene domains (Varrault et al., 2006; Zhao et al., 2006).

Epigenetic marks demonstrate a form of plasticity both during development and in later life which allows them to be modified both temporally and spatially. This means that investigations of epigenetic alterations must be made in the context of developmental stages and tissue-specific epigenotypes. Epigenetic marks appear to be sensitive not only to genomic programming but also to environmental stimuli and to drugs, which can specifically target epigenetic marks (Weksberg et al., 2007).

1.2.1 DNA Methylation

DNA methylation occurs in mammals only on cytosine residues in CpG dinucleotides (Bernstein et al., 2007) or CNG sequences (Denisova et al., 2007). The 5-carbon of the cytosine nucleotide is covalently modified with a methyl group. This has been shown to alter the ability of gene regulatory sequences to interact with key chromatin proteins, such as methyl binding proteins (MBPs), insulator binding proteins, and the DNA methyltransferase enzymes themselves (Robertson, 2005). Patterns of DNA methylation can be faithfully propagated to daughter cells

during tissue growth, making this biochemical modification a very effective way to maintain epigenetic states. CpG dinucleotides are found throughout the genome, but are enriched in so-called CpG islands (CGIs). Since methylated cytosine tends to deaminate spontaneously to thymine, the bulk of the human genome contains the dinucleotide CpG five times less frequently than expected (Jones et al., 1992). The absence of methylation on cytosine slows the rate of mutation to T and CGIs are usually unmethylated. The concept of the CGI today is more of a mathematical description than a precise sequence. It was originally defined as a sequence of at least 200bp having a GC content greater than 50% and a ratio of CG dinucleotides greater than 0.6 based on the number of Gs and Cs in the segment. According to this description the genome contains some 28,000 such islands (UCSC Genome Browser March 2006) based on the criteria published by Gardiner-Garden and Frommer (Gardiner-Garden and Frommer, 1987). Takai and Jones proposed an alteration to the mathematical definition of the CGI to help exclude sequences derived from intragenomic parasites based on updated sequence information on the human genome from chromosomes 21 and 22 (Takai and Jones, 2002). According to their revised definition, a DNA segment >500 bp with a GC content equal to or greater than 55% and an observed CpG/expected CpG of 0.65, identified CGIs associated with the 5' end of genes while excluding most Alu repeat sequences based on their analysis of chromosomes 21 and 22.

Genes with CGIs in their promoter region tend to be expressed, and these CGIs are usually unmethylated (Bird, 1986). In the human genome approximately 60% of genes colocalize with a CGI (Antequera, 2003). On the other hand many of the other CpGs in the genome, lying outside of these CpG-dense islands, are methylated. Methylation of CpG dinucleotides in gene promoters does occur, especially in imprinted regions of the genome, and on the inactive X chromosome in

female cells. In both of these situations methylated CGIs are typically associated with gene silencing (Weber et al., 2005; Weber et al., 2007). CGIs often become methylated in cancer cells – in this setting the pathological gain of methylation can silence tumor suppressor genes, thereby promoting tumor progression (Jones and Baylin, 2002). DNA methylation is only effective in silencing gene expression when the methylated DNA is appropriately packaged into chromatin (Keshet et al., 1986), and we now know that CpG methylation acts in concert with histone modifications to determine chromatin structure and gene activity (Barski et al., 2007; Bernstein et al., 2007). Silencing mechanisms, including DNA methylation, are thought to have evolved in part as a host defense mechanism to silence retrotransposons, endogenous retroviruses, or repetitive sequences (Yoder et al., 1997). In fact, ~45% of the human genome consists of retrotransposons, including the very abundant Alu and L1 elements, and these sequences are indeed often densely methylated (Weisenberger et al., 2005).

DNA methylation is established and maintained by a family of DNA methyltransferases (DNMTs) (Chen and Li, 2004), which are listed and described in Table 1-1. These enzymes transfer a methyl group from S-adenosyl methionine to the 5-carbon position of cytosine bases of duplex DNA. Tracking the changes in DNA methylation in early development is technically difficult. From current information it appears that the genome (or at least many genomic sequences) is extensively demethylated in the first few post-zygotic cell divisions, and then remethylated. Methylation patterns then need to be maintained through successive cell generations. As the DNA replicates semi-conservatively during S-phase, one strand of each daughter duplex is methylated and one non-methylated. The template strand maintains its methylation pattern but the newly methylated DNA is unmethylated. DNMT1, the major

Table 1-1: DNA Methyltransferases

DNMT	Catalytic Activity	Substrate Preference	Knock-Out
1	Yes	CpG, Hemimethylated	Lethal
1o	Yes		Heterozygote knock out lethal last third of gestation
2	Not demonstrated in vivo	CpT, CpA, physiological substrate uncertain	Viable
3a	Yes	CpG, De novo	Lethal
3b	Yes	CpG, De novo	Lethal
3L	No	-	-Male sterility, female lethality -Imprinted expression not maintained

maintenance methylase, has a high affinity for this hemimethylated DNA (Pradhan et al., 1999; Pradhan et al., 1997), and it therefore acts catalytically to restore the original methylation pattern (Figure 1-2). Without DNMT1, passive demethylation can occur, with loss of methylation through successive rounds of cell division. Indeed such passive demethylation, and a less well understood active process of removal of methyl-C, does occur in the early post-zygotic period (Rougier et al., 1998; Santos et al., 2002). In mouse, at least one stage-specific isoform of DNMT1 is known. $DNMT1_O$ is an oocyte derived protein that enters cell nuclei only at the 8-cell stage of the early embryo, and has an essential role in maintaining the correct epigenetic marks (Howell et al., 2001).

In addition to maintenance methylation, methyl groups must also be added "de novo" at various times during development, e.g. to establish parental imprints on the DNA (Kaneda et al., 2004), to regulate tissue specific expression of genes, to methylate centromeric DNA and other constitutive heterochromatin, and to defend the host against foreign DNA integration and expression. The DNMT3 family includes two "*de novo*" DNA methyltransferases, DNMT3a and DNMT3b. These enzymes can methylate CG's that are not in hemimethylated DNA. DNMT2, a member of the DNA methylase family, has sequence homology to known DNA methylases, but lacks the characteristic catalytic signature residues. Another member of the DNMT3 family, DNMT3L, has no catalytic activity but is required to maintain allele-specific methylation in imprinted regions of the genome (Bourc'his et al., 2001).

Figure 1-2: Methylation of DNA after replication.

Once a sequence is methylated, this methylation pattern can be faithfully propagated to daughter cells. This propagation is primarily the responsibility of a DNA methyltransferase enzyme called DNMT1. DNMT1 has a high affinity for hemi-methylated CpG sites, so the daughter strands are rapidly re-methylated after they are synthesized.

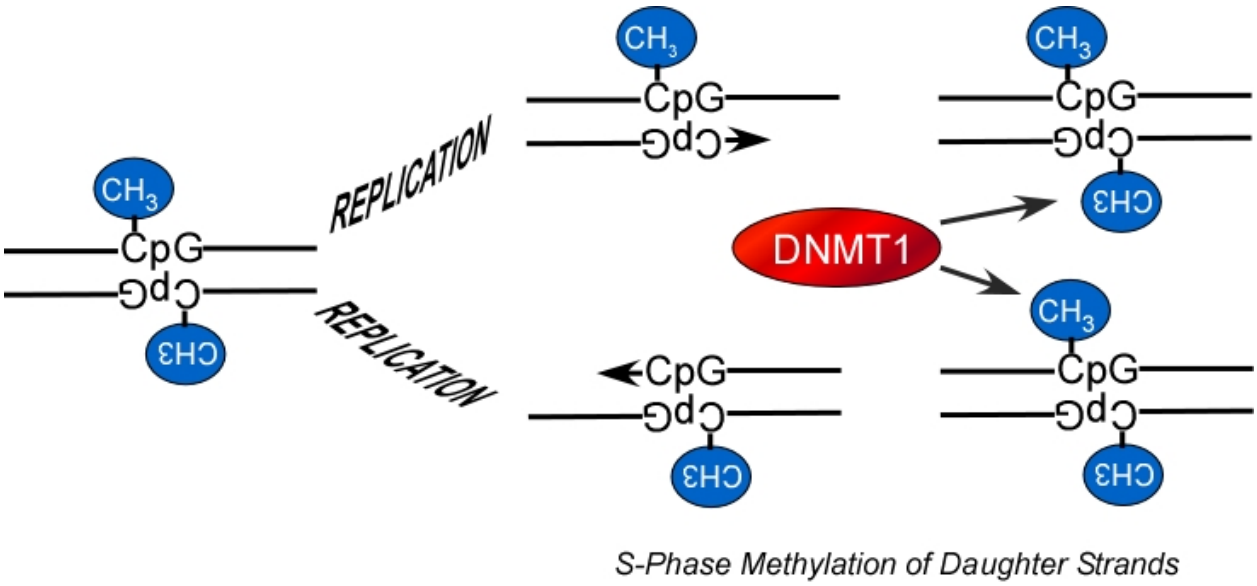

Figure 1-2. Methylation of DNA after replication.

1.2.2 **DNA Methylation Reprogramming**

There are two periods characterized by extensive epigenetic reprogramming, germ cell production and early embryonic development post-fertilization (Reik et al., 2001). In mice, the DNA of the primordial germ cells becomes globally and rapidly demethylated. This erasure of DNA methylation includes the germ-line imprints. This step removes the biparental DNA methylation marks that are present in the progenitors of the germ cell population so that all germ cells can then be remethylated with the appropriate sex-specific germline marks for either sperm or oocyte.

After fertilization, another wave of DNA methylation reprogramming takes place as the paternal genome is again rapidly and actively demethylated. The maternal DNA is also demethylated but more slowly and by a replication-dependent mechanism in the absence of any DNA methyltransferase activity. In contrast to what happens in primordial germ cells, after fertilization genomic imprints remain resistant to the demethylation that occurs in the rest of the genome. It has been suggested that the oocyte-specific form of DNA methyltransferase (*Dnmt1*$_o$) plays a key role in maintaining imprinted marks as it translocates to the nucleus at the 8-cell stage in mice (Ko et al., 2005). A wave of *de novo* methylation establishes the somatic cell pattern of DNA methylation following implantation (Reik et al., 2001). The active demethylation of DNA observed during development has led many to search for a DNA demethylase. Several studies have proposed that MBD2 (Bhattacharya et al., 1999) and GADD45A (Barreto et al., 2007) have the ability to demethylate DNA. However, additional studies have contested the findings reported in these papers (Jin et al., 2008b; Santos et al., 2002)

and the exact mechanism of DNA demethylation remains unclear. DNA demethylation could occur either by a specific demethylase enzyme, which is yet to be found, or via a DNA repair mediated pathway whereby methylated DNA would be removed and new DNA synthesized without methylation (Kangaspeska et al., 2008; Metivier et al., 2008). In either case, it is clear that DNA methylation and other epigenetic modifications play an important role in regulating transcription for both imprinted and non-imprinted genes.

1.2.3 **Non-Coding RNA**

Noncoding RNA transcripts such as *H19* and *KCNQ1OT1* are hallmarks of imprinted domains (Barlow, 1997; Nakabayashi et al., 2002; Smilinich et al., 1999). The exact function of these transcripts in the regulation of genomic imprinting is not fully understood but what is clear is that they are important for the establishment of allele-specific imprinting. What is also intriguing is the variety of RNA mechanisms which are seemingly operating in different clusters. For example, mouse experiments demonstrate that the non-coding transcripts *Kcnq1ot1* and *Air1* act as *cis*-acting silencers although the precise mechanism remains to be defined. In contrast, the *H19* non-coding RNA contains a microRNA (miRNA) and expression of *H19* may simply serve to produce this miRNA. This may also be similarly true for the *SNURF-SNRPN* locus on chromosome band 15q11 where expression of *SNRPN* may serve to express the small nucleolar RNA (snoRNA) contained within this locus (Costa, 2008; Royo and Cavaille, 2008).

miRNAs are 22 nucleotide-long RNA molecules that can have a profound effect in controlling gene expression. Some miRNAs are located intergenically while others are located within genes. miRNAs that are located within genes can be expressed only when the gene they are located in is

expressed or they can have their own transcriptional start site (Rouhi et al., 2008). They are transcribed by RNA polymerase II and then processed in the nucleus into precursor miRNAs. After being exported to the cytoplasm precursor miRNAs are further processed by RNase III Dicer into mature miRNAs. miRNAs can down-regulate gene expression and each miRNA can have multiple targets. When an miRNA binds to its target with complete complementarity it signals for the degradation of the mRNA. miRNAs can also bind with incomplete complementarity that can cause the suppression of mRNA translation (Chuang and Jones, 2007).

SnoRNAs are 60 to 300 nucleotide non-coding RNAs that guide the chemical modification of methylation or pseudouridylation of ribosomal RNAs, small nuclear RNAs and tRNAs. Imprinted snoRNAs do not appear to act like other snoRNAs, by directing methylation or pseduouridylation, and are thus called orphan C/D box snoRNAs (Royo and Cavaille, 2008). For the imprinted HBII-52 snoRNA in the imprinted region on chromosome 15 the function of this RNA has been shown to direct the adenine to inosine RNA editing of the serotonin receptor 5-HT_{2C}R. This editing regulates the alternative splicing of exon V of the 5-HT2CR gene and generates receptor isoforms that differ in their ability to interact with G proteins. This modulates serotonergic neurotransmission in the central nervous system and may contribute to the phenotype seen in Prader-Willi syndrome (Kishore and Stamm, 2006).

1.2.4 **The Regulation of Chromatin Structure by Modifications to Histone Tails**

DNA packaging is a dynamic process that must respond to many signals relevant to processes and functions of the DNA in the nucleus. During processes such as DNA repair, DNA replication and gene transcription, nucleosomes, histones and the strands of DNA themselves are

modified. This active process supports the structural stability and functionality of DNA within the nucleus.

The conformation of chromatin is regulated by a "histone code" that is established by a series of covalent modifications to the tails of the histones (Briggs and Strahl, 2002; Bulger, 2005; Jaenisch and Bird, 2003; Umlauf et al., 2004). High-throughput array and sequencing technologies (ChIP-on-Chip and ChIP-seq) have begun to elucidate the many modifications to histone tails and their higher-order interactions. With respect to histone acetylation and methylation typical patterns of repressive and active chromatin have been described at promoters, insulators, enhancers, and transcribed regions. Actively transcribed promoters are generally associated with acetylated histone H3 and H4 as well as monomethylation of H3K27, H3K9, H4K20, H3K79, and H2BK5. Deacetylated H3 and H4 as well as trimethylation of H3K27, H3K9, and H3K79 are associated with repressed chromatin (Barski et al., 2007). Some histone tail modifications are specifically associated with the transcription start site of a gene (e.g. H3K4 trimethlyation) whereas other modifications mark actively transcribed regions (e.g. H3K36 trimethylation).

1.2.5 **Regulation of Genomic Imprinting and Imprinted Clusters**

An intriguing characteristic of imprinted genes is that they often cluster, forming imprinted domains (Nicholls, 2000; Verona et al., 2003). The concept of an imprinting centre that regulates expression of closely positioned imprinted genes within a domain was first developed by analyzing deletions in patients with Prader-Willi syndrome. Imprinting centres are thought to generate parent-of-origin-specific chromatin states that are propagated bidirectionally over

several hundred kilobases of DNA to regulate imprint switching of the domain (Nicholls et al., 1998). Mutations (either genetic or epigenetic) in imprinting centers may cause failure to reset imprints in the germline and lead to inheritance of an inappropriate "epigenotype" across hundreds of kilobases of DNA (Buiting et al., 1995).

Imprinting centres have been demonstrated to have certain unique characteristics. Imprinting centres usually contain differentially methylated regions (DMRs) that are methylated only on the maternal or paternal allele. These differentially methylated regions are often associated with non-coding RNA transcripts that are expressed from the unmethylated allele (such as *SNRPN* and *KCNQ1OT1*). These functional RNAs seem to be a hallmark of imprinted domains and an important part of their regulatory mechanisms.

Imprinting centres, as well as the genes that are functionally regulated by them, have been shown to have differential histone tail modifications on the maternal and paternal alleles (Diaz-Meyer et al., 2005). As would be expected the active allele is associated with acetylation of histone H3 and H4 and trimethlyation of H3K4. The repressed allele is associated with deacetylated H3 and H4 and trimethylation of H3K9 and H3K27 (Diaz-Meyer et al., 2005). The chromatin status of imprinted regions has also been shown to influence the timing of regional chromosome DNA replication (Brown et al., 1996; Squire et al., 2000).

1.2.6 **Replication Timing**

A common element observed in mammalian genomic sequences that are monoallelically transcribed is replication asynchrony during S-phase of DNA replication. This has been

observed for immunoglobulin genes, olfactory receptor genes, the majority of genes on the X-chromosome and genomically imprinted genes (Ohlsson et al., 1998). Replication asynchrony for the H19/IGF2 region has been demonstrated to show early replication of the paternal allele by most studies (Bergstrom et al., 2007; Squire et al., 2000) however some studies have shown early replication of the maternal allele or synchronous replication (Gribnau et al., 2003; Kawame et al., 1995). These opposing observations may be accounted for by methodological differences between the studies, such as use of chemical agents for cell synchronization.

A recent study in mouse has demonstrated that replication timing in the imprinted H19/IGF2 region may be mediated by the binding of the transcriptional regulator CTCF that normally binds to the maternal allele of the *H19* IC. When the CTCF binding sites are mutated no shift in replication timing is seen when the mutant allele is inherited paternally, but a shift to early replication is seen when the mutated allele is inherited maternally (Bergstrom et al., 2007). The role of asynchronous replication in regions of the genome associated with monoallelic expression patterns and the mechanisms that control it are currently poorly understood. Further elucidation of the role of CTCF in mediating replication timing at other loci characterized by monoallelic expression may help to clarify the mechanisms and functions of replication asynchrony.

1.3 The Evolution of Genomic Imprinting

How genomic imprinting evolved is not completely understood and several theories have been proposed to explain its occurrence. The best known theory is called the "Conflict" or "Haig" hypothesis as it was first proposed by Haig and Westoby in 1989 (Haig, 1993; Haig and Westoby, 1989). The theory suggests that the mother's evolutionary interest is to pass on her

DNA to as many offspring as possible and therefore limits the size of each individual fetus. This means that maternally expressed imprinted genes will tend to restrict growth as is the case with maternally expressed *CDKN1C*, a cyclin dependent cell cycle inhibitor. Conversely, the evolutionary interest of the father is to maximize the fitness of each offspring. Therefore, paternally expressed genes should be growth enhancing as with the paternally expressed insulin-like growth factor 2 (Wilkins and Haig, 2003). Since the majority of the conflict between the maternal and paternal interests takes place *in utero,* the placenta should be a key organ for this conflict. Much support for the conflict hypothesis rests on the fact that many imprinted genes are highly expressed in the fetal compartment of the placenta where they are known to affect fetal growth (Coan et al., 2005; Tycko, 2006; Weksberg et al., 2007). In addition, it appears that the development of genomic imprinting coincided with placentation (Killian et al., 2000; Killian et al., 2001; Lawton et al., 2005; Nolan et al., 2001). It has been noted that not all imprinted genes are involved in modulating growth. However, since imprinting tends to affect clusters of genes it could be argued that such genes are simply "innocent bystanders" in the regulation of the target growth regulatory gene.

Alternative theories, such as the "Evolvability Model" by Beaudet and Jiang (Beaudet and Jiang, 2002), have been proposed. Essentially, this model proposes that imprinted genes provide an organism with a mechanism to adapt to environmental pressures. For example, if a gene was normally imprinted there would be no phenotypic effect, but if increased growth became advantageous the repression of the silenced allele could be rapidly reversed increasing expression and consequently increasing growth. The final theory proposed by Varmuza and Mann (Varmuza and Mann, 1994) is called the "Ovarian Time Bomb" hypothesis. They

hypothesized that by requiring equal parental contributions, the level of growth and development of parthenogenetic embryos, such as hydatidiform moles or teratomas, would be limited thereby protecting the female from ovarian diseases. As placentation led to longer gestational periods and an increased demand on maternal resources, increased protection for the mother during pregnancy would increase her fitness.

Mechanistically, there are many links between the processes of X-inactivation and genomic imprinting. Silenced imprinted regions and the inactive X chromosome share features in common such as DNA methylation, repressive chromatin structure and expression of a functional non-coding transcript (e.g. *XIST*). It has therefore been proposed that these processes shared a common origin. The suggestions that genomic imprinting evolved from X-inactivation or that both of these processes developed from a shared ancestral imprinted chromosome have not been supported by evidence from mammals, marsupials and birds (Edwards et al., 2007). These authors demonstrated that the orthologues of mammalian imprinted genes are dispersed amongst the genomes of both monotremes and marsupials suggesting that the origin of each gene or cluster occurred individually in a stepwise or additive process.

1.4 Imprinting and Human Disease

1.4.1 Genetic and Epigenetic Events in Imprinted Domains Resulting in Disease

There are several well studied imprinting clusters in the human genome. Each is associated with one or more syndromes that exhibit both genetic and epigenetic alterations summarized in Table 1-2. It should therefore be noted that for several genes in each of these imprinted clusters, gene

Table 1-2: Summary of Epigenetic Alterations in Imprinting Disorders

DISEASE	CHROMOSOME LOCATION	UPD	IC METHYLATION ALTERATIONS	CHROM./ DELETION DUPL.	MUTATION IN IMPRINTED GENES	UNKNOWN
Beckwith-Wiedemann syndrome	11p15.5	11p15.5 (pat) 20%	KvDMR LOM (mat) 50% H19 GOM (mat) 5%	translocation 11p15.5 (mat) (<1%) Dup. 11p15.5(pat) (<1%)	CDKNIC (mat) 5%	20%
Prader-Willi syndrome	15q11-q13	15q11.2-q13 (mat) (7%)	15q11.2-q13 GOM (<1%)	Deletion 15q11.2-q13 (70%) Rearrangement 15q11.2 (1%)	None identified	<1%
Angelman syndrome	15q11-q13	5q 11.2-q13 (pat) (7%)	Imprinting defect LOM (3%)	Deletion 15q11.2 – q13 (70%) Rearrangement (Tl & inv) 1%	UBE3A (mat) 11%	10%
Russell-Silver syndrome	7p11.2* and 11p15.5	7 (mat) (10%)R	H19 (chrom 11) LOM (pat) (25%) R	Duplication 11p15.5 (mat) (3%)	None identified	65%
Pseudohypopara thyroidism type 1b	20q13.2	20q13.2 (pat) (N.D.)	GNAS DMR and exon 1A (N.D.)	Microdeletions near GNAS exon 1A disrupting methylation OR NESP55 gene (N.D.)	GNAS Mutations (McCune-Albright syndrome)	N.D.

*exact molecular defect is unknown, however evidence points to this region.

N.D. not determined, accurate number is not currently known

dosage must be tightly regulated and alterations in their levels of expression result in disease phenotypes.

The imprinting disorders listed in Table 1-2 can be caused by multiple mechanisms and the frequency of those alterations tends to be unique to each region. Duplication or deletion of a region including an imprinted cluster is a common mechanism especially in Prader-Willi and Angelman syndrome. These deletions are quite often large and microscopically visible but smaller microdeletions can also cause imprinting disorders (Sparago et al., 2006). Translocations and inversions are also associated with imprinting disorders although these are usually rare events. Uniparental disomy (UPD) results from the inheritance of two copies of a chromosome, or segment of a chromosome, from one parent and none from the other; this causes a gain or loss of imprinted gene expression. Mutations of imprinted genes can also cause imprinting disorders. These events also tend to be associated with pedigrees that show dominant parent-of-origin specific transmission of the mutation.

In addition to the genetic alterations listed above, epigenetic changes (e.g. changes in DNA methylation and presumably chromatin modifications) at imprinting centres also cause imprinting disorders. A gain or loss of the normal differential methylation at an imprinting centre results in altered expression of the imprinted genes regulated by that imprinting centre.

Interestingly, more than one syndrome can be caused by either the upregulation or downregulation of imprinted gene expression at a given locus. For example, on human

chromosome 11p15.5, gain of methylation of the *H19* imprinting centre causes overgrowth and is associated with Beckwith-Wiedemann syndrome whereas the opposite epigenetic change, loss of methylation at this locus, results in the severe inhibition of prenatal and postnatal growth seen in the Russell-Silver syndrome (Bartholdi et al., 2009; Bliek et al., 2006; Bruce et al., 2009; Smith et al., 2007; Yamazawa et al., 2008; Zeschnigk et al., 2008). These observations seem to highlight the conflict of maternal versus paternal genes and growth control lending support to the conflict hypothesis for the evolution of genomic imprinting.

1.4.2 **Beckwith-Wiedemann syndrome**

Beckwith-Wiedemann syndrome (BWS) was reported independently in 1963 and 1964 by Drs. Beckwith and Wiedemann in separate publications (Beckwith, 1963; Wiedemann, 1964). The syndrome was initially called the EMG syndrome based on three clinically significant findings: exomphalos, macroglossia and gigantism. However, Beckwith-Wiedemann syndrome represents a complex disorder both phenotypically and genetically/epigenetically providing unique opportunities to explore a number of intriguing biological phenomena.

1.4.3 **Clinical Synopsis**

Beckwith-Wiedemann syndrome occurs in 1/13,700 individuals and is equally represented in males and females (Pettenati et al., 1986; Thorburn et al., 1970). BWS was initially defined by the presence of gigantism, macroglossia and abdominal wall defects, but can also include other clinical finding such as hemihyperplasia, embryonal tumors, adrenocortical cytomegaly, ear anomalies (anterior linear earlobe creases, posterior helical pits), visceromegaly, congenital renal abnormalities, neonatal hypoglycemia, cleft palate and a positive family history (Pettenati et al.,

1986; Weng et al., 1995a; Weng et al., 1995b). Most cases of BWS are sporadic and demonstrate normal karyotypes. Autosomal dominant pedigrees showing maternal transmission occur in about 10-15% of cases (Li et al., 2001). Additionally, rare chromosomal rearrangements, such as duplication, deletion, translocation and inversion can also cause BWS (Hoovers et al., 1995; Sait et al., 1994).

1.4.4 **Genetics of Beckwith-Wiedemann Syndrome**

Although BWS is genetically complex (Cooper et al., 2005; Weksberg et al., 2005), the key imprinted genes implicated in the etiology of BWS and related tumors all map to the 11p15.5 imprinted region. The following section will detail the chromosome 11p15.5 imprinted cluster and the molecular alterations seen in BWS. A map of the 11p15.5 imprinted region can be found in Figure 1-3.

1.4.5 **Molecular Alterations in Beckwith-Wiedemann Syndrome on Chromosome 11p15.5**

The 11p15.5 chromosome imprinted region can be divided into two distinct regulatory domains each controlled by its own imprinting center (IC). The frequency of molecular alterations occurring in BWS patients is summarized in Figure 1-4.

Domain 1 (regulated by IC1): Domain 1 contains two genes: insulin-like growth factor 2 (*IGF2)* and *H19*. An imprinting centre is located approximately 2 kb upstream of the H19 transcription start site and is differentially methylated (Hark et al., 2000). The maternally expressed *H19* gene encodes a spliced, non-translated RNAPolII transcript with five exons. The *H19* transcript is thought to be functional since there is evolutionary conservation of its

Figure 1-3: The imprinted gene domains on human chromosome 11p15 associated with Beckwith-Wiedemann syndrome.

Paternally expressed genes are indicated by blue arrows and maternally expressed genes are indicated by a red arrow. Differentially methylated regions are represented by squares. Solid squares indicate methylation and hollow squares indicate no methylation. Note that individuals with BWS and duplications, translocations and inversions of chromosome 11 are rare. Several reports have now indicated that in rare cases heritable microdeletions may alter methylation at DMR1 or DMR2. Different epigenetic (above) and genetic (below) alterations associated with BWS and their respective frequencies are shown. Note, only the relevant region is shown in some cases.

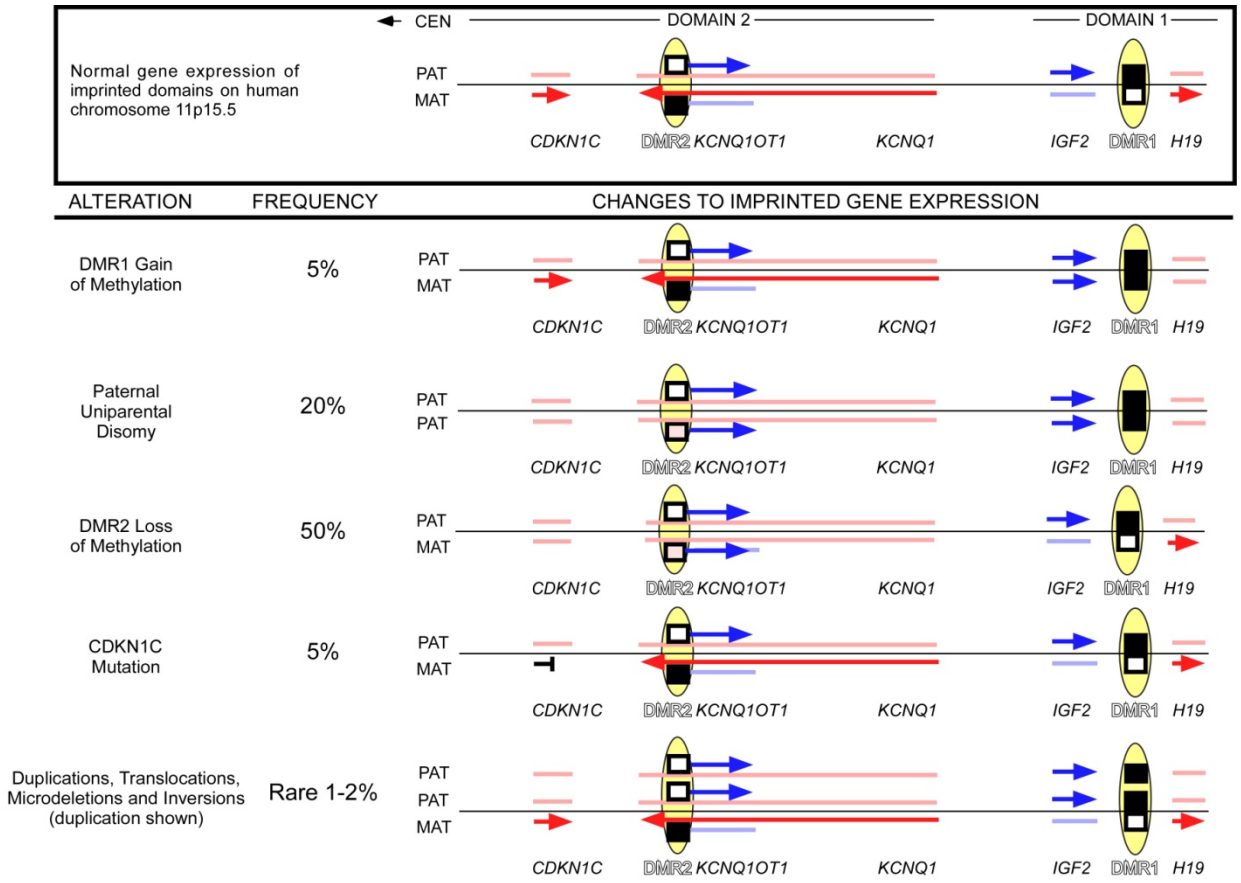

Figure 1-3. The imprinted gene domains on human chromosome 11p15 associated with Beckwith-Wiedemann syndrome.

Figure 1-4: Genetic and Epigenetic Alteration Frequencies in BWS.

The largest molecular subgroup of Beckwith-Wiedemann syndrome patients is the epigenetic defect involving loss of methylation at DMR2 (~50%). Gain of methylation at DMR1 comprises another epigenetic subgroup (~9%). Therefore, approximately 60% of patients carry an epigenetic error at one of the two imprinting centres on 11p15. The next largest category is paternal uniparental disomy (UPD ~20%). Chromosomal alterations are relatively rare and include paternal duplications (<1%) and chromosome 11 inversions and translocations (<1%). Genetic causes of Beckwith-Wiedemann syndrome include mutations in the gene CDKN1C (~10%). Also, microdeletions of IC1 or IC2 occur rarely (<1%). In 10-15% of individuals with Beckwith-Wiedemann syndrome, the molecular anomaly is unknown.

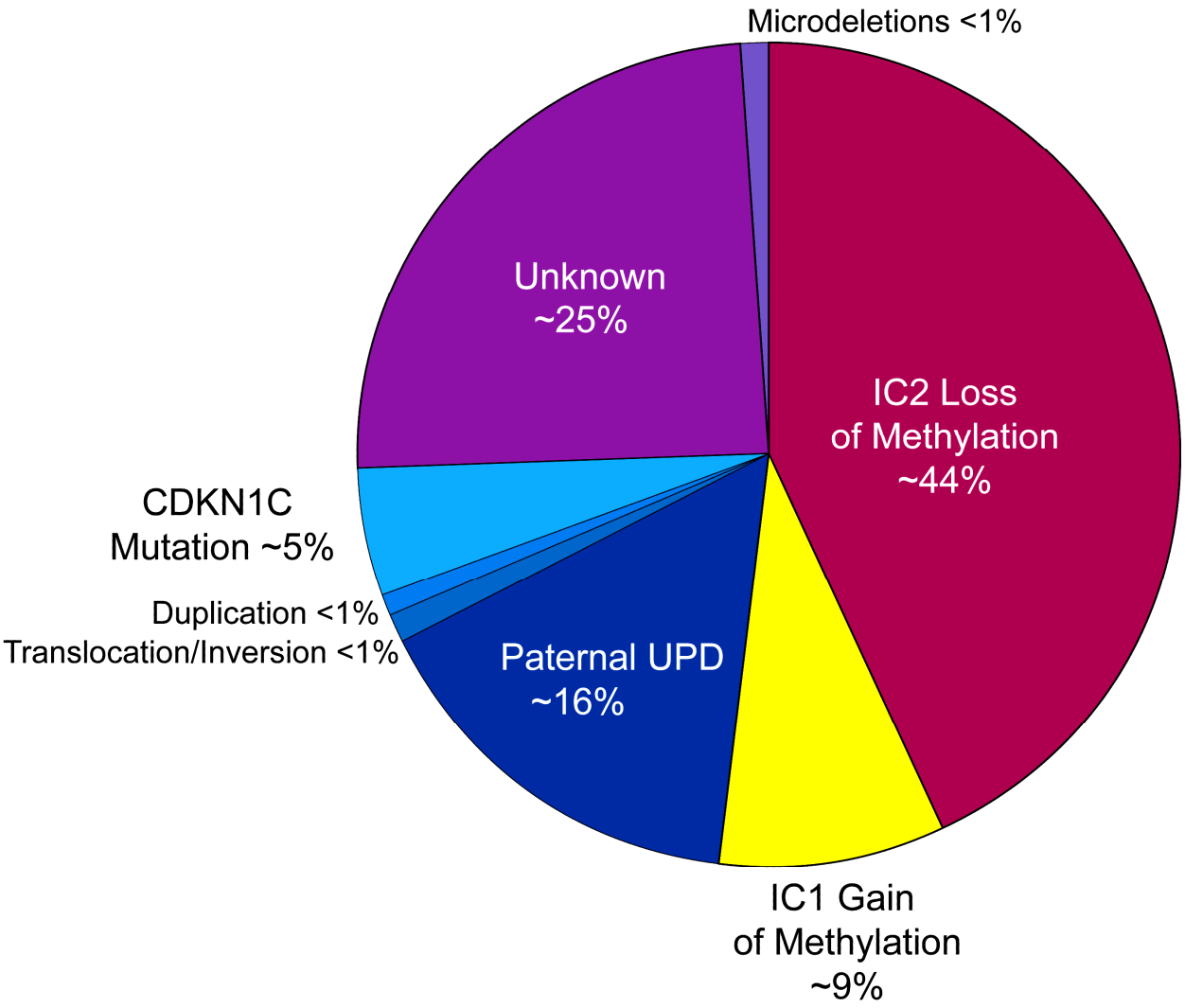

Figure 1-4. Genetic and Epigenetic Alteration Frequencies in BWS.

secondary structure (Juan et al., 2000). The role of *H19* in the regulation of imprinting and gene expression has not been clearly defined; however, the *H19* gene contains the microRNA miR-675 and its function and conservation may simply serve to produce this small RNA. Although the exact function of miR-675 is unknown, the conflict hypothesis suggests that transcription of maternal *H19* should suppress growth pathways via the RNAs that it targets (Cai and Cullen, 2007; Royo and Cavaille, 2008).

The *IGF2* gene encodes a paternally expressed cytokine that plays an important role as a fetal growth factor (Figure 1-3). Its upregulation is thought to play a pivotal role in the pathogenesis of BWS (Maher and Reik, 2000) and in a large variety of sporadic tumors (Schofield et al., 2001; Tycko, 2000). The *IGF2* gene exhibits a pattern of tissue-specific expression that closely parallels the organs exhibiting overgrowth in BWS (Eggenschwiler et al., 1997). Transgenic mice that overexpress *Igf2* exhibit many but not all the features of BWS e.g. overgrowth and macroglossia (Sun et al., 1997). The expression of the *IGF2* gene may be increased by several distinct mechanisms since transcription is modulated by 4 promoters (P2-P4 are imprinted; P1 is non-imprinted) and several tissue-specific regulatory elements including three differentially methylated regions within the *IGF2* gene (Murrell et al., 2008; Vu and Hoffman, 1994). Furthermore, increased expression of *IGF2* may also be caused by paternal duplications of chromosome 11p15 (Weksberg et al., 1990; Weksberg et al., 2003), paternal uniparental disomy, or by loss of imprinting of *IGF2*.

The reciprocal regulation of the *H19* (maternal expression) and *IGF2* (paternal expression) genes is one regulatory mechanism that is demonstrable for these two genes in most normal mouse and human tissues as well as in some human tumors (Figure 1-3). This mechanism was elucidated in a series of elegant mouse experiments that also identified the Domain 1 imprinting center, IC1 (Caspary et al., 1999; Constancia et al., 2000; Drewell et al., 2000; Jones et al., 2001; Sun et al., 1997). The *H19* and *Igf2* genes compete for a common set of downstream enhancers located 3' of the *H19* gene, normally ensuring monoallelic expression of the maternal *H19* allele coincident with monoallelic expression of the paternal *IGF2* allele (Bartolomei and Tilghman, 1997; Caspary et al., 1998). IC1, located 2 kb upstream of the mouse *H19* gene regulates imprinted expression of *H19* and *IGF2* (Domain 1) by functioning as a chromatin "insulator" (Figure 1-5). On the maternal chromosome, IC1 is unmethylated, permitting the binding of a zinc finger binding protein called CTCF. This binding blocks access of the *IGF2* promoter to cognate downstream enhancers. The maternal *H19* gene accesses these enhancers and is therefore transcribed. On the paternal chromosome, methylation of IC1 prevents binding of the CTCF protein to IC1, so that the *IGF2* promoter has access to the downstream enhancers and is expressed while *H19* transcription is silenced (Hark et al., 2000). Although the reciprocal regulation of *H19* and *IGF2* can be understood in the context of the enhancer competition model described above, there are epimutations associated with BWS which cannot be explained using this model. Moreover, it has been acknowledged that not all the data in mouse can be explained by the enhancer-competition model (Jones et al., 2001).

BWS associated with alterations in the IC1 Region: Expression of the normally silent maternal allele of *IGF2* occurs in 25% of BWS cases (Weksberg et al., 1993a) and for most of

Figure 1-5: Model for the regulation of *H19* and *IGF2* reciprocal imprinted expression.

A) H19 is normally maternally expressed, *IGF2* is normally paternally expressed. *H19* is methylated on the paternal allele in the differentially methylated region (IC1, yellow box) located two kilobases upstream. Methylation extends down to the *H19* promoter region (Methylation is indicated by a CH_3). A zinc-finger protein, CTCF, binds to the unmethylated IC1 blocking access of *IGF2* to its shared downstream mesodermal and endodermal enhancers (circle with "E"). *B)* 9% of BWS patients exhibit *H19*-dependent biallelic *IGF2* expression. These patients have gain of methylation, methylation on both the maternal and paternal IC1. CTCF can no longer bind and *IGF2* has access to its downstream enhancers resulting in biallelic expression. *C)* 25-50% of BWS patients have *H19*-independent biallelic *IGF2* expression. These patients do not show a gain of methylation at the maternal promoter region or IC1 of *H19* and often maintain monoallelic *H19* maternal expression. Binding of CTCF to maternal DMR is not known.

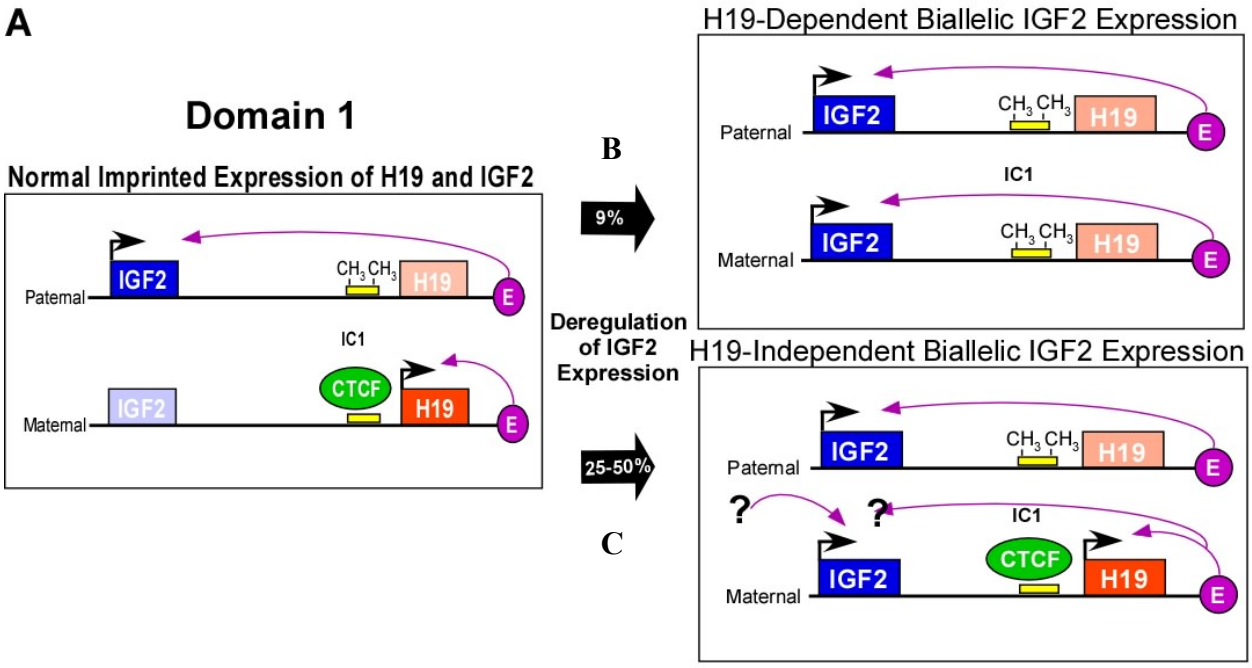

Figure 1-5. Model for the regulation of *H19* and *IGF2* reciprocal imprinted expression.

these cases, the cause whether genetic or epigenetic, is not known. Furthermore, BWS cases with biallelic *IGF2* expression, although occasionally reported in conjunction with other molecular lesions on 11p15.5, have not been systematically investigated for concomitant alterations in Domains 1 and 2. This is due in part to the low baseline expression of *IGF2* in lymphocytes thus requiring a tissue with higher baseline expression of *IGF2*, such as skin or placenta.

Gain of DNA methylation of the IC1 occurs in approximately 9% of patients with BWS (Bliek et al., 2001; Cooper et al., 2005; Gaston et al., 2001; Weksberg et al., 2001). This molecular change can also be seen in sporadic Wilms tumor and some embryonal rhabdomyosarcomas (Anderson et al., 1999; Bjornsson et al., 2007; Steenman et al., 1994). As predicted by the enhancer-competition model, gain of methylation of the maternal IC1 would result in biallelic expression of *IGF2* with repression of *H19* expression (Figure 1-5B). In addition, microdeletions of the IC1 region have been shown to cause gain of DNA methylation at IC1, loss of *IGF2* imprinting and a typical BWS phenotype (Sparago et al., 2004). More commonly in BWS however, there is disruption of the co-ordinate regulation of *H19* and *IGF2* (Brown et al., 1996; Joyce et al., 1997; Squire et al., 2000); i.e. most cases of loss of imprinting of the *IGF2* gene are associated with normal monoallelic maternal expression of the *H19* gene (Figure 1-5C). Loss of imprint of the *IGF2* gene in BWS suggests that dysregulation of the *IGF2* gene can also arise from a yet to be defined epigenetic change in the IC1 region of 11p15.5 that does not affect *H19* expression or methylation. A differentially methylated region within the IGF2 gene, DMR0, could be such a candidate. However, gain of methylation at the *IGF2* DMR0 has been shown in BWS patients that have gain of methylation at IC1 but not with other genetic or epigenetic lesions associated with BWS (Murrell et al., 2008). Experiments in mice indicate that additional

regulatory elements that are tissue-specific likely also play a role in controlling *IGF2* expression independent of imprint regulation at IC1 (Jones et al., 2001).

Domain 2 (regulated by IC2): In Domain 2, there are at least four well characterized human maternally expressed imprinted genes: *KCNQ1, CDKN1C, PHLDA2* and *SLC22A18* (Figure 1-3). The maternally expressed *KCNQ1* gene product forms a subunit of a voltage-gated potassium channel and mutations in the gene cause at least two cardiac arrhythmia syndromes (Neyroud et al., 1997; Wang et al., 1996). This 400kb gene contains several translocation breakpoints associated with BWS (Hoovers et al., 1995; Lee et al., 1999; Lee et al., 1997; Mannens et al., 1994; Sait et al., 1994; Squire et al., 2000). Evidence supporting the existence of the imprinting center IC2 was first obtained from studies of cells from BWS patients. Smilinich and colleagues (Smilinich et al., 1999) and Lee and colleagues (Lee et al., 1999) identified in intron 10 of the *KCNQ1* gene, a DMR, initially called *KvDMR1*, but named 'IC2' in this thesis. Within the DMR of IC2 is the promoter of an imprinted, paternally expressed non-coding RNA transcript called *KCNQ1OT1* that is transcribed in an anti-sense direction to *KCNQ1* (Du et al., 2004; Lee et al., 1999; Smilinich et al., 1999).

The syntenic region on mouse chromosome 7 has a similar organization to the human and has been studied by several investigators to elucidate the mechanisms regulating genomic imprinting in this domain. In mice, *Kcnq1ot1* is a 91kb RNAPolII encoded transcript that is unspliced and not exported to the cytoplasm (Pandey et al., 2008). A targeted deletion of the paternal IC2 in mice, which deleted the *Kcnq1ot1* promoter, led to biallelic expression of *Ckdn1c*, *Kcnq1*, *Phlda2* and *Slc22a18* (Fitzpatrick et al., 2002). Genomic imprinting was retained when the

deletion of IC2 was inherited maternally. In addition, truncation of *Kcnq1ot1* 2 kilobases downstream of the promoter showed that the neighbouring genes are expressed biallelically, when the truncated *Kcnq1ot1* is inherited from the father (Mancini-Dinardo et al., 2006). Further, when the transcription of *Kcnq1ot1* is truncated from 4.9 to 9.2 kilobases, the efficiency of silencing increases (Kanduri et al., 2006). These experiments demonstrate that transcription of *Kcnq1ot1* is necessary for the establishment and maintenance of imprinting and that the length of the transcript is positively associated with stronger establishment of repressive histone marks. Repressive histone modifications in Domain 2 are normally present on the paternal allele while the maternal allele is associated with active marks (Lewis et al., 2004). Ablation of polycomb group proteins or histone methyltransferases that catalyze the addition of repressive histone marks have been shown to activate a subset of imprinted genes in Domain 2 (Mager et al., 2003).

In humans, *KCNQ1OT1* has been less well studied although the regulation of genomic imprinting in Domain 2 is likely to be analogous to mice. Similar to deletion experiments in mice, a targeted deletion of the paternally derived human *KCNQ1OT1* CpG island in chicken DT40 cells led to suppression of *KCNQ10T1* and expression of the normally silent *KCNQ1* and *CDKN1C* genes (Horike et al., 2000). IC2 in humans has been shown to have silencer activity (Du et al., 2003) and in mice to bind CTCF (Fitzpatrick et al., 2007). *KCNQ1OT1* has been shown using RNA FISH to localize to both the *SLC22A18* and *CDKN1C* genes (Murakami et al., 2007) suggesting that the RNA itself may signal the recruitment of the chromatin silencing machinery. It is clear that multiple mechanisms are working to regulate genomic imprinting in Domain 2 and that these are dependent on developmental- and tissue-specific signals that have only been partially demonstrated in humans (Sakatani et al., 2001).

CDKN1C (*p57^{kip2}*) is a maternally expressed growth inhibitory gene that encodes a cyclin-dependent kinase inhibitor and negatively regulates cell proliferation (Matsuoka et al., 1995; Tsugu et al., 2000). *CDKN1C* is a candidate tumour suppressor because of its biochemical function. However, little is actually known about the role of *CDKN1C* in tumorigenesis and cancer progression. Downregulation of *CDKN1C* expression in mouse has been shown to induce prostate cancer that is pathologically indistinguishable from human prostate cancer (Jin et al., 2008a). Similarly, reduced expression of *CDKN1C* RNA was found in breast cancer reinforcing *CDKN1C's* candidacy as a tumour suppressor (Larson et al., 2008). Whether altered *CDKN1C* expression in cancer occurs as a result of the disruption of the long-range regulation by IC2 (such as loss of methylation or loss of heterozygosity) is an important area for future research as a study of *CDKN1C* expression downregulation in colorectal cancer found that alterations in DNA methylation at IC2 were seen in some but not all cases (Nakano et al., 2006).

CDKN1C is an important cell cycle protein that is implicated in the causation of BWS by several lines of evidence. In mouse a targeted deletion of *Cdkn1c* demonstrated increased cell proliferation and alterations in cell differentiation leading to abdominal muscle defects, cleft palate, renal medullary dysplasia, adrenal cortical hyperplasia and cytomegaly as seen in Beckwith-Wiedemann syndrome (Zhang et al., 1997). Finally, parent-of-origin maternal transmission of *CDKN1C* strongly supports a causal role for *CDKN1C* in BWS (Li et al., 2001).

PHLDA2 is imprinted and maternally expressed (Muller et al., 2000). It shows homology to mouse *Tdag51*, a gene involved in Fas-mediated apoptosis. PHLDA2 has been shown to be a

regulator of placental growth with placentomegaly after deletion of PHLDA2 and placental growth retardation after loss of imprinting (Salas et al., 2004). The *SLC22A18* gene, which is imprinted and maternally expressed, functions as an organic cation transporter. Mutations of this gene have been reported in breast cancer and a rhabdomyosarcoma cell line (Schwienbacher et al., 1998). In humans, there are no reports of constitutional mutations either in *PHLDA2* or *SLC22A18*.

BWS associated with alterations in the IC2 region: The most common epigenetic alteration seen in 50% of sporadic BWS is loss of methylation on the maternal allele at IC2 concomitant with loss of imprinting of *KCNQ1OT1* (Lee et al., 1999; Weksberg et al., 2001) (Figure 1-3). Further, biallelic expression of *KCNQ1OT1* is associated with reduction in *CDKN1C* expression in cells lines established from patients with BWS and loss of methylation at IC2 (Diaz-Meyer et al., 2003). Mutations in the *CDKN1C* gene are also associated with BWS (Hatada et al., 1996; Lam et al., 1999; Li et al., 2001). *CDKN1C* mutations occur in only 5-10% of sporadic BWS but in 30-40% of pedigrees with BWS (Hatada et al., 1996; Lam et al., 1999; Li et al., 2001).

BWS associated with alterations to the IC1 and IC2 region: Paternal uniparental disomy for chromosome 11 (usually segmental) occurs in approximately 20% of cases. Uniparental disomy (UPD) in BWS arises from a somatic recombination occurring in early embryogenesis. UPD almost always affects the both imprinted domains and therefore a gain of methylation at IC1 and a loss of methylation at IC2 is seen. The changes in the level of DNA methylation are proportional to the level of somatic mosaicism (Cooper et al., 2007).

Chromosomal alterations also occur in BWS. Duplications of chromosome 11 including the *IGF2* gene occur rarely (<1%) and are always of paternal origin. Apparently balanced reciprocal translocations and inversions also occur (<1%) and are always of maternal origin. These usually have breakpoints within the body of the *KCNQ1* gene (Weksberg et al., 2005).

1.5 Thesis Overview

The IC1 and IC2 imprinted domains are both implicated in the pathogenesis of BWS. A number of observations suggest that regulation of imprinting at chromosome 11p15.5 could be hierarchical (John et al., 2001) i.e., with multiple levels of regulation and not just direct effects of either IC1 or IC2. Additionally, BWS cases with loss of methylation at IC2 can also show loss of imprinting of the *IGF2* gene (Lee et al., 1999; Mitsuya et al., 1999). Thus, there are likely important regulatory signals transmitted over large distances (300 kb) from IC2 in Domain 2 to *IGF2* in Domain 1.

The following three data chapters comprise my work investigating questions involving imprint dysregulation in unique BWS clinical sample sets, with a focus on the IC2 imprinted domain. In Chapter 2, I investigate BWS patients with rhabdomyosarcomas to determine if the same molecular lesions and pathological subtypes exist as in sporadic rhabdomyosaroma. In Chapter 3, I examine the molecular lesions occurring in male and female monozygotic twins with BWS. Finally, in Chapter 4, I examine the role of balanced translocations and inversions associated with maternal transmission of BWS in families.

Chapter 2: Association of Alveolar Rhabdomyosarcoma with the Beckwith-Wiedemann Syndrome

Smith AC, Squire JA, Thorner P, Zielenska M, Shuman C, Grant R, Chitayat D, Nishikawa JL, Weksberg R. Association of alveolar rhabdomyosarcoma with the Beckwith-Wiedemann syndrome. Pediatr Dev Pathol. 2001 Nov-Dec;4(6):550-8. Society for Pediatric Pathologists, Allen Press Inc.

2.1 Summary

Rhabdomyosarcoma (RMS) is a soft tissue tumor of childhood frequently diagnosed between the first and fifth year of life. Children with the Beckwith-Wiedemann syndrome (BWS), a congenital overgrowth syndrome characterized by exomphalos, macroglossia, and macrosomia, have an increased risk of developing childhood tumors including Wilms tumor, hepatoblastoma, neuroblastoma, and RMS. Although an association between RMS and the BWS is well accepted, only four cases have been reported to date, and of these, three were reported as embryonal RMS. Based on these data, an association between BWS and embryonal RMS has been proposed. We report three additional cases of BWS with RMS and review the clinical data for each patient as well as the pathology of their tumors. All three cases of BWS had histology consistent with alveolar RMS and were diagnosed at 6 weeks and 5 and 13 years of age. In two of these BWS cases, constitutional defects of 11p15 imprinting were demonstrated. Furthermore, cytogenetic analysis of the tumors did not detect the t(2;13) or t(1;13) translocations that generate the PAX3- or PAX7-FKHR fusion proteins common to alveolar RMS. These observations suggest that the development of alveolar RMS tumors in BWS may occur without the chromosomal rearrangement producing the PAX-FKHR fusion protein. In summary, we present three new cases of RMS demonstrating anew association between BWS and an uncommon subtype of alveolar RMS. The absence of the translocations commonly associated with alveolar rhabdomyosarcoma suggests a common 11p15 pathway for alveolar RMS and BWS.

2.2 Introduction

2.2.1 Beckwith-Wiedemann syndrome

Beckwith-Wiedemann syndrome (BWS) is a congenital overgrowth syndrome classically involving the triad exomphalos, macroglossia, and macrosomia. Other clinical features include neonatal hypoglycemia, hemihyperplasia, visceromegaly, adrenocorticalcytomegaly, facial nevus flammeus, and ear anomalies (pits and/or creases). BWS is a genetically heterogeneous disorder. A variety of molecular lesions have been described in the 11p15region affecting gene expression for *IGF2, H19, CDKN1C,* and *KCNQ1* (Maher and Reik, 2000; Nicholls, 2000). Specifically, 20% of BWS cases exhibit paternal uniparental disomy (UPD) of chromosome 11p15, 50% have imprinting defects at *KCNQ1* (Engel et al., 2000; Lee et al., 1999; Smilinich et al., 1999), whereas <5% have mutation in *CDKN1C* (Li et al., 2001) or <7% have *H19* hypermethylation (Engel et al., 2000).

Children with BWS are also at increased risk to develop certain types of tumors. Whereas the total cumulative risk of childhood cancer is 0.2% (Robinson, 1997), the risk for the development of cancer in BWS has been reported to be approximately 7.5% (Wiedemann, 1983). Patients with UPD and/or *H19* hypermethylation have been reported to have tumors, but reports of patients with imprinting defects at *KCNQ1* have not been associated with tumors (Bliek et al., 2004) and only rarely with *CDKN1C* mutations (Li et al., 2001). Although embryonal rhabdomyosarcoma (RMS) (Zhan et al., 1994) is often cited as a common tumor associated with BWS, there are only four (3 embryonal, 1 alveolar) reported cases in the literature. Sotelo-Avila and Gooch (Sotelo-Avila and Gooch, 1976) reported a single case of an 11-month-old female with an alveolar RMS. The three other reports of RMS in individuals with BWS are reported to

be of the embryonal subtype. The first was a lower abdominal RMS identified in a 22-month-old male (Matsumoto et al., 1994), the second a RMS in the bladder of a 3-year-old female (Vaughan et al., 1995), and the third a 23-month-old male also with RMS of the bladder (Aideyan and Kao, 1998).

Etiologically, BWS and RMS have both been noted to have alterations at 11p15. At least three different embryonal tumors—embryonal RMS, hepatoblastoma and Wilms tumor—are all seen in association with BWS and have been shown to have loss of heterozygosity (LOH) in the distal region of chromosome 11p (Koufos et al., 1985; Scrable et al., 1989a; Scrable et al., 1989b). Molecular studies have found genetic changes in the 11p15 region in a variety of embryonal tumors such as Wilms tumor (Moulton et al., 1996; Reeve, 1996), hepatoblastoma (Rainier et al., 1995), and embryonal rhabdomyosarcoma (Anderson et al., 1999; Matsumoto et al., 1994). It has been proposed that aberrant imprinting of an unknown tumor suppressor gene in this region of chromosome 11 could also be a common epigenetic change in the embryonal tumors that commonly undergo LOH at 11p15 (Douc-Rasy et al., 1996; Newsham et al., 1995). Such an imprinting alteration(s) may represent a rare common pathway for RMS and BWS.

2.2.2 **Rhabdomyosarcoma**

Rhabdomyosarcoma (RMS) is a soft tissue sarcoma usually seen in children and young adults with an incidence of 1 in 200,000 (Diller, 1992; Maurer et al., 1991; Newton et al., 1995) and accounting for approximately 5%–10% of all pediatric cancers. RMS may occur at any time in the childhood years or even in adulthood; however, the peak incidence is in the 1 to 5-year age-group, with only 10% of cases occurring in the first year of life and 70% appearing in the first

decade. RMS is a small, round cell tumor of mesenchymal origin that can arise anywhere in the body. The tumor is derived from skeletal muscle histogenesis, and the diagnosis is based on the identification of rhabdomyoblastic differentiation in tumor cells. RMS is commonly classified into one of four histologic subtypes: embryonal, alveolar, anaplastic or undifferentiated sarcoma (Qualman et al., 1998). Embryonal RMS is the most frequent subtype, accounting for 50% of tumors, and alveolar RMS accounts for another 30%. Accurate recognition of RMS subtypes is vital because specific treatment protocols are recommended for the different subtypes.

Molecular cytogenetic analyses of RMS indicate that there is often a high degree of chromosomal rearrangement and genomic imbalance occurring in both major subtypes (Pandita et al., 1999). In 90% of alveolar RMS cases one of two characteristic translocations occur. The more common recurrent translocation t(2;13)(q35;q14) involves the forkhead *(FKHR)* gene on chromosome 13 and*PAX3* on chromosome 2, or alternatively, the variant translocation (1;13)(p36;q14) involves *PAX7* on chromosome 1 and *FKHR* again. In contrast to alveolar RMS, no primary molecular genetic aberration analogous to the *FKHR* rearrangements has been detected in embryonal RMS. A high frequency of LOH at 11p15 has been found in embryonal RMS, suggesting the involvement of an unidentified tumor suppressor gene mapping to this chromosomal region (Scrable et al., 1989a). Recently it has been shown that both the embryonal RMS and alveolar RMS subtypes are associated with LOH and loss of imprinting (LOI) of genes mapping to 11p15 (Anderson et al., 1999).

We present three new cases of RMS in association with BWS, all of which show alveolar-type histology. Since only one case of alveolar RMS with BWS has been previously reported; this

report is the first clear demonstration of an association between BWS and alveolar RMS. Furthermore, these cases are of interest not only for their unique clinical presentation but, also in two of our cases, for the significant absence of the *PAX3-FKHR* or*PAX7-FKHR* transcripts commonly associated with alveolar RMS. These data suggest a distinct 11p15associated oncogenic pathway for alveolar RMS lacking the common t(2;13) and t(1;13) translocations.

2.3 Methods

2.3.1 Patients

The cases presented were seen by clinical geneticists and oncologists at the Hospital for Sick Children in Toronto, Ontario, Canada. Research Ethics Board approval for this study was obtained from the Hospital for Sick Children.

2.3.2 Pathology

For light microscopy, tissue was fixed in 10% buffered formalin and embedded in paraffin. Sections were cut at 4 μm.

For immunohistochemistry, paraffin-embedded sections were stained for the following antigens using the Ventana Gen II™ auto-immuno/in situ stainer (Ventana Medical Systems, Tucson, AZ), employing Ventana's ABC/DAB detection system (Cat #250-001): low-molecular-weight keratin (monoclonal, 1/20 dilution; Becton-Dickinson, Mountain View, CA), neuron-specific enolase (polyclonal, 1/400 dilution; Dako, Glostrup, Denmark), S-100 protein (polyclonal, 1/800 dilution; Dako), vimentin (monoclonal, 1/200 dilution; Sigma Laboratories, St. Louis, MO), smooth muscle actin (monoclonal, 1/40 dilution; Dako), desmin (monoclonal, 1/80 dilution;

Dako), CD57 (monoclonal, 1/20 dilution; Becton-Dickinson), CD99 (monoclonal, 1/100 dilution; Signet Labs Inc., Dedham, MA), epithelial membrane antigen (monoclonal, 1/160 dilution; Dako), p53-DO7 (monoclonal, 1/30 dilution; Dako), NB84 (monoclonal, 1/50 dilution; Novocastra Laboratories Ltd., Newcastle upon Tyne, UK), CD45RB (monoclonal, 1/80 dilution; Dako), and myoglobin (polyclonal, 1/5 dilution; Immunon, Pittsburgh, PA).

Staining for WT1 (polyclonal, 1/100 dilution; Santa Cruz Biotechnology, Santa Cruz, CA), myogenin (polyclonal, 1/50 dilution; Santa Cruz Biotechnology), and MyoD-1 protein (monoclonal, 1/10 dilution; Novocastra Laboratories Ltd.) was performed manually using the Elite avidin-biotin detection system (Vector Laboratories, Burlingame, CA). Pretreatment of tissue sections using heat-induced epitope retrieval (HIER) was performed prior to immunostaining for MyoD-1, WT1, P53-DO7, and CD99, while proteolytic pretreatment was performed for low-molecular weight keratin, vimentin, epithelial membrane antigen, NB84, and desmin. Positive controls were run for each antibody.

For electron microscopy, tissue was fixed in a 4% paraformaldehyde–1% glutaraldehyde mixture, post-fixed in osmium teroxide, and embedded in an Epon-Araldite mixture. Sections were cut at 50nm, stained with uranyl acetate and lead citrate, and viewed on a Philips 400 electron microscope.

Reverse transcription–polymerase chain reaction (RT-PCR) for the detection of the *PAX3*- and *PAX7-FKHR* fusion transcripts was performed as previously described by Barr et al. (Barr et al., 1995).

2.3.3 **Analysis of Allele Specific *KCNQ1OT1* Expression**

Total RNA was isolated from lymphoblastoid cell lines using TRIZOL® reagent (GIBCO BRL, Burlington, Canada). Extraction of mRNA from total RNA was done using Quick Prep Micro mRNA Purification kit (Amersham Pharmacia Biotech, Little Chalfont, UK). M-MuLV reverse-transcriptase (MBI Fermentas, Burlington, Canada) was used for reverse transcription reactions. RT-PCR products were gel purified and sequenced to determine allele specific expression.

2.4 Results

2.4.1 **Patient 1**

This female infant was born to a 30-year-old G3P2 mother. Family history was non-contributory. Birth weight at 40 weeks gestation was 2700g (10th percentile). A diagnosis of BWS was made within the first year of life based on the presence of a large omphalocele, macroglossia, nevus flammeus, persistent neonatal hypoglycemia and hypocalcemia, and right leg hemihyperplasia. At 10 months, she was noted to have significant developmental delay and seizures, which were attributed to the persistent neonatal hypoglycemia.

At age 13 years, she was admitted to the hospital 2 months after sudden swelling of her right cheek. A needle biopsy was suggestive of lymphoma. This mass measured 7 - 8 cm over the right cheek and a similar mass over her right temporal region measured 5 cm. A mass was also identified in the right cardiophrenic angle in the chest; the pancreas appeared enlarged with at least two low-density masses (one within the head and one within the junction of the body and tail of the pancreas). There were also soft tissue masses in the hilum of the left kidney.

A treatment regimen including radiation and prednisolone was administered. She deteriorated rapidly despite intervention and died within 8 months of initial diagnosis. Consent was given for postmortem examination of the abdomen only.

2.4.2 **Tumor Pathology**

The retroperitoneal node biopsy contained tumor infiltrating into the surrounding fat. The tumor had a delicate fibrovascular stroma separating loose nests of tumor cells. The tumor cells were poorly cohesive and consisted predominantly of mononuclear cell forms with a high nuclear-to-cytoplasmic ratio. Nuclei ranged from round to oval and some convoluted forms. The cytoplasm consisted for the most part of a thin eosinophilic rim. Many of the cells had one or more large nucleoli. Occasional multinucleated giant cells were present. Although diagnosed as a possible lymphoma at the time, immunohistochemical studies performed for this review showed the tumor cells to be positive for actin, desmin, and myogenin (diffuse nuclear staining), and negative for the other antigens tested (see Methods), allowing a diagnosis of alveolar RMS to be made (Figure 2-1).

Because of the age of the samples, no analysis for the common PAX3-FKHR or PAX7-FKHR fusion proteins seen in alveolar RMS was performed, nor was tissue available for current testing. At autopsy, there was residual tumor in both ovaries and a retroperitoneal lymph node. The primary site of this malignancy was unclear. No malignancy was noted in the pancreas, but rather, areas of fibrosis, necrosis, and foamy macrophage consistent with previous tumor

Figure 2-1: Microscopic appearance of the tumor from patient 1 taken at autopsy.

Top: The tumor is arranged in loosely cohesive nests separated by delicate fibrovascular septa (left, hematoxylin and eosin X175; right, X350). Bottom: By immunohistochemistry, the tumor cells are positive for actin (left, X350) and desmin (right, X350).

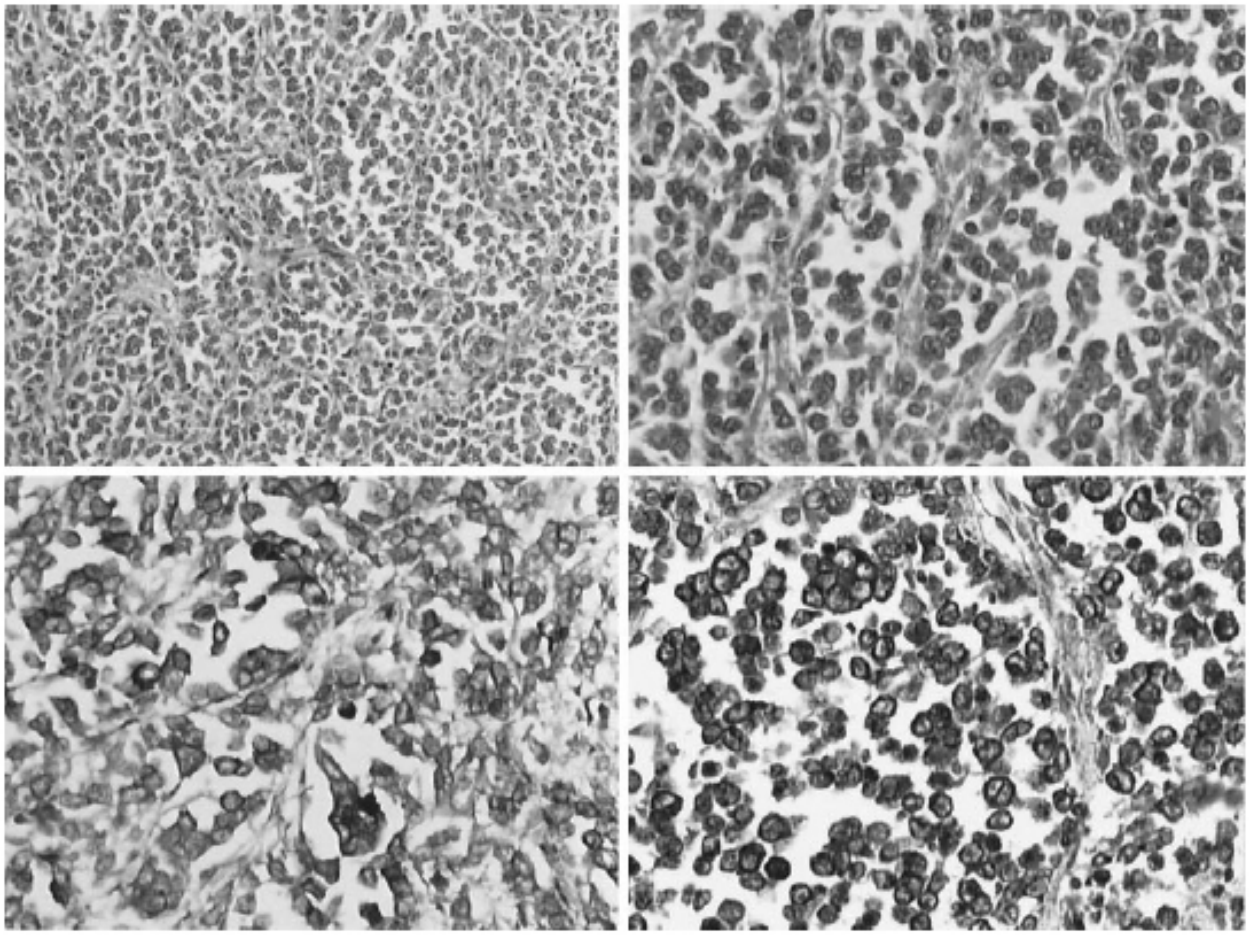

Figure 2-1. Microscopic appearance of the tumor from patient 1 taken at autopsy.

involvement. No cytomegaly was identified in the adrenal glands, nor was there pancreatic islet cell hyperplasia or nephroblastomatosis.

2.4.3 **Patient 2**

This male patient was born to a 26-year-old G2P1mother; family history was non-contributory. The pregnancy was uncomplicated and a rapid vaginal delivery occurred at 38 weeks gestation. Birth weight was 4496 g (>97th percentile). Diagnosis of BWS was made within the first month of life on the basis of the presence of macrosomia, macroglossia, a large umbilical hernia, ear creases and pits on the right ear, nevus flammeus over the forehead and nape of the neck, and inguinal hernias. There was no history of neonatal hypoglycemia and mental development has been normal.

At 5 years of age, he presented with constipation and lower abdominal pain. No diagnosis was made and the symptoms resolved after about 1 week. Approximately 1 month later the symptoms recurred and his mother noted a mass about his left buttock. A computed tomography (CT) scan demonstrated a pelvic mass, and he was admitted for a biopsy. A provisional diagnosis of RMS was made and following this he started chemotherapy with ifosphamide and VP16 (etoposide) plus VAC (vincristine-dactinomycin-cyclophosphamide). A course of abdominal radiation was administered, followed by surgical resection. This patient is now 16 years of age and disease-free.

2.4.4 **Tumor pathology**

Microscopically the sections showed a lymph node partly replaced by nests of tumor cells separated by fibrous bands. The tumor cells were characterized by high nuclear-to-cytoplasmic ratios, marked pleomorphism, a high mitotic rate, and individual cell necrosis. The tumor cells showed no evidence of differentiation at the light microscopic level, but by immunohistochemistry, the tumor cells were positive for desmin, as well as for myogenin with diffuse nuclear staining. Electron microscopic analysis showed primitive cells with perinuclear aggregates of cytoplasmic intermediate filaments. Thin and thick filaments and Z-band material were not seen. A diagnosis of alveolar RMS was made on the basis of these results. We were unable to demonstrate the presence of the PAX3-FKHR or PAX7-FKHR fusion proteins by RT-PCR commonly seen in alveolar RMS.

Molecular analysis of lymphoblasts from this patient showed no uniparental disomy or exonic mutations of *CDKN1C*. However, analysis of imprinting status at *KCNQ1* demonstrated biallelic expression of *KCNQ1OT1* in this patient (Figure 2-2). *KCNQ1OT1* is an expressed antisense transcript located within the *KCNQ1* gene (Lee et al., 1999; Smilinich et al., 1999). Molecular analysis also demonstrated normal methylation of *H19*. Fibroblasts from this patient, required to perform *IGF2* expression studies, were not available.

2.4.5 **Patient 3**

This female patient was born to a 35-year-old G2P1 mother. Family history was non-contributory. Pregnancy was complicated by gastroenteritis at 8 weeks gestation. The first fetal

Figure 2-2: Loss of imprinting of *KCNQ1OT1*.

Location of SNP1, indicated by arrows. SNP1 is contained within EST AA331124 (Smilinich et al., 1999) and within a transcribed region of *KCNQ1OT1*. Reverse transcription-polymerase chain reaction (RT-PCR) reactions were carried out on RNA isolated from a control patient and patient 2. Control and patient 2 are heterozygous for SNP1, 5'-AGCTCTGACC(G/A)TCAGACCCCC -3' (genomic DNA). The control sample showed monoallelic expression of *KCNQ1OT1* at SNP1, whereas the sample from patient 2 showed biallelic expression. RT-PCR was always performed in parallel, in the presence and absence of reverse transcriptase, and only those reactions with no products in the -RT lane were sequenced (cDNA). Sequencing reactions were carried out using the reverse primer.

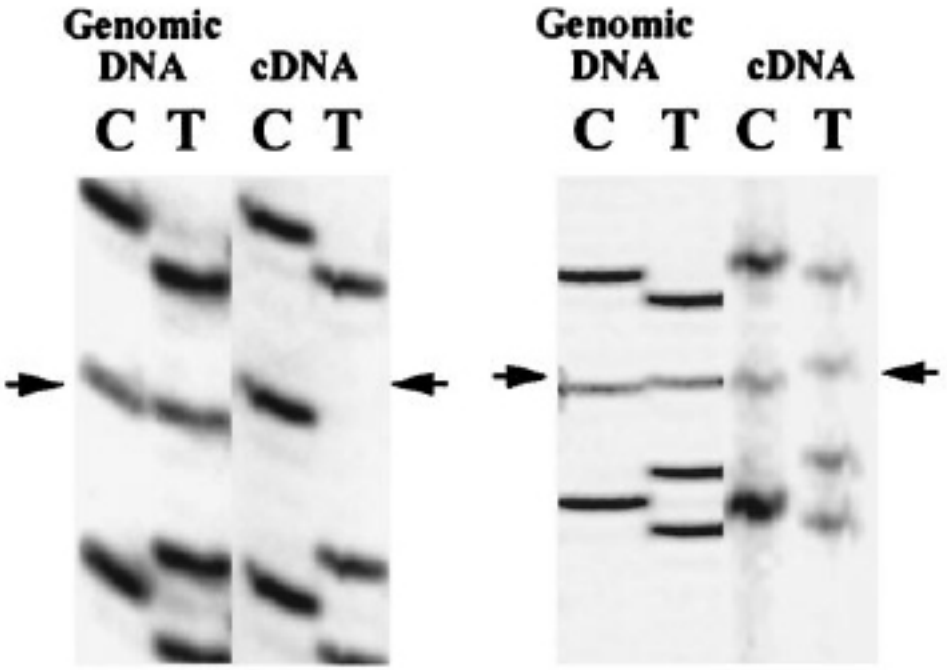

Figure 2-2. Loss of imprinting of KCNQ1OT1

ultrasound appeared normal, however, fetal ultrasounds done at 15 and 18 weeks showed a small omphalocele and Dandy-Walker variant (partial absence of the lower cerebellar vermis).

The infant was born at 37 weeks gestation by spontaneous vaginal delivery. Birth weight was 3100 g (50th percentile) with Apgar scores of 6 and 9 at 1 and 5 minute, respectively. Omphalocele was repaired at 4 days post-delivery. Diagnosis of BWS was made within the first month of life based on the presence of omphalocele, macroglossia, hypoglycemia, nephromegaly, and medullary renal cysts.

At approximately 6 weeks post-delivery the patient presented with multiple small nodules on the left arm and right chest wall and a large nodule on the right thigh. A CT scan confirmed that no additional lesions of the internal organs were detectable. The large mass in the right thigh measured 2.5 x 4.7 cm. Tissue biopsy of the chest wall mass was performed and, based on a provisional diagnosis of alveolar RMS, the patient started on chemotherapy consisting of VP-16, ifosphamide, and VAC.

2.4.6 **Tumor pathology**

The biopsy from the chest wall showed a tumor composed of primitive undifferentiated cells that formed cohesive solid clusters with intervening fibrous stroma. The nuclei were round to elliptical in shape and hyperchromatic. Most cells had a scant amount of cytoplasm, with occasional cells showing some eccentric eosinophilic cytoplasm suggesting rhabdomyoblastic differentiation. By immunohistochemistry, the tumor cells were positive for vimentin, desmin, myoD1, and myogenin with a diffuse nuclear staining pattern. Based on these results, a diagnosis

of solid variant of alveolar RMS was made (Figure 2-3, 2-4). RT-PCR analysis was unable to detect the presence of the PAX3-FKHR or PAX7-FKHR fusion proteins commonly seen in alveolar RMS. We were also unable to detect the presence of WT1 RNA, t(11;22) for both Ewing/PNET and desmoplastic small round cell tumor.

Lymphocytes from the patient were tested for constitutional molecular alterations of 11p15 associated with BWS. No uniparental disomy of 11p15, *H19* hypermethylation, or exonic mutations of the *CDKN1C* (*p57KIP2*) gene were detected. However, imprinting analysis at *KCNQ1* demonstrated biallelic expression of *KCNQ1OT1* in lymphoblasts from this patient. Fibroblasts from this patient, required to perform *IGF2* expression studies, were not available.

2.5 Discussion

The three new cases of RMS with the Beckwith-Wiedemann syndrome reported here are of interest because they are all of the alveolar subtype with an unusually broad age range at presentation (6 weeks to 13 years). The alveolar RMS subtype has only been reported once previously in a patient with BWS (Sotelo-Avila and Gooch, 1976). Thus, this paper contributes to the current literature by expanding the subtypes and age at presentation of RMS in patients with BWS. Furthermore, the absence of the *PAX-FKHR* rearrangement in patients 2 and 3 is also unusual and it suggests a distinct 11p15 associated oncogenic pathway for alveolar RMS and BWS.

Figure 2-3: Example of one of the multiple tumor nodules (arrow) visible on the skin of patient 3.

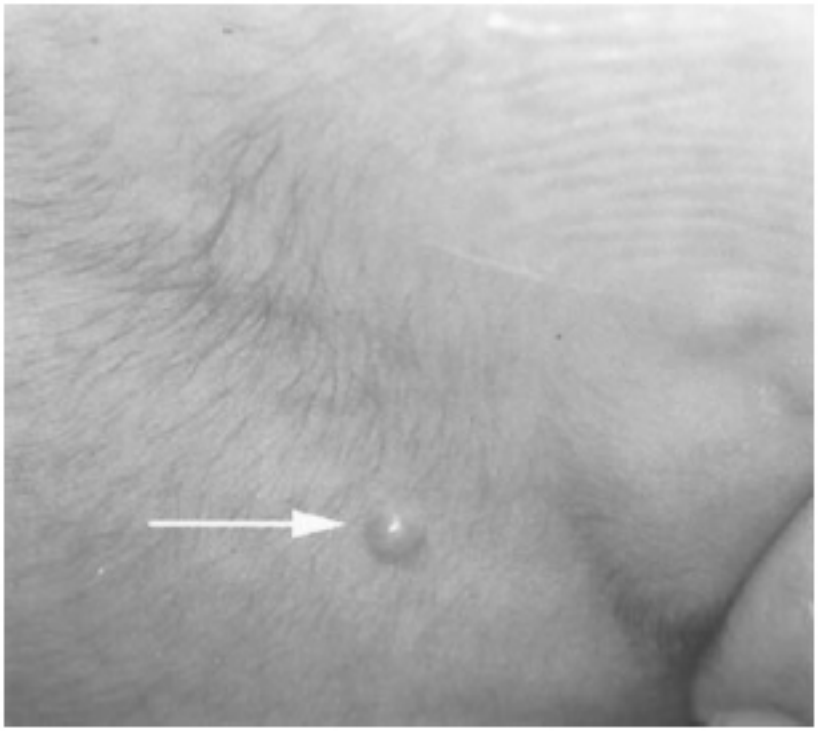

Figure 2-3. Example of one of the multiple tumor nodules (arrow) visible on the skin of patient 3.

Figure 2-4: Microscopic appearance of the chest wall tumor from patient 3.

Top: The tumor is arranged in solid nests separated by thick fibrous septa (left, hematoxylin and eosin, X175; right, X350). Bottom: By immunohistochemistry, the tumor cells are positive for desmin (left, X350) and myogenin (right, X350).

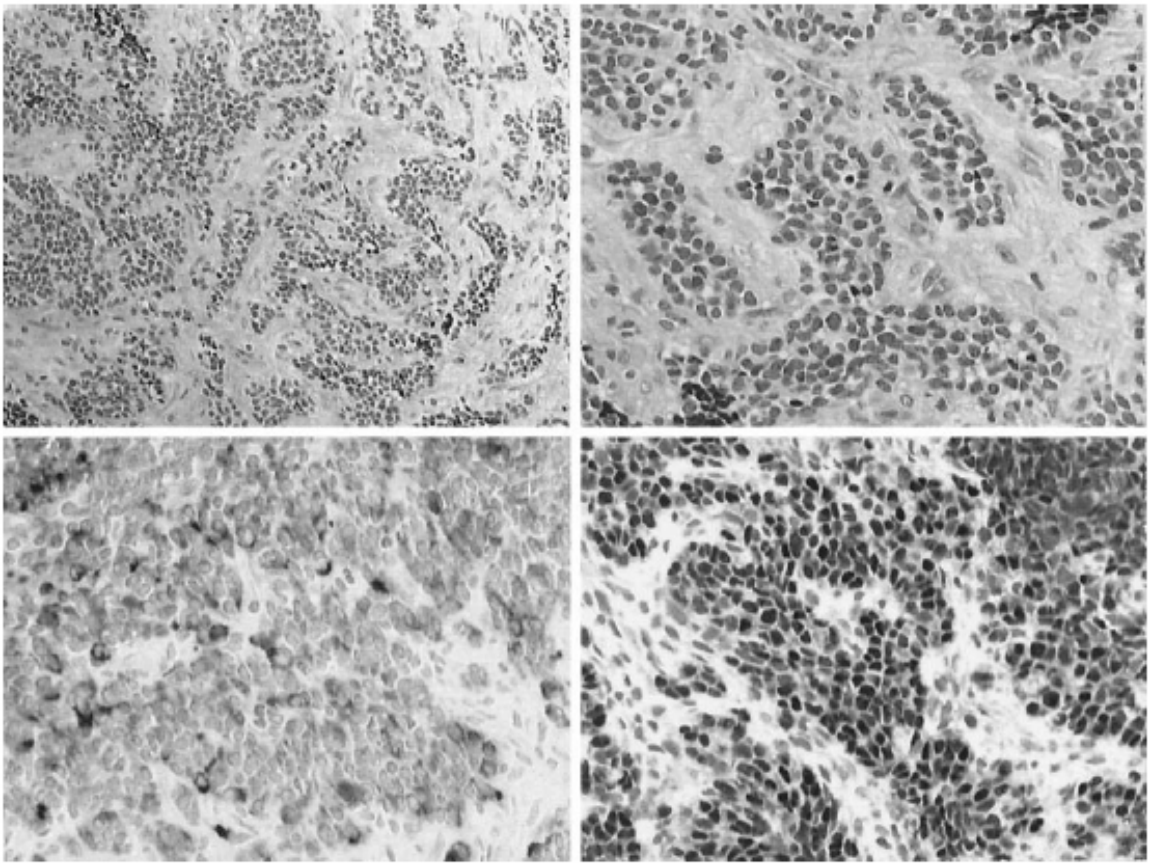

Figure 2-4. Microscopic appearance of the chest wall tumor from patient 3.

The earlier reports of BWS and RMS in the literature were all published before the solid variant form of alveolar RMS was recognized; previously, such solid variants were usually classified as embryonal tumors by default since they lacked classic alveolar histology even when the *PAX-FKHR* rearrangement was detected. Unfortunately, a review of the histology of these previously published BWS cases with embryonal RMS was not possible, as the histology of these cases was not illustrated in the reports.

BWS has been found to segregate with genetic markers on 11p15 (Koufos et al., 1989; Ping et al., 1989) and the elucidation of multiple chromosomal and molecular alterations found in BWS has directed study on the pathomechanism to this region (Maher and Reik, 2000; Mannens et al., 1994; Nicholls, 2000; Weksberg et al., 1993a; Weksberg et al., 1993b). It has been proposed that monoallelic expression of *IGF2* and *H19* is maintained by a putative imprinting center located 2 kb upstream of the *H19* transcription start site (Hark et al., 2000). Hypermethylation in the *H19* upstream region can be associated with biallelic expression of *IGF2*. However, aberrant expression of *IGF2* has been demonstrated in approximately 50% of sporadic BWS (Li et al., 1997; Weksberg et al., 1993a) usually independent of *H19* expression or methylation changes (Engel et al., 2000; Li et al., 2001). This particular finding is important because dysregulation of *IGF2* expression has also been implicated in the pathogenesis of both embryonal and alveolar RMS (Anderson et al., 1999; Scrable et al., 1987; Zhan et al., 1994). Pedone et al. (Pedone et al., 1994) demonstrated that 82% of the RMS tumors studied, regardless of histologic subtype, had two active copies of *IGF2* either by relaxation of imprinting or

duplication of this region. This indicates that a loss of imprint of *IGF2* is an important step in the development or progression of alveolar RMS tumorigenesis.

The elucidation of potential pathways involved in alveolar RMS and the possible role of the 11p15 region in such pathways were recently demonstrated by cDNA microarray analysis of downstream targets of the fusion proteins generated by the common translocations (Khan et al., 1999). At first, a link between alveolar RMS and the 11p15 region is not immediately evident because the common chromosomal rearrangement in alveolar RMS is either a t(2,13)(q35–37; q14) or t(1,13)(p36; q14). These translocations involve the *PAX3* and *PAX7* genes on chromosomes 2 and 1, respectively, and the generation of a chimeric fusion protein with forkhead in RMS (FKHR) on chromosome 13 (Barr, 1999). *PAX3* and *PAX3-FKHR* were introduced into NIH 3T3 cells, and the resultant gene expression changes were analyzed with a murine cDNA microarray. Khan et al. (Khan et al., 1999) found that *PAX3-FKHR* but not *PAX3* was able to activate a number of genes, including *IGF2*. Up-regulation of the expression of *IGF2* seen in these experiments suggest that *IGF2* is a candidate downstream target of *PAX3-FKHR*. Since IGF2 is a strong autocrine growth factor implicated in RMS tumorigenesis, its involvement is likely an important component in initiation or progression of this small cell tumor.

Interestingly, in our study, the two cases of alveolar RMS with material available did not have the common t(2;13) or t(1;13) translocation. This indicates that the development of alveolar RMS in BWS may result from an uncommon or alternate molecular pathway.

For two patients (patients 2 and 3), tissues available for constitutional molecular analysis also showed biallelic expression of *KCNQ1OT1* (the paternally expressed antisense transcript located within the *KCNQ1* gene on 11p15). Biallelic expression of this transcript in >50% of BWS cases has been reported in the literature (Engel et al., 2000; Lee et al., 1999; Smilinich et al., 1999) but has not yet been associated with tumor development (Bliek et al., 2001). The possibility that the lack of the common t(2;13) or t(1;13) translocation in two patients' tumors combined with the biallelic expression of *KCNQ1OT1* indicates that this antisense transcript may be involved in an alternate pathway for tumor development on 11p15. Some individuals with BWS and *KCNQ1OT1* imprinting defects also show LOI at *IGF2*. It is conceivable that dysregulation of the genomic imprinted regions encompassing *IGF2* and/or *KCNQ1OT1* may abrogate the need to have *PAX-FKHR* activation as a primary oncogenic event in alveolar RMS. Unfortunately, tissue for studying the constitutional expression of *IGF2* was not available for analysis from our patients.

Future studies of RMS in BWS may elucidate the critical 11p15 alterations common to BWS and alveolar RMS. The involvement of multiple genes in the 11p15 imprinted region may promote tumorigenesis, as it has been suggested that the 11p15 region of genes modulate cell growth (Schwienbacher et al., 1998).

The development of this highly malignant small cell tumor by the three patients described here suggests that alveolar RMS should be included in the spectrum of tumors that individuals with BWS can develop. The dysregulation of the 11p15 region has been

shown to be an integral part of the genetic aberrations associated with BWS and has also been implicated in a number of tumors, including both major subtypes of RMS. The three BWS patients reported here have unusual presentations of alveolar RMS, and in two cases do not demonstrate the common translocations associated with this tumor subtype. Future studies of alveolar RMS in BWS cases should provide a clearer understanding of translocation-independent routes for development of this type of alveolar RMS and the nature of the constitutional molecular changes in BWS that predisposes to the development of this tumor.

Acknowledgements

This research was supported by the National Cancer Institute of Canada with funds from the Canadian Cancer Society. Special thanks go to Agnes Chan for critical review of the manuscript.

Chapter 3: New Chromosome 11p15 Epigenotypes Identified in Male Monozygotic Twins with Beckwith-Wiedemann Syndrome

The published version of this article appeared in:

Smith, A.C, Rubin T, Shuman C et al: Cytogenet Genome Res 2006;113:313-317

The chapter that follows is a pre-print version.

3.1 Summary

Beckwith-Wiedemann syndrome (BWS) is an overgrowth syndrome demonstrating heterogeneous molecular alteration of two imprinted domains on chromosome 11p15. The most common molecular alterations include loss of methylation at the proximal imprinting center, IC2, paternal uniparental disomy (UPD) of chromosome 11p15 and hypermethylation at the distal imprinting center, IC1. An increased incidence of female monozygotic twins discordant for BWS has been reported. The molecular basis for eleven such female twin pairs has been demonstrated to be a loss of methylation at IC2, whereas only one male monozygotic twin pair has been reported with this molecular defect. We report here two new pairs of male monozygotic twins. One pair is discordant for BWS; the affected twin exhibits paternal UPD for chromosome 11p15 whereas the unaffected twin does not. The second male twin pair is concordant for BWS and both twins of the pair demonstrate hypermethylation at IC1. Thus, this report expands the known molecular etiologies for BWS twins. Interestingly, these findings demonstrate a new epigenotype-phenotype correlation in BWS twins. That is, while female monozygotic twins with BWS are likely to show loss of imprinting at IC2, male monozygotic twins with BWS reflect the molecular heterogeneity seen in BWS singletons. These data underscore the need for molecular testing in BWS twins, especially in view of the known differences among 11p15 epigenotypes with respect to tumor risk.

3.2 Introduction

Beckwith-Wiedemann syndrome (BWS) is an overgrowth syndrome characterized by pre- and postnatal overgrowth, visceromegaly, macroglossia, abdominal wall defects, ear abnormalities, hemihyperplasia, neonatal hypoglycemia (Cohen, 2005; Elliott et al., 1994; Pettenati et al., 1986; Weng et al., 1995a), and an increased risk for childhood tumours (DeBaun and Tucker, 1998; Rump et al., 2005; Weksberg et al., 2001; Wiedemann, 1983).

The molecular etiology of BWS is heterogeneous; however, to date, all known causes involve a cluster of genes on chromosome 11p15 (Bliek et al., 2001; Cooper et al., 2005; DeBaun et al., 2002; Gaston et al., 2001; Weksberg et al., 2001) (Table 3-1). While most cases of BWS are sporadic, dominant inheritance with preferential maternal transmission is seen in 10–15% of cases (Aleck and Hadro, 1989; Best and Hoekstra, 1981; Pettenati et al., 1986). In 1–2% of cases there are chromosome abnormalities such as maternally derived trans-locations and inversions of chromosome 11p15 or paternally derived trisomy of chromosome 11p15 (Sait et al., 1994; Slavotinek et al., 1997). Paternal uniparental disomy (UPD) of chromosome 11p15 occurs in 15–25% of BWS cases (Bliek et al., 2001; Cooper et al., 2005; DeBaun et al., 2002; Gaston et al., 2001; Weksberg et al., 2001). UPD in BWS arises almost invariably as a post-zygotic mitotic recombination error that results in exclusively paternal origin of genes for variable-length segments of chromosome 11p occasionally extending into 11q. This mechanism leads to mosaicism for UPD of 11p15.

Table 3-1: Spectrum and Frequency of Molecular Etiologies in BWS:

Genetic/Epigenetic Alteration	Frequency in BWS Cases (%)	Male MZ Twin Pairs	Female MZ Twin Pairs
11p15 translocations/duplications	1-2		
UPD for 11p15	15-25	1	
Gain of Methylation at IC1	5-10	1*	
CDKN1C mutation	5-8		
Loss of methylation at IC2/ biallelic expression of KCNQ1OT1	50	1	11
Unknown	~10		

*MZ twin pair is concordant for BWS whereas all other MZ twin pairs reported in the table are discordant for BWS. Data compiled from Weksberg et al., (2002) and Gaston et al., (2001).

Molecular changes observed in patients with BWS include both genetic and epigenetic alterations on chromosome 11p15 (Bliek et al., 2001; Cooper et al., 2005; DeBaun et al., 2002; Weksberg et al., 2001; Weksberg et al., 2005) (Table 1). Coding mutations in the *CDKN1C* gene, a maternally expressed cyclin-dependent kinase inhibitor, have been found in 5% of sporadic BWS cases, and approximately 30–50% of dominantly transmitted cases of BWS (Li et al., 2001; Weksberg et al., 2001). Epigenetic alterations can be identied in either one of the two imprinting control regions (IC1 & IC2) by changes in methylation or histone modifications. IC1 is associated with *H19* and *IGF2* (insulin-like growth factor 2) and IC2 is associated with *KCNQ1OT1* and the downstream target gene *CDKN1C*. Loss of methylation at the maternal IC2 allele is common in BWS (50% of cases) and results in de-repression of the maternal *KCNQ1OT1* transcript (Diaz-Meyer et al., 2003). Gain of methylation at the maternal IC1 allele is rare in BWS (5–10% of cases) and results in repression of the maternal *H19* transcript and de-repression of the paternal *IGF2* transcript (Weksberg et al., 1993a).

Many monozygotic twin pairs with BWS have been reported in the literature (Bose et al., 1985; Brown, 1986; Chien et al., 1990; Clayton-Smith et al., 1992; Franceschini et al., 1993; Leonard et al., 1996; Litz et al., 1988; Schier et al., 2000; Weksberg et al., 2002). Monozygotic twins result from a single fertilization and are often said to be genetically identical, although it has been repeatedly reported that there are differences between monozygotic twins in terms of discordance for disease or chromosomal abnormalities (Machin, 1996). This discordance in monozygotic twins could arise from a myriad of

post-zygotic mitotic errors. In fact, it has also been proposed that a genetic event prior to twinning may give rise to two separate clonal populations of cells. This, in turn, creates mutual repulsion triggering the twinning process itself (Machin, 1996).

Studies in monozygotic twins are challenging because attribution of molecular defects to a specific twin requires tissue(s) other than blood. Previous twin studies have shown that even discordant monozygotic twins can display the same molecular or chromosomal defect in blood because of sharing of the fetal blood supply *in utero* (Hall and Lopez-Rangel, 1996; Marcus-Soekarman et al., 2004; Weksberg et al., 2002). However, when other tissues are available for testing, e.g. fibroblasts, the alteration can be restricted to the affected twin. This is important to consider when assessing the validity of data for monozygotic twin pairs.

There are very few reports of BWS and monozygotic twins which identify the molecular basis for the BWS phenotype. Our previous study of BWS twins demonstrated a clear excess of female monozygotic twins discordant for BWS (Weksberg et al., 2002). This study showed discordance for loss of methylation at IC2 for 10 twin pairs (9 female and 1 male) (Weksberg et al., 2002). Gaston et al. reported two sets of female monozygotic twins discordant for BWS with the same molecular defect (Gaston et al., 2001). These studies demonstrated that there was a strong correlation between IC2 methylation changes in BWS and female monozygotic twinning. Notably, there are few reports available regarding the molecular etiology of BWS in male monozygotic twins.

We report here two cases of male monozygotic twin pairs, one pair concordant for BWS and the other discordant with altered 11p15 epigenotypes not previously reported for BWS monozygotic twins. Molecular studies reveal paternal UPD of 11p15 in the affected proband of the discordant pair and hypermethylation of IC1 in both twins of the concordant pair.

3.3 Methods

3.3.1 Subjects

This study was approved by the Research Ethics Board of the Hospital for Sick Children. Clinical information was provided by the referring geneticist and/or genetic counselor for each twin pair.

3.3.2 Patient material

Blood samples were obtained from each twin for molecular analysis. Blood samples were also obtained from parents whenever possible.

3.3.3 Tissue culture

Lymphoblastoid cell lines were established by Epstein Barr virus transformation of blood from patients diagnosed with BWS. Lines were maintained in RPMI 1640 medium with 15% fetal calf serum and 1% antibiotics at 37°C and 5% CO2.

3.3.4 DNA extraction

DNA was extracted from lymphoblastoid cells by the standard phenol-chloroform extraction protocol. Briefly, 20 ml of a lymphoblastoid cell culture or whole blood was

centrifuged at 250 g to isolate cells. Nuclei were then lysed, resuspended in physiological saline and digested by proteinase K. Samples were then mixed with phenol and then phenol/chloroform, spun in Phase Lock Gel tubes (Eppendorf) and the aqueous phase decanted. DNA was then spooled and rehydrated in TE.

3.3.5 **UPD analysis**

Quantitative multiplex-PCR using highly polymorphic STR markers was performed using DNA markers within the BWS critical region at chromosome 11p15.5 (D11S1984, D11S922, TH), several DNA markers along 11p (D11S2362, D11S1997, D11S1996 & D11S1993) as well as two DNA markers mapping to the q arm of chromosome 11 (D11S1998 & D11S1974) in order to detect paternal UPD of this region. Amplification products were separated on a 6% denaturing polyacrylamide gel on an ABI 377 PRISM DNA Sequencer (PE Biosystems). The allele sizes and corresponding peak areas were determined using Genescan software. The percentage of paternal UPD of informative alleles at chromosome 11p15.5 in the proband was determined based on the following calculation:

% UPD = (Peak area of paternal allele – peak area of maternal allele) / area of paternal and maternal alleles.

In order to designate a proband as exhibiting mosaic paternal UPD of 11p15, a minimum of two markers within the BWS critical region had to demonstrate an increase in dosage of greater than 20% for the paternal allele.

3.3.6 **Methylation analyses**

5ug of genomic DNA was digested with either Eco*RI* and Not*I* or Pst*I* and Mlu*I* or Pst*I* and Sma*I* for IC2, IC1 and the *H19* promoter, respectively. Digested DNA was electrophoresed on a 0.8% agarose gel and transferred overnight to a positively charged nylon membrane (Hybond N+, Amersham Biosciences) in 0.4 N NaOH. Membranes were neutralised and prehybridised in modified Church's buffer with salmon sperm DNA as a blocking agent. ^{32}P-dCTP random labeled probe was added overnight at 65°C and washed with serial washes of SSPE (2x, 1x, 0.5x, all containing 0.5% SDS). Membranes were then exposed to Phosphor screen for at least 24 h and imaged by Storm Phosphorimager (Molecular Dynamics). Methylation index was calculated by dividing the optical density of the band uncut by the methylation sensitive enzyme by the sum of the optical densities of both bands.

3.4 **Results**

3.4.1 **Clinical synopsis**

Discordant twin pair MZA1 and MZA2.

MZA1 is a male monozygotic twin with the following findings: macroglossia, auricular pits (father also has auricular pits), cardiomegaly, nephromegaly, Wilms' tumor and mild developmental delay. No clinical features indicative of BWS were found in twin MZA2. Monozygosity was established (probability >99.9%) by analysis of polymorphic microsatellite markers (data not shown).

Concordant twin pair MZB1 and MZB2.

Diagnosis for both MZB twins was made on the basis of macroglossia causing occlusion of the airway, hepatomegaly, splenomegaly, weight above the 90th percentile, prominent eyes, relative microcephaly, diastasis recti, severe apnea and polycythemia. MZB1 had an umbilical hernia. MZB2 had a capillary nevus flammeus. Both MZB twins had a normal karyotype and shared a normal variant duplication of chromosome 15q11.2-q13 with their mother. The father's karyotype was normal. Monozygosity was established (probability >99.9%) by analysis of polymorphic microsatellite markers (data not shown).

3.4.2 **Uniparental disomy testing for chromosome 11p15**

Paternal uniparental disomy of chromosome 11p15 was detected in lymphoblasts from patient MZA1. It was not detected in lymphoblasts from patient MZA2. Testing of lymphoblasts from both MZB1 and MZB2 did not reveal UPD of 11p15 (Figure 3-1).

3.4.3 **Methylation analysis**

Further molecular analyses of lymphoblastoid cells from MZB1 and MZB2 included methylation analyses for IC1 and IC2. Methylation at IC2 was normal. However, methylation at both the *H19* promoter and the IC1 was shown to be hypermethylated (Figure 3-2).

Figure 3-1: UPD analysis for STR microsatellite markers on human chromosome 11.

Idiogram of chromosome 11 is shown (left) indicating the approximate location of microsatellite markers tested. Idiogram drawn with Colored Chromosomes package (Böhringer et al., 2002). Results for MZA and MZB monozygotic twins shown. Twin MZA1 shows paternal uniparental disomy for chromosome 11 whereas twin MZA2 does not. The MZB twins do not show UPD for any of the tested markers. Since UPD in BWS demonstrates somatic mosaicism, signals over 20% are considered isodisomic for the microsatellite region tested.

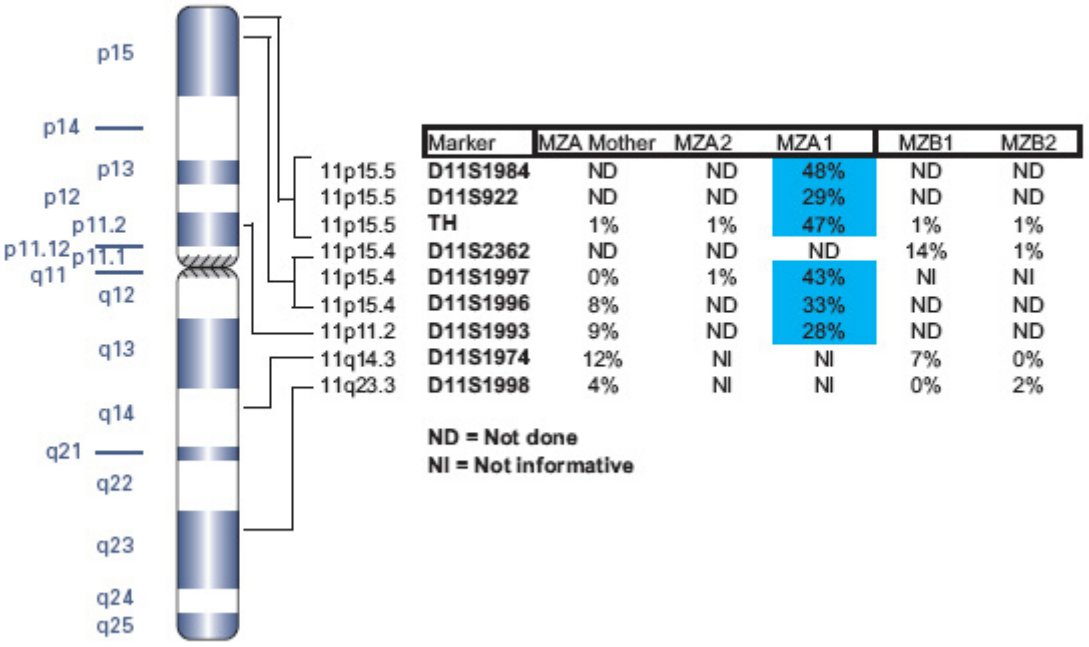

Marker	MZA Mother	MZA2	MZA1	MZB1	MZB2
D11S1984	ND	ND	48%	ND	ND
D11S922	ND	ND	29%	ND	ND
TH	1%	1%	47%	1%	1%
D11S2362	ND	ND	ND	14%	1%
D11S1997	0%	1%	43%	NI	NI
D11S1996	8%	ND	33%	ND	ND
D11S1993	9%	ND	28%	ND	ND
D11S1974	12%	NI	NI	7%	0%
D11S1998	4%	NI	NI	0%	2%

ND = Not done
NI = Not informative

Figure 3-1. UPD analysis for STR microsatellite markers on human chromosome 11.

Figure 3-2: Methylation analysis of MZB twins.

(Top) Schematic of relevant imprinted genes on human chromosome 11p15. Expressed allele is shown by an arrow. Maternally expressed genes are shown in red and paternally expressed genes in green. Imprinting centers are indicated by squares and labeled IC1 or IC2. A closed square represents methylation whereas an open square is unmethylated. Methylation-restriction enzyme digestion and Southern blotting were performed for IC2, IC1 and the H19 promoter. IC2 digestion was done with Pst I and Not I producing a 4.2-kb maternal band and a 2.7-kb paternal band in control samples (representative control shown). MZB1 and MZB2 showed normal methylation patterns for IC2. Digestion of DNA from MZB twins with Pst I and Mlu I and followed by probing for the IC1 region generates a 2.4-kb (paternal) and 1.2-kb (maternal) band. Both MZB twins showed hypermethylation at IC1. Digestion of the MZB DNA with Pst I and Sma I generates 1.8-kb and 1.0 kb bands. The MZB twins also showed hypermethylation at the H19 promoter.

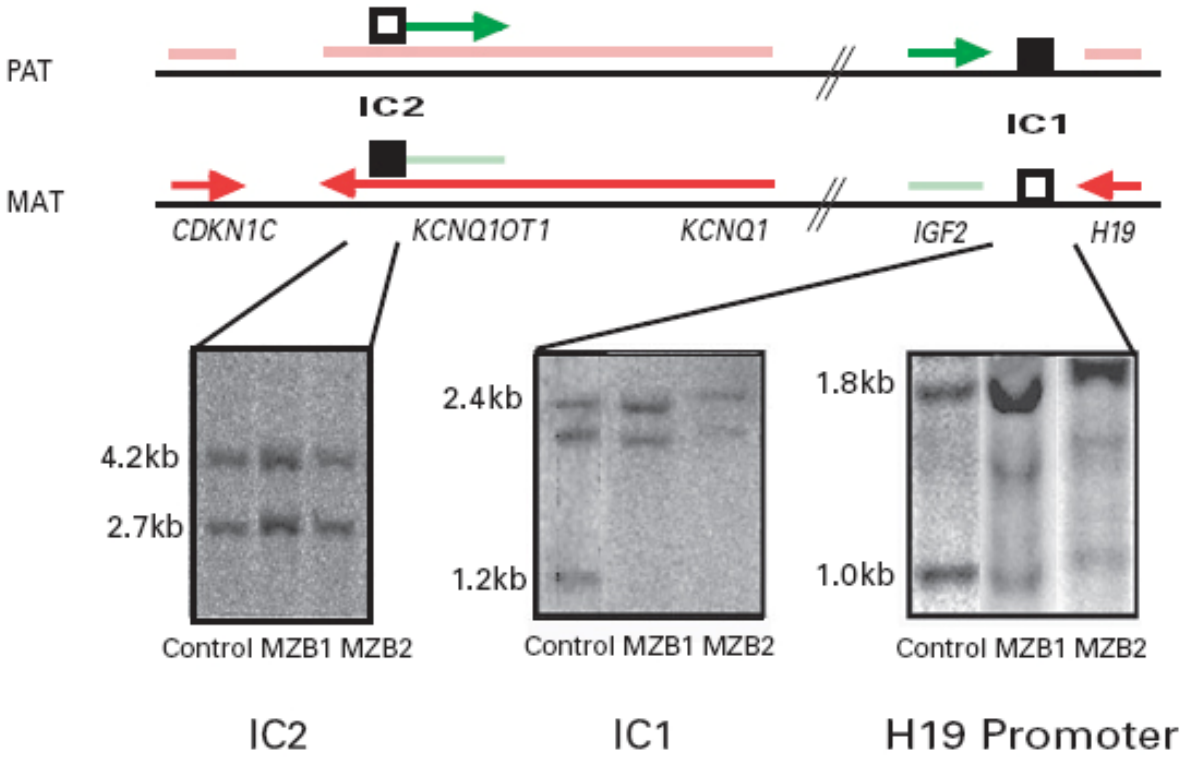

Figure 3-2. Methylation analysis of MZB twins

3.5 Discussion

We report two new male monozygotic twin pairs with BWS, one discordant and the other concordant for the condition. For the discordant monozygotic twin pair, there was evidence of UPD for chromosome 11p15 in the affected twin. For the concordant monozygotic twin pair, hypermethylation at IC1 was demonstrated in both twins. These twin pairs are, to our knowledge, only the second and third monozygotic male twin pairs with BWS for whom molecular findings have been reported. This report broadens the spectrum of molecular heterogeneity associated with BWS in male monozygotic twin pairs, as the only molecular defect previously reported in a male BWS twin pair was hypomethylation at IC2 (Weksberg et al., 2002). Further, these data demonstrate that the molecular heterogeneity seen in BWS singletons occurs in male but not female monozygotic twins with BWS.

All analyses on the patients presented in this report were undertaken on blood products (lymphocytes, lymphoblastoid cell lines) and fibroblasts/other tissues were unavailable for testing. The MZB twins were concordant for BWS as well as the molecular defect, whereas the molecular data for the MZA twins reflected the discordant phenotypes in that UPD of 11p15 was found only in the twin affected with BWS. Given that the molecular findings reflect the clinical phenotypes of these twin pairs, it is likely that these are the true epigenotypes for each twin. However, the conclusions presented in this study are based only on the molecular data within each twin pair and not between the twins for

each pair because the molecular studies were carried out on lymphocytes or their derivatives.

A number of different epigenotype-phenotype correlations have been described for BWS (Bliek et al., 2001; Cooper et al., 2005; DeBaun et al., 2002; Engel et al., 2000; Gaston et al., 2001; Li et al., 2001; Weksberg et al., 2001). UPD for chromosome 11p15 is strongly associated with hemihyperplasia as well as a high risk for tumor development. Patients with methylation defects at IC1 also have a higher cancer risk than BWS patients with either *CDKN1C* mutations or loss of methylation at IC2. Abdominal wall defects, such as exomphalos, are highly correlated with *CDKN1C* mutations or IC2 loss of methylation although umbilical hernias tend to be more common in patients with IC1 methylation or UPD for 11p15. Ear pits and creases are most prevalent in patients with *CDKN1C* mutations and methylation defects at IC2. Finally, cleft palate has been reported only in BWS cases with *CDKN1C* mutations.

The data we present in this paper extend previous molecular information available for monozygotic twins with BWS. Previous reports for twelve monozygotic twin pairs (11 female, 1 male) discordant for BWS found that every pair had a methylation defect at IC2 (Gaston et al., 2001; Weksberg et al., 2002). In our previous work we postulated that lack of a critical element, such as DNMT1o, during the pre-implantation phase of development (Howell et al., 2001) might disrupt proper resetting of imprints in the embryo (Weksberg et al., 2002). Two clonal populations of cells could result with only

one of the two monozygotic twins carrying a methylation defect. This can explain the discordance for an epigenetic error in female BWS monozygotic twins.

The finding of a large number of female monozygotic twin pairs with a single epigenetic etiology suggested to us that male versus female monozygotic twin pairs with BWS might be etiologically distinct. Since UPD for 11p15, loss of methylation at IC2 and gain of methylation at IC1 are all found in male monozygotic twins with BWS, the association between loss of methylation at IC2, monozygotic twinning and BWS is limited to female monozygotic twins. These data demonstrate an important new epigenotype-phenotype correlation for female monozygotic twins with BWS and loss of methylation at IC2. This suggests that those developmental processes limited to female rather than male monozygotic twins likely increase the rate of epigenetic errors at IC2. Such developmental processes include X-inactivation and its associated developmental time lag for female embryos in the pre-implantation phase of development (Lubinsky and Hall, 1991). This report is the first description of paternal UPD of chromosome 11p15 and hypermethylation of IC1 in BWS monozygotic twins. The majority of twins (in particular discordant females) demonstrate loss of methylation at IC2 (Gaston et al., 2001; Weksberg et al., 2002). However, this report clearly demonstrates that male monozygotic twins with BWS, although rarer than female monozygotic twins with BWS, can carry heterogeneous molecular defects associated with BWS, specifically, UPD of 11p15 or hypermethylation of IC1. This finding also has important clinical implications. Even though all children with BWS have a higher relative risk of cancer development, especially between 1 and 4 years of age (DeBaun and Tucker, 1998), patients with BWS

who have UPD for 11p15 or hypermethylation at IC1 are at a greatly elevated risk for the development of Wilms' tumor and hepatoblastoma (Bliek et al., 2004; Bliek et al., 2001; Cooper et al., 2005; DeBaun et al., 2002; Gaston et al., 2001; Weksberg et al., 2001). These cases highlight the importance of molecular testing for monozygotic twins with BWS.

Chapter 4: Maternal Gametic Transmission of Translocations and Inversions Involving the Human Chromosome 11p15.5 Domain Demonstrates Abnormal Regional DNA Methylation and Downregulation of CDKN1C Expression

4.1 Summary

Beckwith-Wiedemann syndrome (BWS) is associated with dysregulation of expression for one or more imprinted genes on human chromosome 11p15.5. Both genetic and/or epigenetic mechanisms that cause BWS include alterations of DNA methylation at one of the two imprinting centres, paternal uniparental disomy, and loss of function mutations in the *CDKN1C* gene. More rarely, chromosomal translocations or inversions of chromosome 11p15.5 with breakpoints in the imprinted domain are associated with BWS. In our collection of translocation and inversion patients with BWS the chromosomal alteration is in most cases associated with normal differential DNA methylation of the imprinting centres and monoallelic expression of the non-coding RNA *KCNQ1OT1*. Based on these results we hypothesized that either microdeletions or microduplications (below the resolution of standard cytogenetic methods) occur near the breakpoints disrupting sequences important for the regional regulation of imprinted gene expression. In addition, we also hypothesized that epigenetic alterations of as yet unknown regulatory DNA sequences, (i.e. other than the imprinting centres) could cause dysregulation of gene expression and explain BWS in these patients. In order to answer these questions a high resolution Nimblegen custom microarray was designed representing all non-repetitive sequence from the first 33 MB of the short arm of human chromosome 11. DNA methylation was also assayed on this microarray for the same 33 MB of chromosome 11 using the Hpa*II* tiny fragment enrichment by ligation-mediated PCR (HELP) technique. No regions of gain or loss around the breakpoints were detected using array complete genomic hybridization that would account for BWS in our patients. However, high-resolution DNA methylation microarray analysis revealed a gain of DNA methylation

that was seen in translocation and inversion patients affecting the p-ter segment of chromosome 11 including the imprinted domain. In BWS patients with a maternal transmission of a translocation or inversion they were also associated with reduced expression of the growth suppressing gene, *CDKN1C*. We propose that translocations and inversions can alter regional DNA methylation patterns and when the translocation breakpoints occur in regions such as the imprinted domain on 11p15.5 it could alter chromatin structure and alter the expression of neighbouring genes. Specifically, in BWS that maternal transmission of a translocation or inversion results in a regional gain of DNA methylation and may cause downregulation of the maternally expressed gene *CDKN1C*.

4.2 Introduction

Beckwith-Wiedemann syndrome (BWS) is characterized by somatic overgrowth, macroglossia, omphalocele, and an increased risk (1000-fold) of embryonal tumours (DeBaun and Tucker, 1998; Rump et al., 2005; Weksberg et al., 2001). BWS is associated with dysregulation of gene expression in an imprinted gene cluster on chromosome band 11p15.5 (Figure 4-1). The 11p15.5 region is divided into two domains controlled by two imprinting centres (IC). Imprinting centres are characterized by differential, parent-of-origin specific methylation and the presence of non-coding transcripts that regulate the expression of neighboring genes in cis over distances up to one megabase (Diaz-Meyer et al., 2003; Du et al., 2004; Fitzpatrick et al., 2002). Molecular changes observed in patients with BWS include both genetic and/or epigenetic alterations on chromosome 11p15.5 (Cooper et al., 2005; Weksberg et al., 2005). Epigenetic alterations can be identified in either one of the two imprinting centres (IC1, IC2) by changes in DNA methylation or histone modifications (Diaz-Meyer et al., 2005; Weksberg et al., 2005; Weksberg et al., 2003).

In Domain 1, IC1 is associated with the genes *H19* (a non-coding RNA of unknown function) and insulin-like growth factor 2 (*IGF2*) (Figure 4-1). Gain of methylation at the maternal IC1 allele accounts for 9% of BWS cases (Sasaki et al., 2007), with repression of the maternal *H19* transcript and de-repression of the maternal *IGF2* transcript (Weksberg et al., 1993a).

Figure 4-1: Schematic map of the 11p15.5 region

A) This schematic representation of the chromosome 11p15.5 imprinted cluster from UCSC genome browser coordinate chr11:1 900 000 – 3 000 000 (http://genome.ucsc.edu). The 11p15.5 imprinted cluster is divided into two domains (Domain 1 is telomeric, while Domain 2 is more centromeric) with an imprinting centre for each Domain. Biallelically expressed genes are shown in black. Maternally expressed imprinted genes are noted by red text colour and paternally expressed imprinted genes are noted by blue text colour. Direction and approximate length of the transcript are indicated by arrows. IC1 is a differentially methylated region upstream of the *H19* transcription start site. IC2 is a differentially methylated region upstream of the non-coding RNA *KCNQ1OT1*. The approximate locations of the breakpoints are shown on the map based on previously published mapping (Hoovers et al., 1995; Sait et al., 1994; Squire et al., 2000) and validated by our BAC FISH.

B) The IC1 differentially methylated region in detail. The location of the *H19* transcript is noted by the red arrow (maternal expression) and the location of CpG islands and the *H19* DMR are shown by green and yellow boxes respectively. The location of the seven putative CTCF binding sites are shown by small blue boxes and the location of the pyrosequencing and Southern assays are indicated.

C) The IC2 differentially methylated region in detail. The location of the *KCNQ1OT1* transcript is noted by the blue arrow (paternal expression) and the location of CpG island and the *KCNQ1OT1* DMR are shown by green and yellow

boxes respectively. The location of the pyrosequencing and Southern assays are indicated. The *KCNQ1* (maternally expressed) transcript passes through this region in the antisense orientation although there is no coding sequence as this region is contained within intron 10 of *KCNQ1*.

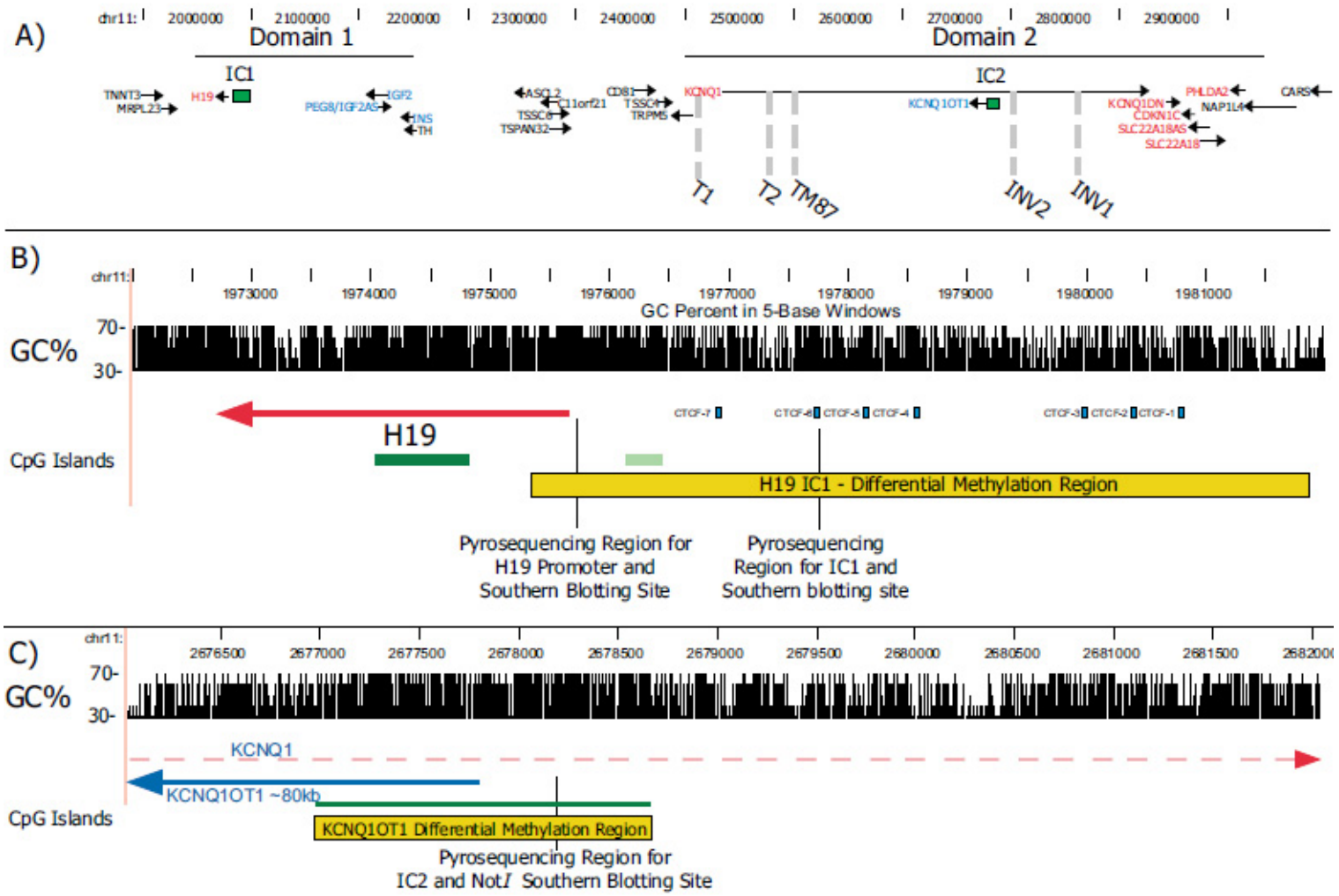

Figure 4-1. Schematic map of the 11p15.5 region

In Domain 2, IC2 is associated with *KCNQ1OT1* (non-coding RNA) and several downstream target genes implicated in BWS, including the *CDKN1C* gene (cyclin-dependent kinase inhibitor 1C). The *KCNQ1OT1* promoter is a differentially methylated region (IC2) found within intron 10 of the *KCNQ1* gene in Domain 2 (Smilinich et al., 1999). IC2 also contains the promoter for *KCNQ1OT1* (Du et al., 2004), a paternally expressed, non-coding RNA, which downregulates the expression of nearby genes on the paternal chromosome e.g. *KCNQ1* and *CDKN1C* (Diaz-Meyer et al., 2003; Murakami et al., 2007) (Figure 4-1). Loss of maternal methylation of IC2 is seen in 50% of patients with sporadic BWS (Bliek et al., 2001; Cooper et al., 2005; Gaston et al., 2001; Weksberg et al., 2001). Deletion of the orthologous sequence in mouse results in loss of imprinting of several genes neighbouring *KCNQ1* indicating that this IC is critical for maintaining imprinted gene expression in Domain 2 (Fitzpatrick et al., 2002). In humans, loss of methylation on the maternal chromosome at IC2 has been shown to be associated with reduction of *CDKN1C* expression, thereby explaining the pathophysiology of such cases of BWS (Diaz-Meyer et al., 2003). Other genetic alterations associated with BWS include paternal uniparental disomy of chromosome 11 (~20%), mutations in the *CDKN1C* gene (5-10%) and less frequently microdeletions involving IC1 (Sparago et al., 2004) and rarely IC2 (Niemitz et al., 2004) (<1%).

Other rare chromosomal changes associated with the Beckwith-Wiedemann syndrome phenotype include chromosomal rearrangements (<1%) including paternally transmitted duplications of chromosome 11p15 and maternally transmitted translocations. Unbalanced chromosome rearrangements involving chromosome 11p15.5 alter the copy

number of imprinted genes thus presumably changing the dosage of growth controlling genes such as *IGF2* and *CDKN1C*. Most reports of unbalanced translocations or inversions associated with BWS show duplications of the *IGF2* gene that are paternally inherited with two copies of the active *IGF2* allele (Delicado et al., 2005; Fert-Ferrer et al., 2000; Grundy et al., 1998; Han et al., 2006; Krajewska-Walasek et al., 1996; Mikhail et al., 2007; Ogur et al., 1988; Slavotinek et al., 1997; Turleau et al., 1984).

Apparently balanced translocations and inversions that are associated with BWS typically occur following maternal transmission (Hoovers et al., 1995; Lee et al., 1999; Lee et al., 1997; Sait et al., 1994; Squire et al., 2000; Weksberg et al., 1993b). Individuals with a paternally derived translocation or inversion are apparently normal. Patients with maternally transmitted 11p15.5 apparently balanced translocations or inversions exhibit typical features of Beckwith-Wiedemann syndrome. The mechanism by which such balanced translocations and inversions of the imprinted cluster on 11p15.5 result in the BWS phenotype is not understood. In the case of such balanced rearrangements there are no known associated changes in copy number and are all maternally rather than paternally inherited.

FISH mapping studies have indicated that translocations and inversions associated with a BWS phenotype have a cluster of breakpoints near the *KCNQ1* gene – encompassing a region of over 400 kilobases. Balanced translocations and inversions associated with BWS with breakpoints that lie several megabases centromeric to *KCNQ1* also occur (such as sample B10.1 in (Hoovers et al., 1995)) however the mechanism that results in

the BWS phenotype is not clear. The authors suggested that position effects leading to altered gene expression of the 11p15.5 imprinted cluster over large distances might cause BWS.

Recent literature indicates that chromosomal rearrangements that are apparently balanced by standard cytogenetic methods may involve unexpected complexity when investigated using high resolution technologies (Gribble et al., 2005; Sismani et al., 2008). We hypothesized that microdeletion of regulatory elements when passed through the maternal germline could lead to the BWS phenotype. Further, since apparently balanced translocations and inversions only produce a BWS phenotype upon maternal transmission we also hypothesized that an epigenetic mark that could not be reset in the female germline could cause the BWS phenotype. By investigating the latter possibility *cis*-acting elements important in the establishment or maintenance of imprinting on chromosome 11p15.5 could be discovered.

We demonstrate that translocations and inversions disrupting the imprinted domain on chromosome band 11p15.5 can result in regional changes in DNA methylation. Further, dysregulation of the maternally expressed growth suppressing gene, CDKN1C, occurs in affected patients that have a maternally derived translocation or inversion. We conclude that translocations and inversions can alter DNA methylation several megabases away from the breakpoints and cause the dysregulation of gene expression.

4.3 Methods

4.3.1 Tissue Culture

Lymphoblastoid cell lines were established by Epstein-Barr virus transformation of blood from patients diagnosed with BWS. Lines were maintained in RPMI 1640 media with 15% fetal calf serum and 50 units of pencillin plus 50 ug of streptomycin per millilitre at 37˚C and 5% CO_2. Fibroblast cell strains were obtained from standard punch biopsies of tissues, surgical resections or from aborted fetuses subsequently treated with collagenase to obtain enriched cultures of fibroblast cells. Cells were passaged in alpha modified Eagle's medium with 10% fetal calf serum and 50 units of pencillin plus 50 ug of streptomycin per millilitre at 37˚C and 5% CO_2. Fibroblast strains were not cultured beyond 10 passages to reduce the influence of any culture-related changes.

4.3.2 Patient Samples

This study was approved by the Research Ethics Board of the Hospital for Sick Children. All families gave their informed consent to participate. Our collection of 8 samples with 5 unique maternally derived translocations and inversions mapped to the Domain 2 region of chromosome 11p15. The translocation and inversion rearrangements in our sample are summarized in Table 4-1. Control samples (CNF1, CNF2, CNL1, CNL2) are from healthy individuals and have been tested for DNA methylation at imprinting centres IC1 and IC2.

Table 4-1: Translocation and Inversion Patients

Patient Sample	Tissue	Karyotype	Previously Published	Previous Name
INV1U	**Fibroblast**	Inv(11)(p15.5; q13), pat		
INV1A	**Fibroblast**	Inv(11)(p15.5; q13), mat	**Squire et al 2000**	**INV11**
INV2A	**Fibroblast**	inv(11)(p11.2;p15.5), mat	**Hoovers et al 1995**	**CV581**
T1U	**Lymphoblast**	t(11;22) (p15.5;q11.23)	**Weksberg et al 1993, Squire et al 2000**	**T1**
T1A	**Lymphoblast**	t(11;22) (p15.5;q11.23) mat	**Weksberg et al 1993, Squire et al 2000**	**T1**
T1A-F	**Fibroblast**	t(11;22) (p15.5;q11.23) mat	**Weksberg et al 1993, Squire et al 2000**	**T1**
T2	**Lymphoblast**	t(11;16) (p15.5;q12)	**Weksberg et al 1993**	**T2**
TM-87	**Rhabdoid Tumor Line**	t(11;22)(p15.5;q12.23)	**Karnes 1991, Hoovers et al 1995, Lee et al 1997, Lee et al 1999**	**TM-87**

4.3.3 **DNA Extraction**

DNA was extracted from lymphoblastoid and fibroblast cells by standard phenol-chloroform extraction and protocol (Dracopoli, 1994). Briefly, for lymphoblastoid cell lines, 5-20ml of cell culture or whole blood was centrifuged at 250 x g to pellet cells. For fibroblast cultures cells were harvested from culture dishes by scraping after being briefly washed with phosphate buffered saline. Nuclei were then lysed and digested by proteinase K. Samples were then mixed with phenol and then phenol/chloroform, spun in Phase Lock Gel tubes (Eppendorf, Mississauga, Canada) and the aqueous phase decanted. DNA was then spooled and rehydrated in TE. DNA quality was tested by gel electrophoresis and spectrophotometry.

4.3.4 **RNA extraction and cDNA preparation**

Total RNA was extracted from lymphoblastoid cell lines and fibroblast strains by RNeasy kit (Qiagen GmbH, Germany) according to the manufacturer's instructions. Briefly, 5mL (approx 1,000,000 cells/mL) or one 10cm plate of fibroblasts were suspended in buffer RLT. After centrifugation of the lysate at 10,000×g for 3 minutes, the supernatant was transferred to a fresh tube and mixed with an equal volume of 70% ethanol. The mixture was then transferred to the RNeasy spin column and centrifuged at 10,000 × g for 15 seconds. The RNA was washed by Buffer RW1 and RPE (QIAGEN®) and eluted in 30 µl RNase-free water.

Potentially contaminating DNA was removed from the RNA samples by DNaseI (Invitrogen, Burlington, Canada) treatment for 15 minutes at room temperature followed by heat inactivation. cDNA was prepared by Reverse-iTTM 1st strand synthesis kit (Thermo-Fisher Scientific/ ABgene, Rochester, NY) according to the manufacturer's instructions. The first-strand cDNA was synthesized from 2 μg of total RNA by incubation with Reverse-iTTM RTase blend, random decamers, 5× first strand synthesis buffer, dNTP mix and DTT at 47°C for 50 minutes. For each sample, a parallel reaction was also prepared without reverse transcriptase to provide a control to rule out DNA contamination.

4.3.5 **Methylation Analyses – Southern Blotting**

5-10 μg of genomic DNA was digested with Eco*R1* and Not*I* or Pst*I* and Mlu*I* or Pst*I* and Sma*I* for the IC2 region, IC1 region and the H19 promoter, respectively. Digested DNA was electrophoresed on 0.8% agarose gels and transferred overnight to positively charged nylon membranes (Hybond N+, Amersham Biosciences, Piscataway, NJ) in 0.4N NaOH. Membranes were neutralized and prehybridized in modified Church's buffer with salmon sperm DNA as a blocking agent. ^{32}P-dCTP random labeled probe was added overnight at 65˚C and washed with serial washes of SSPE (2X, 1X, 0.5X, all containing 0.5% SDS). Membranes were then exposed to Phosphor screen for at least 24 hours and imaged by Storm Phosphorimager (GE Healthcare, Piscataway, NJ). Bands were quantitated by Fluorchem Software (Alpha-Innotech, San Leandro, CA) by dividing the band intensity of the undigested fragment, indicating a methylated product, by the sum of the digested

and undigested fragments as previously described (Smilinich et al., 1999; Weksberg et al., 2001; Weksberg et al., 2002). Probe locations are listed in Table 4-3.

4.3.6 **Bisulphite Modification**

1 µg of DNA sample was used in the Qiagen Epitect 96 Bisulphite Modification kit (Qiagen GmbH, Germany) according to the manufacturer's instructions. Briefly, sodium bisulfite-mediated conversion of unmethylated cytosines was accomplished by exposing the samples to reaction mix containing sodium bisulphite followed by 3 cycles of denaturation (95°C) at 5 minutes for each cycle and incubation (60°C) of 25, 85 and 175 minutes for cycles 1-3. Single-stranded DNA samples were then bound to the membrane of an EpiTect 96 Plate, washed and desulfonated. The desulfonating agent was then removed by washing and converted DNA was collected by elution.

4.3.7 **Methylation Analyses - Pyrosequencing**

Pyrosequencing (Biotage, Uppsala, Sweden) reactions for the *KCNQ1OT1* IC2 differentially methylated region (DMR), IGF2DMR, *H19* promoter, *H19* enhancers and *H19* DMR region were designed using the Pyrosequencing Assay Design Software. PCR product of each region was used for the individual sequencing reaction (Table 2). The biotinylated PCR product (40 uL) was purified using streptavidin-Sepharose beads (Amersham Biosciences, Piscataway, NJ). Purification with streptavidin-Sepharose HP beads followed by denaturation of the biotinylated PCR products and the sequencing primer (15 pmol per reaction) were conducted following the PSQ 96 sample preparation guide using the pyrosequencing vacuum prep tool (Biotage AB). Reactions were

designed as recommended by the manufacturer's instructions with the single-strand PCR product providing a template. After primer annealing, sequencing was carried out with a PSQ 96MA system using the Pyrogold reagent kit according to the manufacturer's instructions. Raw data were analyzed with the Pyro-Q-CpG software provided with the instrument. Percent methylation was calculated for the H19 CTCF region (sixth CpG site) and IGF2 DMR by analyzing the unmethylated and methylated peak height for each CpG analyzed. All Pyrosequencing reactions were performed using a universal biotinylated primer solution previously published by Royo and colleagues (Royo et al., 2007; Royo et al., 2006). Primer information for all Pyrosequencing reactions is contained in Table 4-2.

4.3.8 **Fluoresence In-Situ Hybridization**

Chromosome spreads were prepared for FISH analysis according to established cytogenetic and hybridization protocols (Beatty et al., 2002). At least 20 metaphase nuclei were analyzed from each sample using the Vysis Quips FISH Imaging System (Vysis, Inc.). The following probes RP-11-542-J6, RP-11-373, RP-11-38L8 and RP-11-81K4 were end-labeled by nick translation with Texas Red or FITC and were used to validate the location of the translocation and inversion breakpoints. Since many of the studies published regarding the breakpoint locations were performed before the final draft of the human genome sequence was completed we wished to confirm the location of each breakpoint.

Table 4-2: Pyrosequencing Primer Sequences

Primer Type	Primer Name	Sequence
KCNQ1OT1 (IC2) Methylation		
Universal	M13-Biotin	5'-Biotin-CGCCAGGGTTTTCCCAGTCACGAC
Forward	BW3	5'-GTGATGTGTTTATTATT
Reverse	M13-BW2	5'-CGCCAGGGTTTTCCCAGTCACGACCTAAACRCCCACAAACCTCCA
Sequencing	BW3	5'-GTGATGTGTTTATTATT
H19 (IC1) CTCF Binding Site 6		
Universal	M13-Biotin	5'-Biotin-CGCCAGGGTTTTCCCAGTCACGAC
Forward	H19-Cts6-Bis-F-5	5'-TGAGTGTTTTATTTTTAGATGATTTT
Reverse	M13-H19-Cts6-Bis-R-5	5'-CGCCAGGGTTTTCCCAGTCACGACACAATACAAACTCACACATCACAAC
Sequencing	H19-Cts6-Seq-5	5'-GTGGTTTGGGTGATT
H19 Downstream Enhancer Region 1		
Universal	M13-Biotin	5'-Biotin-CGCCAGGGTTTTCCCAGTCACGAC
Forward	H19-Enhancer 1-reverse-F-1	5'-TGAAATAATGGTATGGAGGGAGTA
Reverse	M13-H19-Enhancer 1-reverse-R-1	5'-CGCCAGGGTTTTCCCAGTCACGACCAACCAAAAAAACAAATCTTAATA
Sequencing	H19-Enhancer 1-reverse-S-1	5'-AAATGTTAGGAGTTAAGGG
H19 Downstream Enhancer Region 2		
Universal	M13-Biotin	5'-Biotin-CGCCAGGGTTTTCCCAGTCACGAC
Forward	H19-Enhancer 2-F-2	5'-GTGATTTGTGGTTTGGGAGATA
Reverse	M13-H19-Enhancer 2-R-2	5'-CGCCAGGGTTTTCCCAGTCACGACACCTACCTCTACCACCCTCAAAA
Sequencing	H19-Enhancer 2-S-2	5'-TTGTGGTTTGGGAGAT
H19 Promoter		
Universal	M13-Biotin	5'-Biotin-CGCCAGGGTTTTCCCAGTCACGAC
Forward	H19-Promoter-Seq-2	5'-TATTTTAGTTAGAAAAAGTT
Reverse	M13-H19-Promoter-Bis-R-2	5'-CGCCAGGGTTTTCCCAGTCACGACTCTCCTCCAACACCCCATCT
Sequencing	H19-Promoter-Seq-2	5'-TATTTTAGTTAGAAAAAGTT

Table 4-3: Southern Probe Sequences

Probe Region	Coordinates of Probe (Hg18 Genome Browser:genome.ucsc.edu)	Size of Probe
IC2 (KCNQ1OT1) Differentially Methlyated Region	chr11:2679514–2679910	396 bp
IC1 Differentially Methylated Region (CTCF Site 6)	chr11:1979443–1979743	300 bp
H19 Promoter Region	chr11:1975199–1975482	283 bp

4.3.9 **Quantitative real-time PCR**

Quantitative real-time RT-PCR was performed to assess *CDKN1C* and *IGF2* expression using the ABI Prism 7900 Sequence Detection System (Applied Biosystems Inc., Foster City, CA) with SYBR Green PCR incorporation. The amplification mix (20 µl) contained a cDNA template derived from 5 ng of total RNA, 200 nM or 100 nM of each specific primer set (Table 4-4), 10 µl SYBR Green Mix and RNase-, DNase-free water. The PCR reaction was initiated by incubation at 95°C for 10 minutes to activate hot-start Taq polymerase followed by 40 cycles of denaturation at 95°C for 10 seconds, then annealing at 60°C for 1 minute and followed by elongation at 72°C for 1 minute. Fluorescence detection was performed immediately following each cycle and the purity of each amplification product was confirmed by generating dissociation curves. For all samples, real-time RT-PCR was performed with cDNA templates generated from reactions with and without reverse transcriptase. No PCR product was observed when reverse transcriptase was not added. Relative expression of each gene was determined using the standard curve method (Rutledge and Cote, 2003) and normalized by the expression of the housekeeping genes GAPD, YWHAZ and HPRT1 (Vandesompele et al., 2002).

4.3.10 **Allelic Expression Analysis by SNaPshot**

Single nucleotide primer extension assay was used on the SNaPshot platform (Applied Biosystems, Foster City, CA) to determine the allelic expression profile for coding *KCNQ1OT1* single nucleotide polymorphisms (SNPs) (Guo et al., 2008; Lee et al., 1999).

Table 4-4: Allele Specific Primers for SNAPSHOT and Q-PCR Primers

Target Name	Forward primers (5'- 3')	Reverse primers (5'-3')
KCNQ1OT1rs10832514	TTTCCAAACTTCACTTCCTCCGT	TGGGCCATCCACCTAGACAG
CDKN1C-QPCR	CAGTGTACCTTCTCGTGCAGAATAC	GGGACCGTTCATGTAGCAGC
IGF2-QPCR	CAGGTGTCATATTGGAAGAACTTGC	TCCTGGAGACGTACTGTGCTACC
YWHAZ-QPCR	ACTTTTGGTACATTGTGGCTTCAA	CCGCCAGGACAAACCAGTAT
HPRT1-QPCR	TGACACTGGCAAAACAATGCA	GGTCCTTTTCACCAGCAAGCT
GAPD-QPCR	TGCACCACCAACTGCTTAGC	GGCATGGACTGTGGTCATGAG

Reverse-transcribed PCR products (cDNA) were analyzed when patients were heterozygous for *KCNQ1OT1* SNPs. Primers are listed in Table 4-4. Briefly, DNA and cDNA amplicons encompassing SNP sites were treated with shrimp alkaline phosphatase (SAP) and subjected to Exonuclease I (Exo) (USB) treatment. SNP genotyping was performed using SNaPshot™ single-basepair extension reactions (Applied Biosystems Inc., Foster City, CA), which contained 7µl of cleaned PCR product (at a concentration of 0.01 to 0.4 pmol PCR product), 2 µl of SNaPshot™ multiplex enzyme mix and 50 ng of primer for a total volume of 10 µl. Conditions for the 25 extension reaction cycles included 96ºC for 10 seconds, 50ºC for 5 seconds and 60ºC for 30 seconds. 1 µl of SNaPshot reactions was suspended in 9 µl of Hi-Di formamide (ABI) and run on an ABI 3100 genetic analyzer (Applied Biosystems, Foster City, CA) using the POP4 polymer and dye set E5. Results were analyzed using the software GeneMapper ver. 3.5.

Since *KCNQ1* is transcribed in an anti-sense direction and from the opposite strand to *KCNQ1OT1* detection of the *KCNQ1* nascent transcript with this assay is a possibility. However, detection of the *KCNQ1* unspliced RNA by single-nucleotide primer extention or by direct sequencing of cDNA has never been reported (Kohda et al., 2001; Lee et al., 1999; Li et al., 2001; Mitsuya et al., 1999; Tanaka et al., 2001; Weksberg et al., 2001; Weksberg et al., 2002).

4.3.11 **Array Design**

Arrays representing 33 megabases of the p-terminal segment of chromosome 11 were generated by DNA synthesis by maskless photolithograpy (Nuwaysir et al., 2002) (Nimblegen, Iceland). Representation of the first 33 megabases of sequence from chromosome 11 for array CGH and DNA methylation was performed as follows. Array CGH probes were selected from only non-repetitive DNA. Using the RepeatMasker track from the UCSC genome browser coordintates chr11:1-33,000,000 (http://genome.ucsc.edu, Human Genome Build 36.1 (NCBI) Genome Browser March 2006 version, with HG18 annotation track) all repetitive sequences (15,727,426 nucleotides) were removed from our design. The remaining 17,272,574 nucleotides were represented by 300,000 isothermal oligonucleotides of approximately 50 nucleotides in length (feature). Each feature was checked for uniqueness against the genome to minimize possible cross-hybridization. The 300,000 features gave an average resolution of 58 bp between probes.

The remaining ~85,000 features were designated for HELP (**H**paII tiny fragment **E**nrichment by **L**igation-mediated **P**CR) (Khulan et al., 2006). First, an in-silico digest was performed with HpaII (CCGG) for the first 33 megabases of chromosome 11, excluding repetitive sequences, and selection of fragments between 50 and 2000bp were retained for probe design. A 50-mer oligo was then designed every 5 base pairs and tested for uniqueness against the genome (www.ncbi.nlm.nih.gov/blast). Eight oligonucleotides were then selected to represent each HpaII fragment based on a selection algorithm that counts the number of oligos per HpaII fragment and give penalties for

degree of overlap of each oligo in a sliding 15-mer window and for stretches of G's or C's longer than 3 nucleotides or A's and T's longer than 5 nucleotides. After the first oligo is selected the remaining oligos are positioned to achieve an optimal spacing of oligos across the entire HpaII fragment.

4.3.12 **Array CGH Hybridization**

Genomic DNA samples for INV1U, INV1A, T1U and T1A were fragmented by sonication to a size range of 500-2000bp. For labelling, 1 ug was denatured at 98ºC in the presence of Cy3 and Cy5-labelled oligonucleotides and random primers. The denatured samples were chilled on ice. The samples were then incubated with Klenow fragment (100 units exo-) and dNTPs (6mM each) at 38ºC for 2 hours. After termination of the reaction with 0.5M EDTA, samples were precipitated with isopropanol and resuspended in water. The translocation and inversion samples were hybridized with Cy5 and the reference sample with Cy3. The reference sample consisted of a pool of six male individuals (Promega, Madison WI). Samples were then hybridized to the array and scanned at the Nimblegen Service Laboratory.

4.3.13 **Isoschizomer representations**

Ten µg of DNA from CNL1, CNL2, CNF1, CNF2, INV1U, INV1A, INV2A, T1U and T1A were digested using HpaII or MspI. After cleaning the DNA by phenol-chloroform extraction and rehydration in TE pH 8.0 one-tenth of the sample was incubated with T4 DNA ligase with the following primers, HELP 1 - 5' –

CGACGTCGACTATCCATGAACAGC – 3', HELP – 2 - 5' – GTACTTGTCGGC – 3'. The mix was incubated for 5 minutes at 55°C and then the temperature was gradually reduced to 4°C over 1 hour. At this time an additional unit of T4 DNA ligase was added and the reaction was incubated overnight at 16°C.

To perform ligation-mediated polymerase chain reaction (LM-PCR), 1/50 of the MspI or 1/25 of the HpaII sample was amplified using the HELP-1 oligonucleotide. An extension for 10 minutes at 72°C was followed by 20 cycles of 95°C for 30 seconds and 72°C for 3 mintues. A final polishing step was performed at 72°C for 10 minutes. The products of the amplification were purified by Qiagen PCR purification kit as per the manufacturer's instructions and then quantitated by spectrophotometry.

Each of the translocation and inversion samples was labeled for microarray with Cy3 or Cy5-conjugated olignucleotides and random primers. The *Hpa*II and *Msp*I representations were cohybridized to the microarray in the NimbleGen Service Laboratory and scanned to quantify the fluorescence at each oligonucleotide on the microarray.

4.3.14 **Array CGH Data Analysis**

Copy number analysis was performed by importing the array CGH data from each test and reference sample into R (www.r-project.com) and applying the normalize.qspline function (Workman et al., 2002) from the bioconductor package (www.bioconductor.org). Log_2 ratios for each probe were averaged into 800bp, 1600,

and 4000bp segmentation files to quantitate the presence of gains or losses for the first 33 megabases of chromosome 11.

4.3.15 **HELP Methylation Data Analysis**

Visual analysis of each cohybridization was performed to ensure uniform signals were observed on the microarrays. Each restriction fragment generated by the HELP method was represented by 8 oligonucleotides on the the microarray. The median signal intensity was calculated for each fragment. Normalization of signals was performed as described previously (Khulan et al., 2006) to centre log ratios across the entire array.

In order to visualize global patterns of DNA methylation in each of the samples methylation ratios were averaged into 0.5 megabase bins for the first 33 megabases of chromosome 11. Lymphoblast and fibroblast samples were analyzed separately so as to minimize inherent tissue specific differences in methylation. Each DNA methylation signature for individual patient samples was plotted against the average of the controls subtracted from each sample. This manipulation then represents DNA methylation in the patient samples as a deviation from the control average. Deviations below zero represent greater methylation in patient samples and deviations above zero represent less methylation in patient samples.

Heat maps for methylation data were created using the Integrative Genomics Browser (http://www.broad.mit.edu/igv/index.html). A red-blue colour spectrum was generated

for each methylation data point with red representing unmethylated regions, white representing differential methylation and blue representing methylated regions.

4.4 Results

4.4.1 Translocation and Inversion Breakpoint Confirmed by FISH

The patient samples tested in our study are shown in Table 4-1. Each translocation and inversion was given a unique code. Unaffected parental samples are identified by a "U" and affected probands by an "A". Translocations are designated with a "T" and inversions by "INV". Each rearrangement is given a unique number so that when a parent and child have the same rearrangement but one is affected and the other unaffected they can be differentiated e.g. T1U is a translocation in an unaffected individual, T1A is the same rearrangement in an affected individual. For some samples we have lymphoblastoid and fibroblast cell lines which are indicated in Table 4-1. In an effort to be consistent with previously published studies we have also listed the names of the translocations or inversions as they appeared in previous publications in Table 4-1.

Clinical features for patient INV1A include macroglossia, macrosomia, ear creases/pits and omphalocele. Patient INV2A was aborted and has probable macroglossia and omphalocele with an extracorporeal liver. Patient T1A had macroglossia, ear creases/pits, organomegaly, neonatal hypoglycemia and an umbilical hernia. Although this sample is too small to draw any conclusions regarding the phenotype seen commonly in translocation and inversion patients with BWS it is worth noting that macroglossia, ear creases and omphalocele are clinical features that are commonly seen together in patients with *CDKN1C* mutations (Li et al., 2001). However, these are also common features in BWS as macroglossia is seen in 95% of patients, omphalocele in 70% and ear creases in 60%.

Using four previously published mapping studies (Hoovers et al., 1995; Lee et al., 1999; Lee et al., 1997; Sait et al., 1994; Squire et al., 2000) and our own FISH mapping with RP-11 library BAC clones, we confirmed the approximate breakpoint locations of the translocations and inversions in our study sample (Figure 4-1). We chose four RP-11 BAC library clones that spanned the 400kb *KCNQ1* gene from 5' to 3' (RP11-542J6, RP-11-373H8, RP11-38L8 and RP11-81K4). Since most of the previous mapping studies pre-dated the completion of the human genome sequence, we wanted to confirm the location of the breakpoints based on clones that map to the *KCNQ1* region on chromosome band 11p15.5.

INV1U is an unaffected mother with a pericentric inversion inv(11)(p15.5,q13) inherited from her father (Norman et al., 1992). INV1A is the daughter of INV1U and is affected with the BWS. This inversion produces a split signal by FISH using the RP11-81K4 confirming that the breakpoint in in the 3' end of *KCNQ1* in the region chr11:2,755,275-2,927,014 (171,740 base pairs). INV2A is a proband affected with BWS for which we do not have parental material. The breakpoint for INV2A is also in the 3' end of *KCNQ1*. This paracentric inversion does not include the q-arm as in INV1 as the breakpoint is inv(11)(p11.2,q15.5). This inversion produces a split signal by FISH using the RP11-38L8 in the region chr11:2,624,682-2,805,692 (181,011 base pairs) and is within 50 kb of the differentially methylated region IC2. T1U is an unaffected mother with a translocation between chromosomes 11 and 22, t(11;22)(q15.5;11.23). T1A, her affected child, has the same translocation and showed a split signal using the FISH probe RP11-

373H8 indicating the break point is in the region chr11:2,261,657-2,468,447 (205,791 base pairs). For T1A we have two available tissues, a lymphoblastoid cell line and a fibroblast cell line (T1A-F) derived from resected tongue tissue. T2U is an unaffected mother carrying a translocation t(11;16)(q15.5;q12). TM-87 is a rhabdoid tumor cell line derived from a patient that did not have BWS. The TM-87 translocation breakpoints were determined to be t(11;22)(q15.5;q12.23) (Hoovers et al., 1995; Karnes et al., 1991; Lee et al., 1997). Both T1 and TM87 involve chromosome 22 with a breakpoint on band q11.23 for T1, just distal to the 22q11 deletion syndrome region, and band q12.23 for TM87 – a distance of 8 megabases between these two breakpoints.

4.4.2 **Maintenance of DNA Methylation at IC1 and IC2**

IC2 Methylation

Since the BWS-associated translocations cluster around IC2 (within 300 kilobases on either side of IC2), we looked for loss of methylation at IC2 and biallelic expression of *KCNQ1OT1* as is commonly seen in over 50% of BWS patients. Surprisingly, an investigation of DNA methylation at the *KCNQ1OT1* IC2 showed normal methylation and allelic expression of *KCNQ1OT1* for all informative samples (Figure 4-2). Although the translocations disrupt this locus as they are all within 300kb of IC2 and all except one do not disturb the establishment of methylation at the *KCNQ1OT1* DMR even on transmission through the maternal germline. In the inversion patient, INV2A previously named CV581 (Hoovers et al., 1995; Lee et al., 1999), with the breakpoint very close to the *KCNQ1OT1* DMR (IC2) the methylation is absent on both alleles (Figure 4-2A) (Hoovers et al., 1995). Methylation results obtained by Pyrosequencing were validated

Figure 4-2: DNA methylation and allele specific expression of *KCNQ1OT1*.

A) DNA methylation of the differentially methylated promoter of *KCNQ1OT1* (IC2) was assayed by Pyrosequencing. The average DNA methylation of 5 CpG sites in the differentially methylated region was tested and is shown for each sample tested in duplicate with standard deviation indicated by the error bars. All samples showed normal methylation except for sample INV2A which showed a complete loss of methylation. BWIC2 is patient with BWS and a loss of methylation at IC2. All Pyrosequencing results correspond directly with methylation-sensitive Southern blotting results for the same region (data not shown).

B) Allele specific expression of the non-coding transcript *KCNQ1OT1*. The samples T1A, T2U and TM-87 are informative for the single nucleotide polymorphism rs10832514 (A/G). The traces show expression of one allele only. Patients with BWS and loss of methylation at IC2 typically show biallelic transcription of *KCNQ1OT1*. This shows in these translocations and inversion samples that DNA methylation and imprinting at this locus is maintained despite the disruption of the region by the translocation/inversion breakpoints. Applied Biosystems dye set E5 labels nucleotides with the following colours, A Green, C Black, G Blue, T(U) Red. Molecular size marker is run in all reactions labeled with a red fluorophore.

A

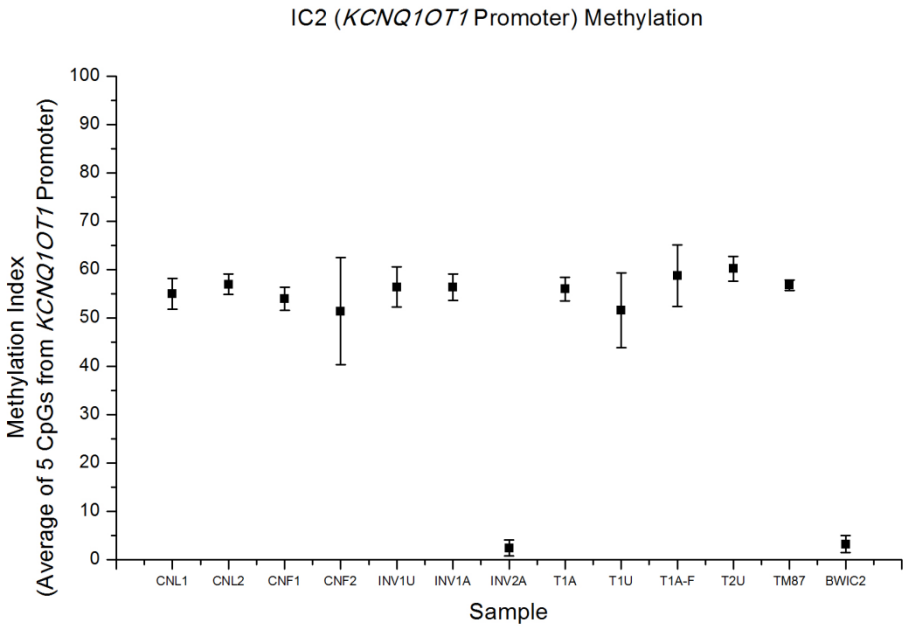

B

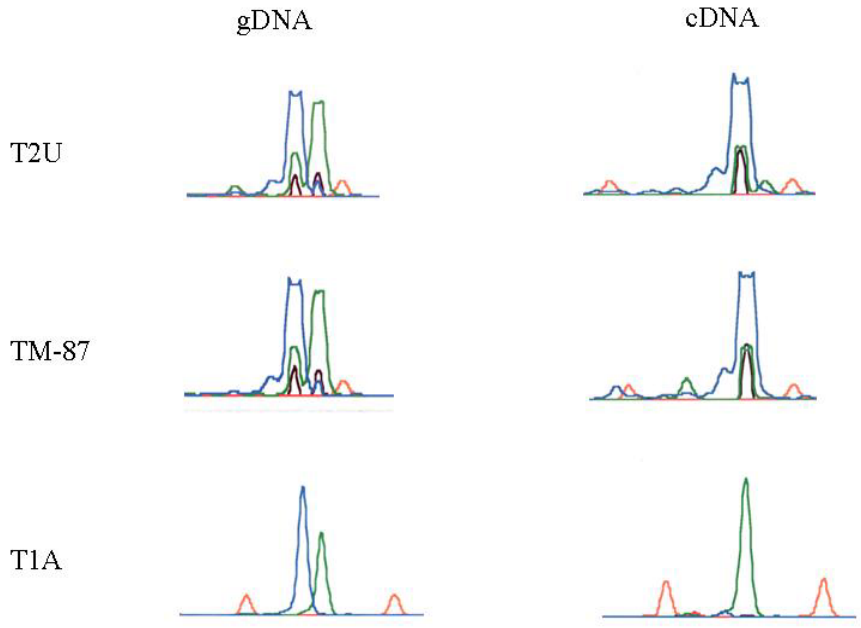

Figure 4-2. DNA methylation and allele specific expression of KCNQ1OT1.

by Southern blotting (data not shown). These findings indicate that regulatory elements other than the *KCNQ1OT1* promoter region (IC2) or its transcript can regulate imprinting on 11p15 to produce the BWS phenotype. For INV2A loss of methylation at IC2 could account for the BWS phenotype, however the usual mechanism presumed in BWS with loss of methylation at IC2 and without translocations or inversion is that the *KCNQ1OT1* is expressed biallelically and this causes a downregulation of *CDKN1C* likely due to a change in the chromatin structure of the region (Diaz-Meyer et al., 2003; Diaz-Meyer et al., 2005). In the case of INV2A the inversion breakpoint is between IC2 and *CDKN1C* which likely disrupts the chromatin context resulting in reduced *CDKN1C* expression.

Differential IC1 Methylation (*H19* Promoter and Differentially Methylated Region)

Nine percent of patients with BWS have gain of methylation of the entire IC1 region including the promoter. Investigation of DNA methylation at the H19 IC1 of all five test subjects showed normal methylation for all samples tested at the sixth putative CTCF binding site in the differentially methylated region by Pyrosequencing (Figure 4-3A). We also tested the H19 promoter region which is two kilobases downstream by Pyrosequencing and found that samples INV1U, INV1A, T1A-F, T2U and TM-87 showed loss of methylation at the H19 promoter (Figure 4-3B). Normally, methylation at IC1 and the H19 promoter are concordant. That is, in BWS patients who have gain of methylation of IC1 there is also gain of methylation at the H19 promoter. All samples that showed loss of methylation at H19 promoter were fibroblast samples except for T2U which may indicate that the isolated loss of methylation in the promoter region is a tissue

Figure 4-3: Methylation analysis of the IC1 and *H19* Promoter by Pyrosequencing.

A) DNA methylation of the differentially methylated IC1 region upstream of the *H19* gene was assayed by Pyrosequencing. The average DNA methylation of 3 CpG sites in the differentially methylated region was tested and is shown with standard deviation for each sample tested. All samples showed normal methylation (~50%) and were done in duplicates. BWIC1 is a sample from a patient with BWS that has gain of methylation of the *H19* IC1 region. All Pyrosequencing results were confirmed by methylation-sensitive Southern blotting results for the same region.

B) DNA methylation of the differentially methylated *H19* promoter region was assayed by Pyrosequencing. The average DNA methylation of 2 CpG sites in the differentially methylated region was tested and is shown with standard deviation for each sample tested. INV1U, INV1A, T1A-F, T2U and TM-87 showed loss of methylation at the *H19* promoter. All Pyrosequencing results were confirmed by methylation-sensitive Southern blotting results for the same region.

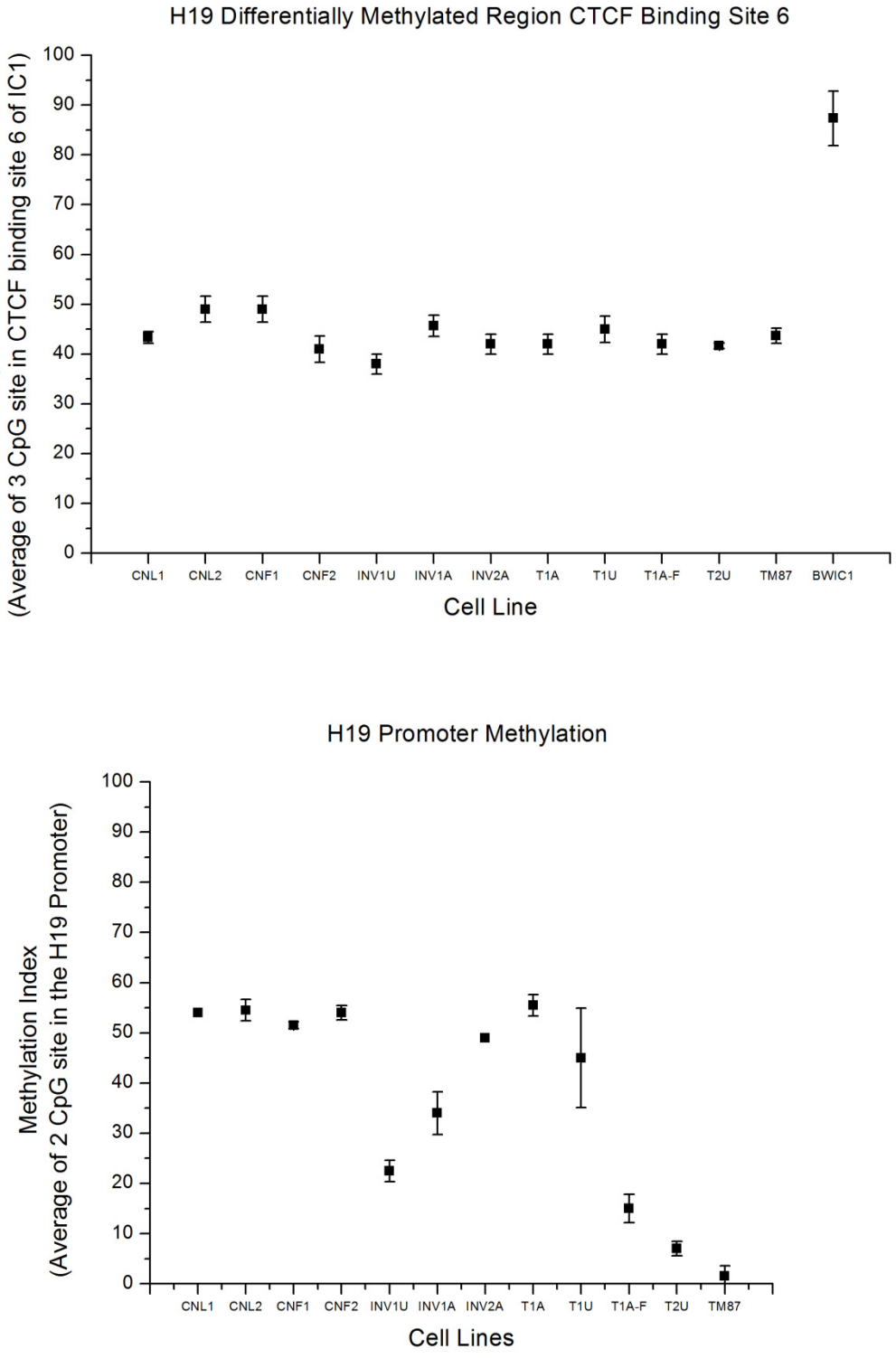

Figure 4-3. Methylation analysis of the IC1 and *H19* Promoter by Pyrosequencing.

specific phenomenon. Variable loss of methylation at the H19 promoter in fibroblast cells in tissue culture has been reported previously (DeBaun et al., 2002).

4.4.3 Reduced *CDKN1C* Gene Expression in Patients with BWS and Translocations and Inversions

Using fibroblast cells derived from INV1U (inv(11)(q15.5,q13)), INV1A (inv(11)(q15.5,q13), and TM-87 t(11;22)(p15.5;q12.23) we assessed total transcription of *CDKN1C*. We found that this imprinted gene is downregulated in INV1A and TM-87 presumably as a result of the translocations but independently of IC2 DNA methylation and expression of the non-coding RNA *KCNQ1OT1* (Figure 4-4A). The extent of this downregulation is equivalent to the level of a fibroblast strain with loss of methylation at IC2 and a concomitant downregulation of CDKN1C (BW1). CDKN1C is expressed at very low levels in lymphoblastoid cell lines and therefore could not be tested in other samples.

Expression of *IGF2* was also assessed using fibroblast cell lines. We did not find increased expression of *IGF2* above control levels of expression in any of our samples (Figure 4-4B). Two additional patients with BWS and without translocations or inversions were used as additional controls (BW1 and BW2). BW1 is a patient with a loss of methylation at IC2 and a downregulation of *CDKN1C* expression but normal expression of *IGF2*. BW2 is a patient with BWS showing upregulation of *IGF2* expression.

Figure 4-4: Reduced *CDKN1C* Expression in Translocation and Inversion samples with BWS.

A) Real-time PCR for *CDKN1C* was performed on fibroblast samples since *CDKN1C* expression is not detectable in lymphoblasts. Expression of *CDKN1C* was normalized to that of housekeeping genes *GAPD*, *HPRT1* and *YWHAZ* according to the method published by Vandesompele et al (Vandesompele et al., 2002). INV1U, an unaffected mother, shows normal expression of *CDKN1C* whereas INV1A and TM-87 show reduced expression of *CDKN1C*. Five normal fibroblast control samples were tested to compare the expression of the BWS patients. BW1 is a fibroblast line from a patient with BWS that has loss of methylation at IC2 and shows reduced expression of *CDKN1C* normally seen in BWS patients with this lesion.

B) Normal *IGF2* expression in Translocation and Inversion samples with BWS. Real-time PCR for *IGF2* was performed on fibroblast samples. Expression of *IGF2* was normalized to that of housekeeping genes *GAPD*, *HPRT1* and *YWHAZ* as above. Translocation and inversion patients do not show an elevation of *IGF2* expression compared to controls. Patient BWS2 is a patient with BWS, a loss of methylation at IC2 and no elevation of *IGF2* expression. Patient BWS3 is a patient with BWS and an upregulation of *IGF2* expression.

A)

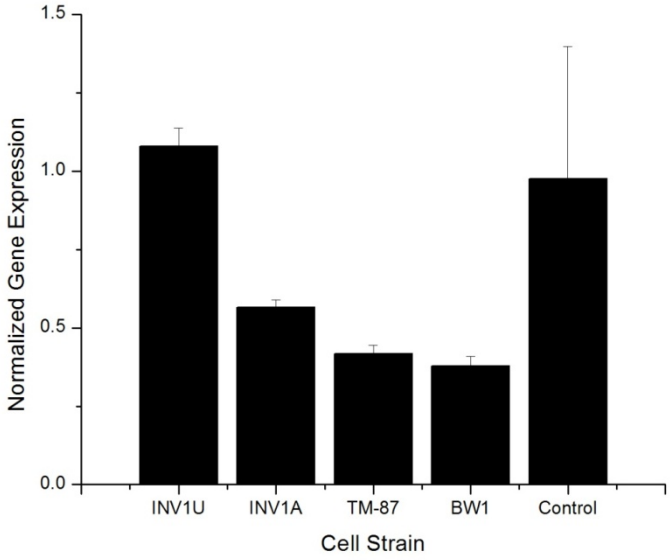

B)

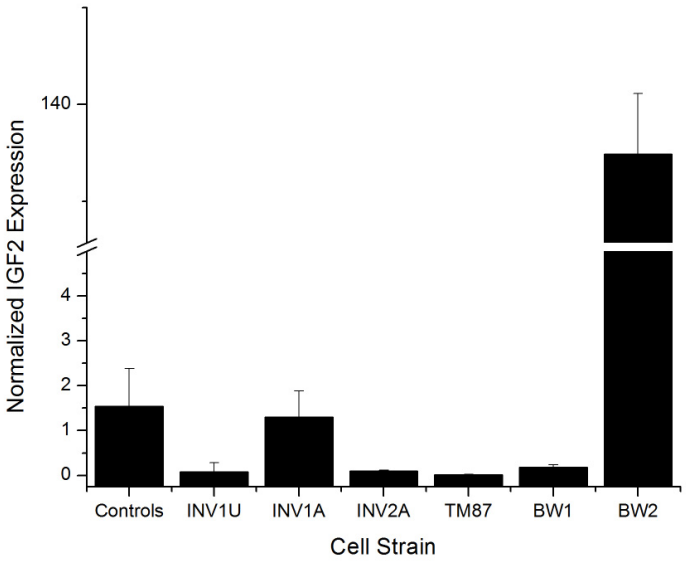

Figure 4-4. A) Reduced *CDKN1C* Expression in Translocation and Inversion samples with BWS. B) Normal *IGF2* expression in Translocation and Inversion samples with BWS.

4.4.4 No Microduplications or Microdeletions Detectable by Array Complete Genomic Hybridization in BWS-Associated Translocation/Inversion Breakpoints

We developed a custom array covering 33,000,000 base pairs of sequence from the 11pter segment of chromosome 11 to chromosome band 11p13 (chr11:1-33,000,000; hg18 Mar 2006) using Nimblegen's custom array platform. Using 300,000 features on the 385,000 feature Nimblegen custom microarray of 11pter we represented this region at an average resolution of 58bp between consecutive probes. Repetitive sequences are not represented on the array as they cross-hybridize at many genomic locations (Figure 4-5). We used the array CGH to test our hypothesis that microdeletions or microduplications may have occurred during maternal transmission. We tested the two translocation and inversion pedigrees for which we had matched tissue samples from both the mother and affected proband (INV1U/INV1A - fibroblast, T1U/T1A – lymphoblastoid cell lines). Despite the high level of resolution on our microarrays we were unable to detect any microdeletions or microduplications associated with the breakpoint regions in the affected probands (Figure 4-5). This indicates that the breakpoint regions are apparently balanced and do not show any rearrangement complexity. The breakpoints may be in the repetitive sequence elements but any single copy microdeletions or microduplications would have to be very small to escape detection by our custom array.

The detection of copy number variations was minimized by our study design because we used of a pooled reference DNA (Promega, Madison, WI.). However, very small

Figure 4-5: Microduplications or Microdeletions Were Not Detected by Array CGH. Array Comparative Genomic Hybridization using the 385,000 feature Nimblegen oligonucleotide microarray of the first 33 megabases of chromosome 11 is shown for four samples. The genes in the imprinted region are shown above the array results as seen in Figure 4-1 to illustrate the location of the two Domains, imprinting centres and approximate location of the rearrangement breakpoints. The location of the BAC clones that were used to verify the location of the breakpoints are shown below the gene track in addition to the location of the one potential copy number polymorphism for this region in the database of genomic variants (www.tcag.ca). Repetitive elements in the region are displayed extracted from the repeat masker track from the UCSC genome browser. The level of shading in the graphical display reflects the amount of base mismatch, base deletion, and base insertion associated with a repeat element. The higher the combined number of these, the lighter the shading. Signal ratios for each of the 300,000 CGH probes from the test and reference samples were normalized using NimbleScan and converted to $\log_2$ ratios for each probe on chromosome 11. Signals either above or below zero indicate a gain or loss of genetic material (+ 0.5 indicates a gain of 1 copy and – 0.5 indicates a loss of one copy on the $\log_2$ scale) in these samples indicating a cryptic imbalance (an imbalance undetected by conventional cytogenetic techniques such as G-banding). INV1U, INV1A, TIU and T1A showed no changes in DNA copy number in the known breakpoint region.

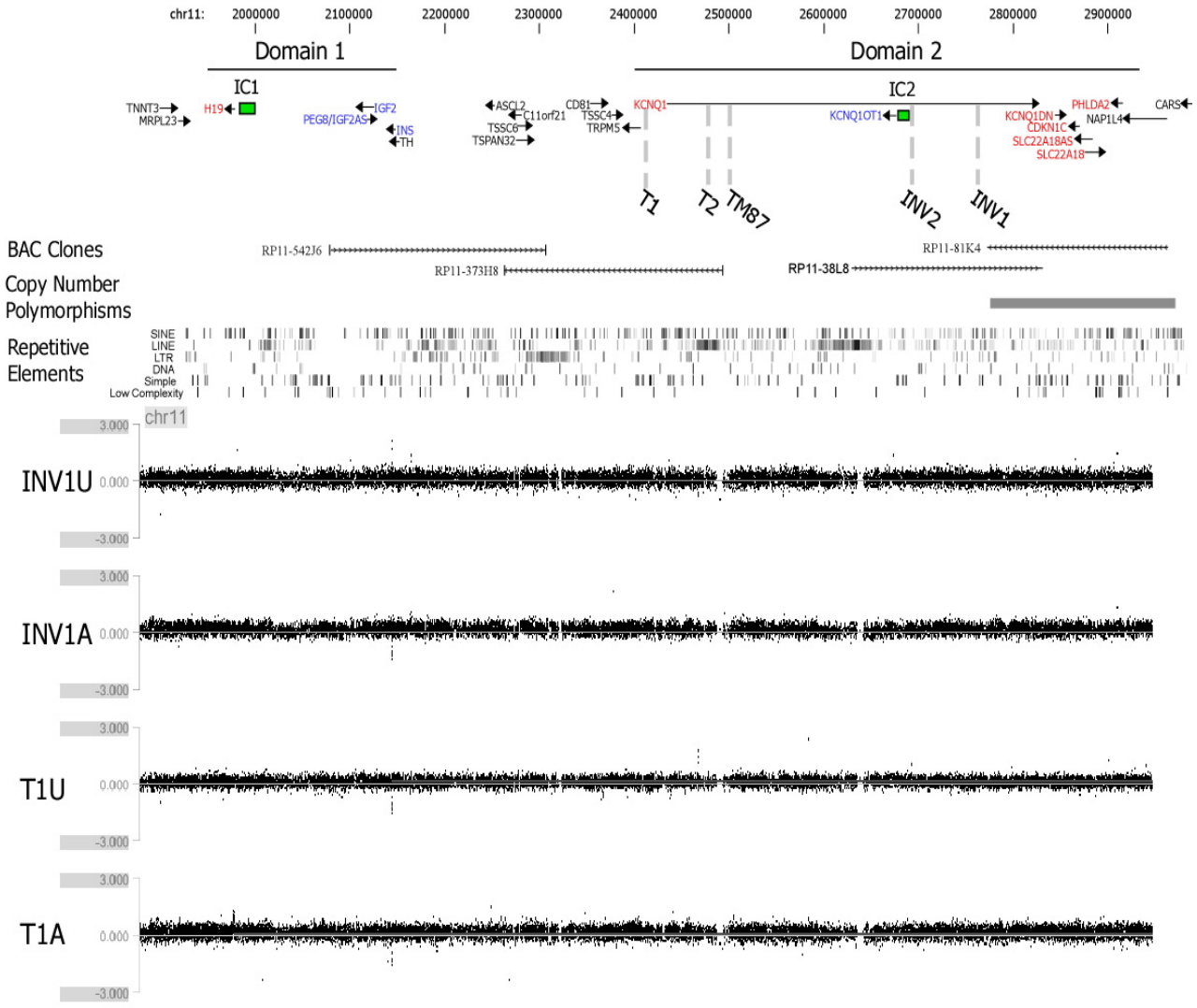

Figure 4-5. Microduplications or Microdeletions Were Not Detected by Array CGH

changes in copy number were still detected as demonstrated by the detection of a loss in two samples and a gain in one of a segmental duplication (http://genome.ucsc.edu, located at chr11:10486286-10488459) of approximately 2 kb in size (Figure 4-6).

4.4.5 Regional Gain of DNA Methylation in BWS Patients with Translocations and Inversions

In addition to the 300,000 features for array CGH we also analyzed 85,000 features for methylation using the HELP assay representing approximately 10,000 locations (Khulan et al., 2006) on the distal 33 Mb of chromosome 11p. For analysis, samples were used from pedigrees in which a maternal transmission of the translocation or inversion had occurred; provided we had the same tissue available for parent and offspring. In this way, tissue-specific methylation differences would be minimized in the analysis. In order to analyze methylation differences across samples and tissues, we compared the variability between *Msp*I representations among all arrays. The *Msp*I representation represents all the potential cut sites for *Msp*I regardless of whether they are methylated and therefore a high correlation validates our expectations. All arrays showed coefficients of determination (R^2) above 0.90 for all the analyzed lymphoblast (CNL1, CNL2, T1U, T1A) and fibroblast (CNF1, CNF2, INV1U, INV1A, INV2A) samples. This confirms previously published results of this technique (Khulan et al., 2006) and shows that the representation of the methylation insensitive enzyme *Msp*I is consistent among samples. Correlation coefficients between *Hpa*II and *Msp*I/*Hpa*II ratios are expectedly lower as methylation differences between tissues, affected and control sample methylation are reflected in this value (R^2 range = 0.4983 – 0.9235).

Figure 4-6: Detection of ~2kb Segmental Duplication Region.

Two known segmental duplication regions (UCSC Segmental Duplication at chr11:10486286-10488459) at 10.5 Mb on chromosome 11 were detected by high resolution array CGH. Normalized $\log_2$ ratios for each probe on the array are plotted on the y-axis for patients T1A, T1U, INV1A and INV1U with chromosome 11 position indicated at the top of the figure. Gains are shown as ratios above 0 and losses as ratios below 0 with (~ 0.5 gain of one copy, ~ -0.5 loss of one copy). Genes in the region are shown below the array CGH results in blue with rectangles representing exons and lines representing introns. Chevrons represent the direction of transcription. CpG islands are indicated by green boxes. The locations of repetitive sequences are shown as black bars at the bottom of the figure. Segmental duplications are defined as sequences of duplicated DNA >1kb that are >90% identical. Some segmental duplications in the human genome may be variable in their copy number (Kim et al., 2008). Patient T1U shows additional copies of this region versus the reference DNA whereas patients T1A and INV1A show less copies of this sequence versus the reference DNA.

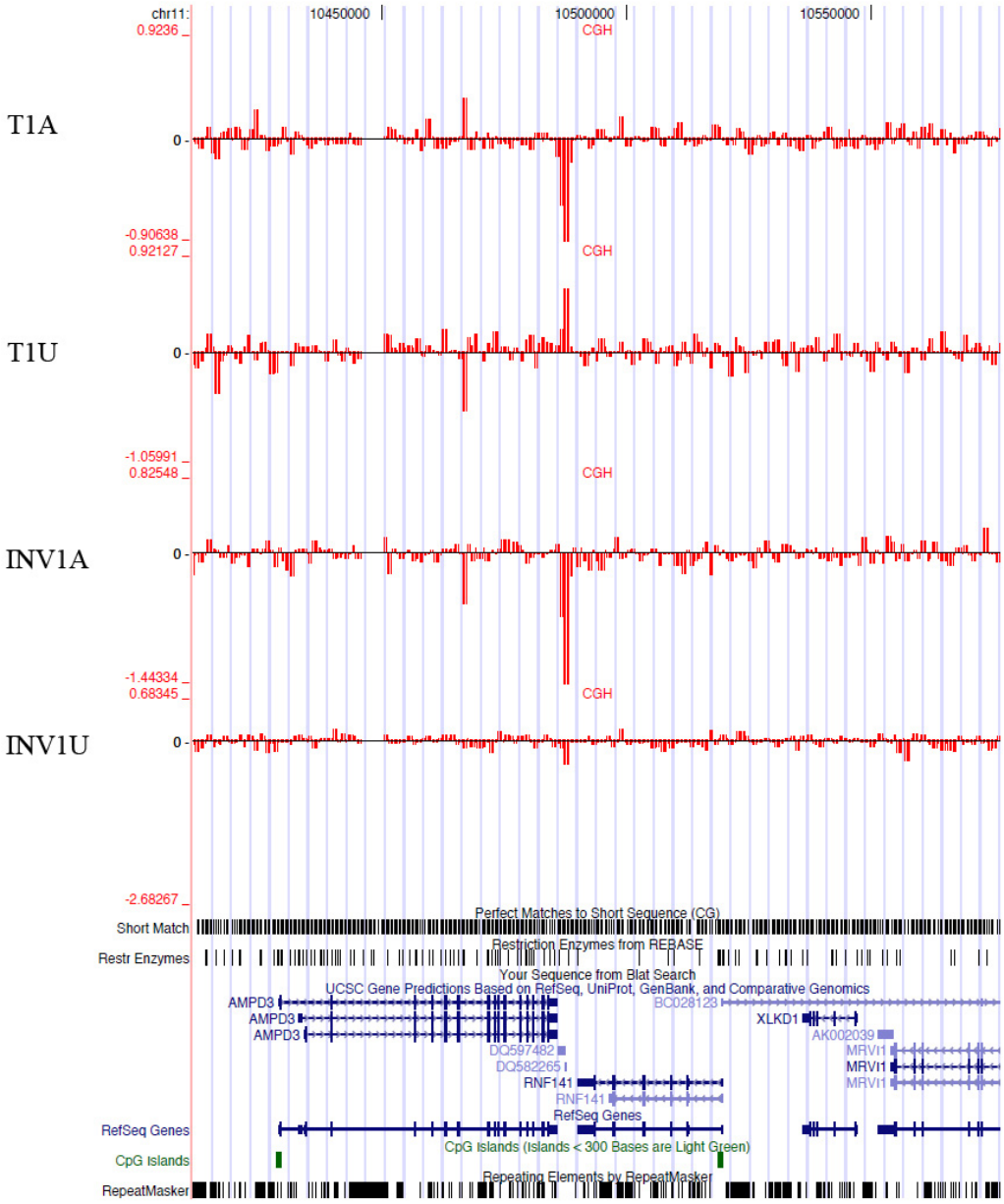

Figure 4-6. Detection of ~2kb Segmental Duplication Region.

We also observed that global patterns of DNA methylation were consistent among all cell lines as seen in Figure 4-9A and Figure 4-10A. Most CpG's in the human genome are methylated with the notable exception of CpG's that are in CpG islands (Bird, 1986; Robertson, 2005; Takai and Jones, 2002; Weber et al., 2005; Weber et al., 2007). Our samples also showed hypomethylation of CpG containing promoters and general hypermethylation of surrounding sequences (Figure 4-8).

Our hypothesis that chromosome 11p15.5 translocations and inversions cause BWS due to an alteration in one or several specific methylated regions where the methylation signature is altered in affected probands after maternal transmission was not supported. DNA methylation in translocation and inversion fibroblast samples is altered over very large genomic distances likely as a result of the translocation or inversion itself (Figure 4-8B). Methylation values for control fibroblasts were averaged and then all methylation values were substracted by the control average to aid in the visualization of the changes in DNA methylation in translocation and inversion patients. INV1A and INV2A show DNA gain of methylation throughout the BWS imprinted cluster from 1.9 Mb to 3.0 Mb. They also showed gain of methylation at 11, 16, 21-22 and 30-31 Mb. In contrast the unaffected mother, INV1U, shows regions of loss of methylation especially at 5, 16, 21-27 and 29-31 Mb illustrating that chromosomal rearrangements have long-range effects on DNA methylation. The gain of methylation of the BWS imprinted cluster is seen in the fibroblasts of both of our affected patients.

Figure 4-7: HELP Methylation Data Heat Map for 33 Megabases on Chromosome 11.

Methylation microarray results for 85,000 probes on the p-terminal of chromosome 11 (chr11:1-33,000,000) for each individual sample are shown. Each log-centred methylation ratio is the average of eight oligonucleotides. An ideogram of chromosome 11 is shown at the top of the figure, a hollow red box indicates the region represented on our microarray. The heat map shows methylation data for each individual sample where blue bars represent hypermethylation and red bars represent hypomethylation. Most CpG sites represented by the array are methylated in agreement with the observation that the bulk of the genome is methylated with the exception of CpG islands. The red bar above the heatmap represents the location of the imprinted region on chromosome 11p15.5.

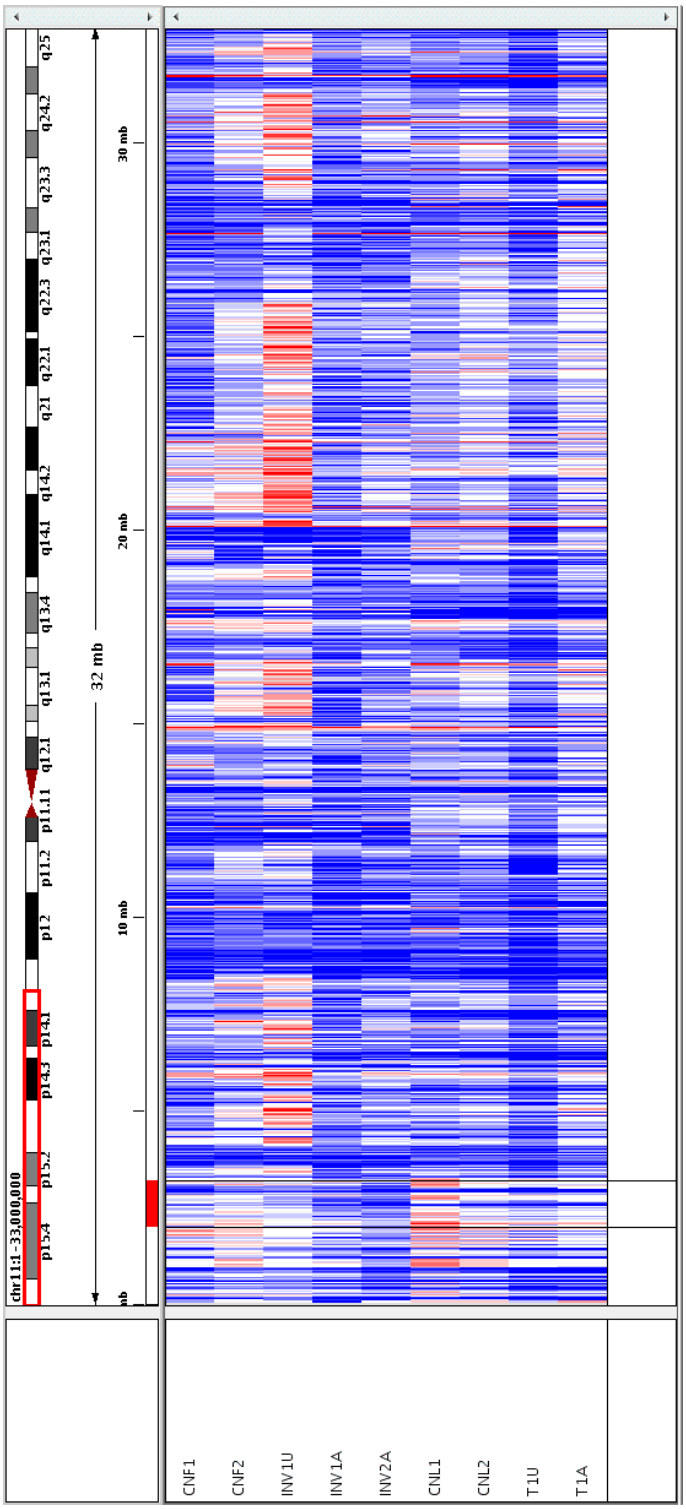

Figure 4-7. HELP Methylation Data Heat Map for 33 Megabases on Chromosome 11.

Figure 4-8: HELP DNA methylation heat map for the imprinted region on chromosome 11p15.5.

Methylation results for the imprinted region on chromosome 11 (chr11:1,900,000-3,200,000) are shown for each sample. Each log-centred methylation ratio is the average of eight oligonucleotides. An ideogram of chromosome 11 is shown at the top of the figure, a red box indicates the location of the imprinted region displayed in the heat map below. The heat map shows methylation data for each individual sample where blue bars represent hypermethylation and red bars represent hypomethylation. The location of the genes in the region are shown below the heat map is.

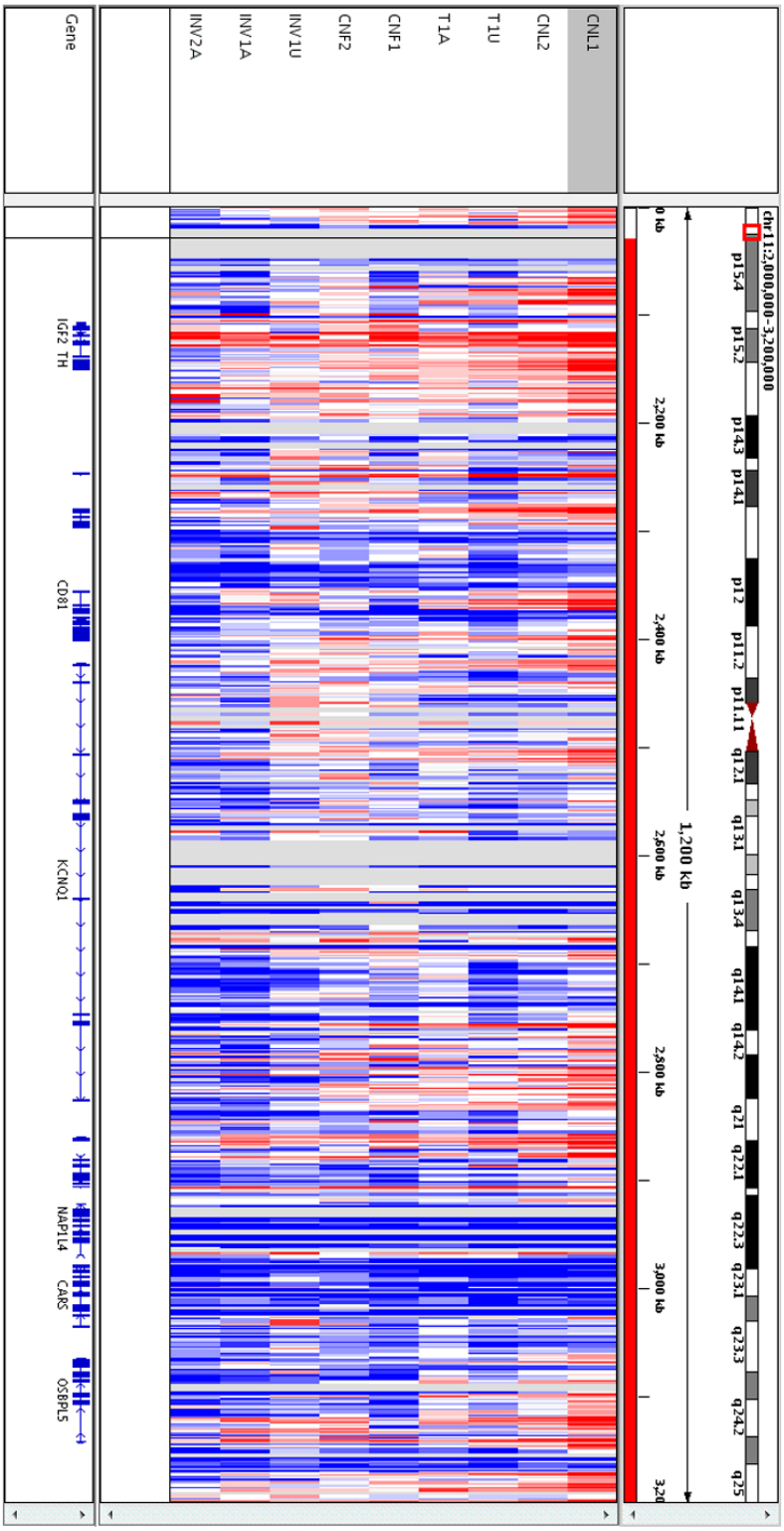

Figure 4-8. DNA methylation heat map for the imprinted region.

Figure 4-9: Translocation and Inversion Disrupt DNA Methylation in Fibroblasts

A) DNA methylation data for two control fibroblast samples (CNF1 and CNF2) are shown. DNA methylation ratios are averaged in 0.5 Mb bins and plotted on the y-axis. The first 33 Mb of chromosome 11 are represented on the x-axis. Increased DNA methylation is represented by a negative ratio and a lack of DNA methylation by a positive ratio.

B) DNA methylation in translocation and inversion fibroblast samples is shown. Control fibroblast methylation values have been averaged and then all methylation values were substracted by the control average. This conversion sets the control methylation as "zero" which aids in the visualization of the changes in DNA methylation in translocation and inversion patients. Deviations below zero represent DNA hypermethylation compared to controls and deviation above zero represent hypomethylation compared to controls. INV1A and INV2A show a gain of DNA methylation throughout the BWS imprinted cluster from 1.9 Mb to 3.0 Mb (red box). They also show regions with gains of DNA methylation at 11, 16, 21-22 and 30-31 Mb. In contrast the unaffected mother, INV1U, shows regions with loss of DNA methylation especially at 5, 16, 21-27 and 29-31 Mb illustrating that chromosomal rearrangements may have long-range effects on DNA methylation. Gain of DNA methylation in the BWS imprinted domain on chromosome 11p15.5 is seen in all affected patients.

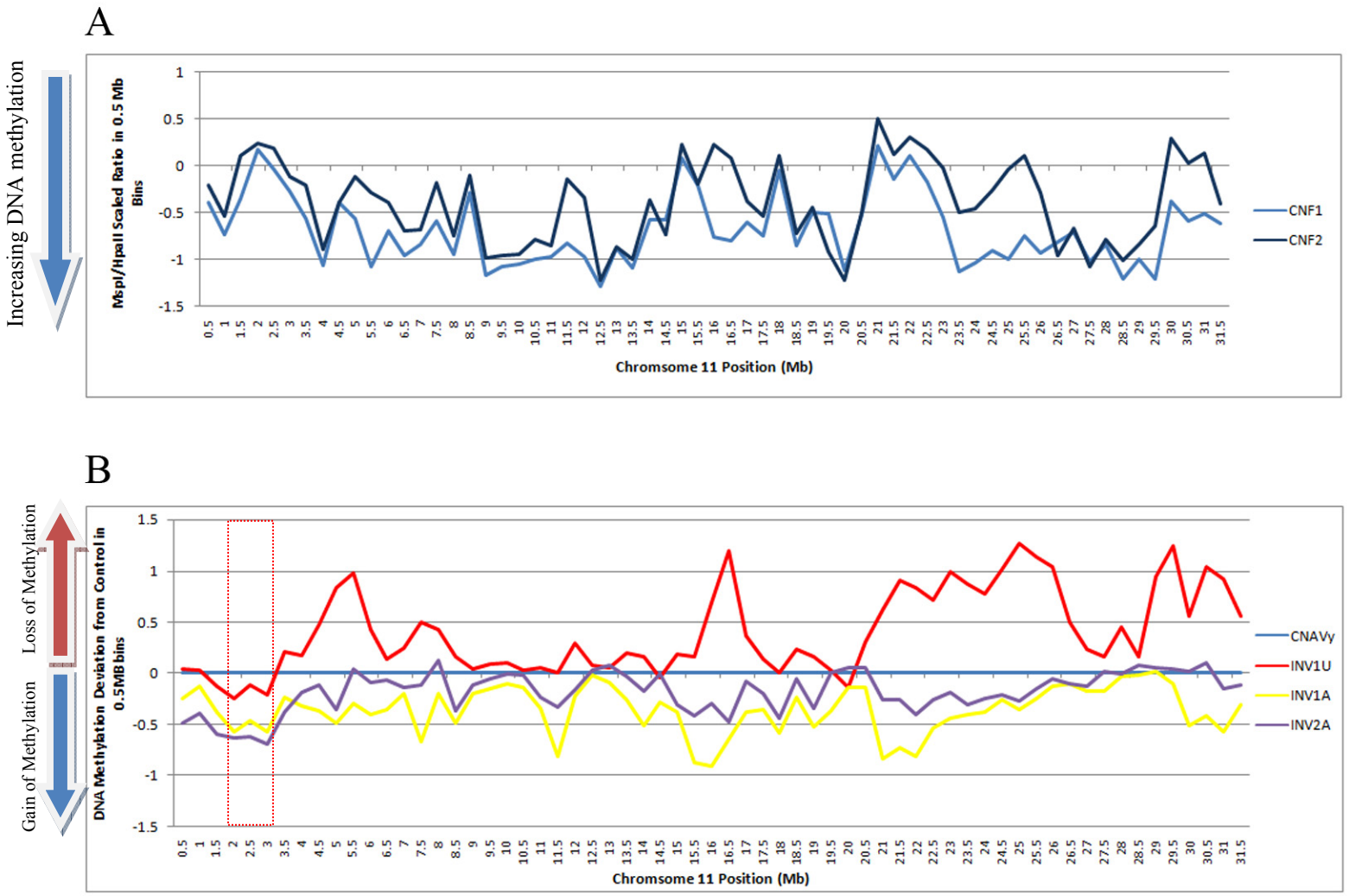

Figure 4-9. Translocation and Inversion Disrupt DNA Methylation in Fibroblasts

Figure 4-10: Translocation and Inversion Disrupt DNA Methylation in Lymphoblasts

A) DNA methylation data for two control lymphoblast samples (CNL1 and CNL2) are shown. DNA methylation ratios are averaged in 0.5 Mb bins and plotted on the y-axis. The first 33 Mb of chromosome 11 are represented on the x-axis. Increased DNA methylation is represented by a negative ratio and a lack of DNA methylation by a positive ratio.

B) DNA methylation in translocation and inversion lymphoblast samples is shown. Control lymphoblast methylation values have been averaged and then all methylation values were subtracted by the control average. This conversion sets the control methylation as "zero" which aids in the visualization of the changes in DNA methylation in translocation and inversion patients. Deviations below zero represent gain of DNA methylation compared to controls and deviation above zero represent hypomethylation compared to controls. T1U and T1A show a gain of DNA methylation from the 11p terminal throughout the BWS imprinted domain (red box) to 4.0 Mb. After 4.0 Mb T1A methylation returns to control levels whereas T1U has higher levels of DNA methylation for the sequence represented on the microarray with DNA methylation trending towards control levels of methylation. T1U is unaffected with BWS despite showing higher levels of DNA methylation in the BWS region, however the translocation may be on the paternal chromosome whose genes are normally silent in this region and may not have an effect.

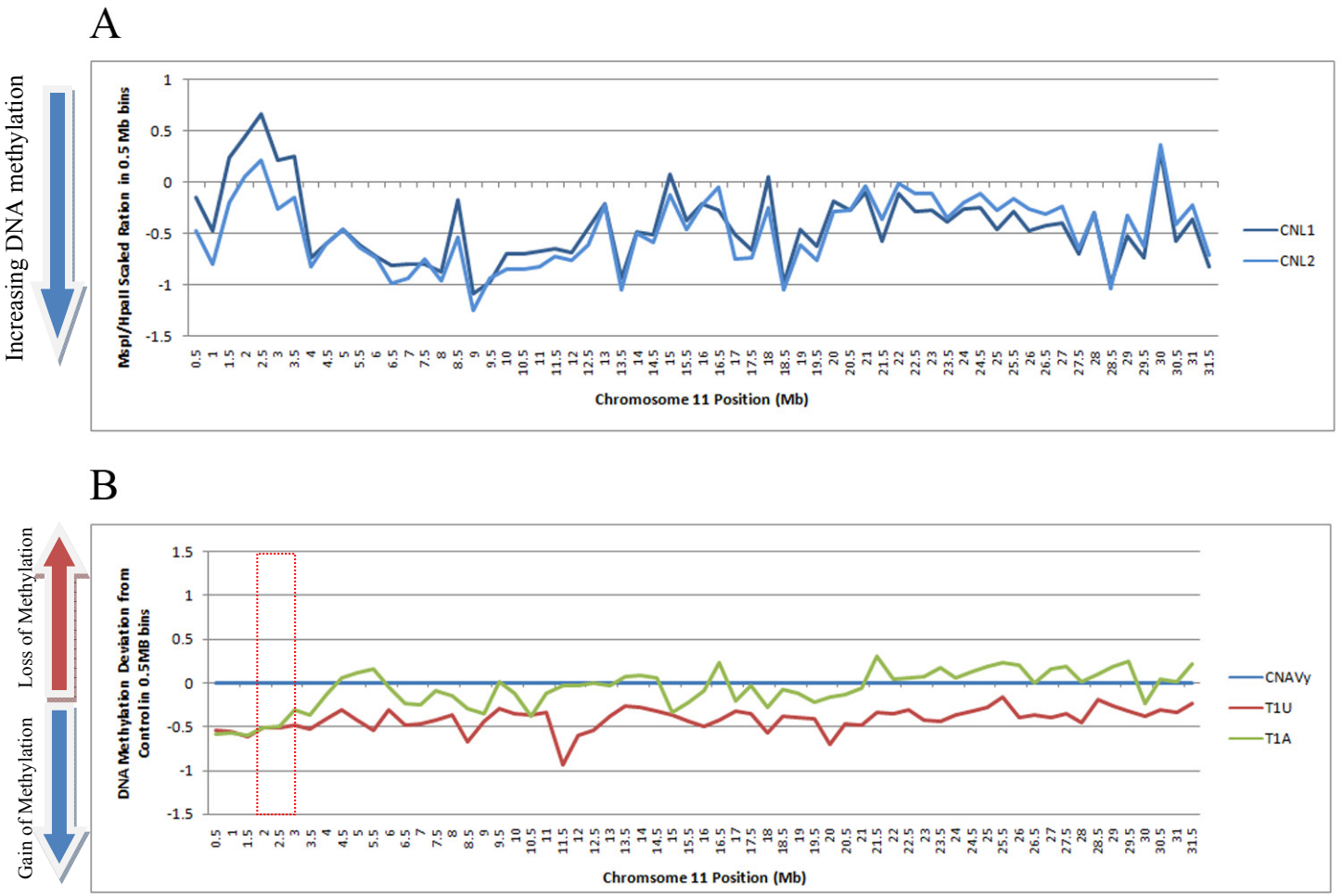

Figure 4-10. Translocation and Inversion Disrupt DNA Methylation in Lymphoblasts

DNA methylation in lymphoblast samples from BWS cases with translocations were converted as the fibroblast samples to illustrate the changes in DNA methylation (Figure 4-10B). T1U and T1A show gain of DNA methylation from the 11-pter throughout the BWS imprinted cluster to 4.0 Mb. After 4.0 Mb T1A methylation returns to control levels whereas T1U has gain of methylation for the rest of the chromosome 11 that was investigated with DNA methylation trending towards control levels of methylation with increased distance from the translocation breakpoint. T1U is unaffected with BWS despite showing a gain of DNA methylation in the BWS region. However the T1U translocation should be on the paternal chromosome whose genes are normally silent in this region and may not have an effect.

Analysis of CpG island methylation in gene promoter regions shows that the majority of CpG islands located near a gene promoter that were represented on the array are unmethylated (Figure 4-11). There are 408 CpG islands in the first 33 megabases of chromosome 11 and 110 are located near a gene promoter for which DNA methylation data was available. An inspection of the data for the CpG islands shows that in all samples >50% of CpG islands are unmethylated. Further, a small number of CpG islands are methylated in a tissue specific manner, i.e. completely unmethylated in lymphoblasts and methylated in fibroblasts or vice versa. Further several CpG islands located in the first 4 megabases of chromosome 11 appear to have variable patterns of DNA methylation among samples indicating that DNA methylation may not be tightly regulated in these specific regions in this particular tissue. No CpG island within the

Figure 4-11: Changes in DNA Methylation Do Not effect CpG Islands

A) The first 33 megabases of chromosome 11 has 405 CpG islands defined by the UCSC genome browser (for CpG island definition and criteria see Chapter 1, page 6). Gene promoters that were associated with CpG islands were selected and merged with methylation microarray data using the Galaxy Bioinformatics package developed by Penn State University (http://galaxy.psu.edu). 110 CpG islands that were associated with a promoter region and were represented on the array were selected. A heatmap showing the methylation status for those CpG island containing promoters are shown where red represents unmethylated DNA in a gradient towards blue representing methylated DNA. The majority of CpG islands that are associated with gene promoters are unmethylated.

B) Percentage of gene promoters in CpG islands that are methylated and unmethylated in fibroblast samples. There is a slight decrease in CpG promoter methylation in INV1U showing ~55% unmethylated CpG islands compared to the other samples which all show between 65%-70% unmethylated CpG islands.

C) Percentage of gene promoters in CpG islands that are methylated and unmethylated in lymphoblast samples. CNL1 shows a higher number of unmethylated CpG islands at 80% whereas CNL2, T1U and T1A show 65%-70% of CpG islands unmethylated.

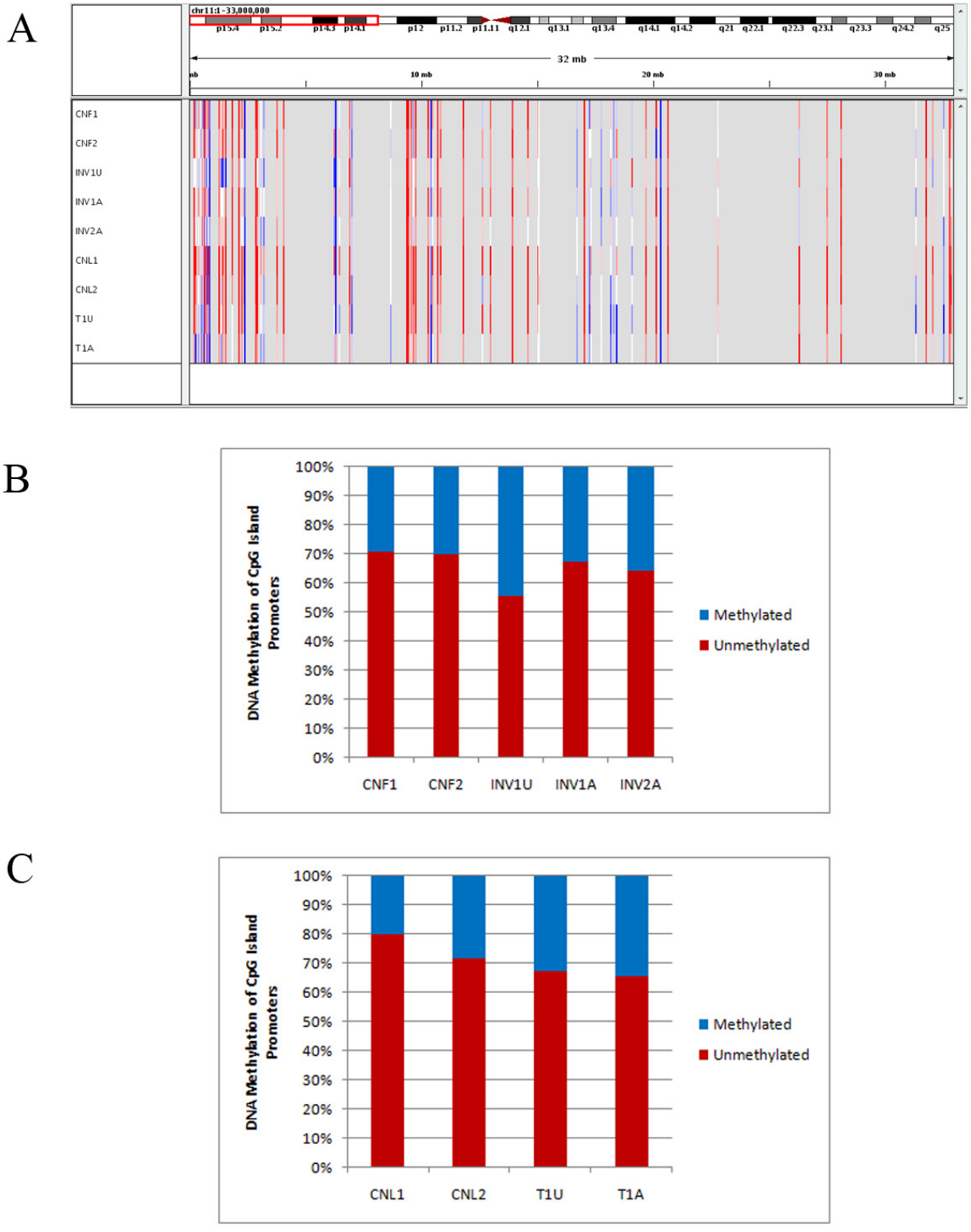

Figure 4-11. Changes in DNA Methylation Do Not Affect CpG Islands

imprinted cluster on chromosome 11p15.5 showed a methylation change in either the fibroblast or lymphoblast samples that was specific to the affected probands.

4.5 Discussion

Although chromosomal aberrations in Beckwith-Wiedemann syndrome are rare (1-2% of all BWS cases) such cases provide excellent opportunities for studying the pathomechanisms of BWS and elucidating more generally the control of imprint regulation in humans. We present data that translocations and inversions associated with Beckwith-Wiedemann syndrome and involving the *KCNQ1* gene on chromosome 11p15.5 upon maternal transmission induce a regional gain of DNA methylation (Figures 4-9B and Figure 4-10B) and changes in imprinted gene expression (Figure 4-4). This result demonstrates that long-range epigenetic defects occur in these patients that can alter the transcription of *CDKN1C*.

Although changes in DNA methylation are detected over large distances in patients with translocations and inversions, the methylation of CpG island promoter regions remains largely unchanged. It is likely therefore that the expression of most genes on the derivative chromosome 11, outside the imprinted region, is not altered. The imprinted region on chromosome 11p15.5 is likely more susceptible to position effect for two reasons. Firstly, imprinted genes are expressed normally from only one allele and are dosage sensitive. So any perturbation to the active allele can substantially change the amount of transcript. Secondly, the expression of imprinted genes on chromosome 11p15.5 is under long-range control from both of the imprinting centres (IC1 and IC2). In fact, the maternal allele may be much more susceptible to changes in the local chromatin environment because of the long-range regulation of imprinted genes that are normally only expressed from the maternal allele explaining the disruption of gene expression only after maternal transmission. It could also explain why some rare translocations that do not

occur in the *KCNQ1* gene body, like B10.1 t(4;11)(p15.2;p15.4) (Hoovers et al., 1995), can cause BWS by imposing a long-range position-effect on this region.

Recent microarray data have shown that cytogenetically balanced translocations and inversions can have rearrangement complexity resulting in a phenotype (Gribble et al., 2005; Sismani et al., 2008). We hypothesized that the BWS breakpoint region may be associated with just such microdeletions and microduplications. These genomic alterations could disrupt genomic imprinting in this region by changing the copy number of critical elements contained within the *KCNQ1* gene. This hypothesis was not supported by our array CGH analysis as no such genomic alteration was detected. It is possible, however, that small gains or losses may have been missed because no repetitive sequence was represented. Within the breakpoint regions in the *KCNQ1* gene are several large blocks of repetitive sequence (for examples, see Figure 4-5, repetitive elements at approximately 2.5 and 2.6 megabases chromosome 11 position). Although we were unable to put these sequences on the array it is also not likely that they contain conserved elements critical for imprint regulation. In addition it is also possible that the breakpoints may indeed be balanced or essentially so causing no noticeable change in copy number even at the high resolution available on our custom microarray.

Further refinement of the breakpoints in these rearrangements would help elucidate the mechanisms by which rearrangements occur in this region. Some recurrent rearrangements are caused by the presence of low copy repeat sequences mediating non-allelic homologous recombination. This mechanism was suggested by Russo et al (Russo et al., 2006) to potentially mediate unbalanced rearrangements causing BWS that they detected; however, there are no

segmental duplications within the gene *KCNQ1*. Since a majority of BWS causing translocations and inversions breakpoints are inside *KCNQ1* it is likely that another mechanism may be responsible. In fact, non-homologous end joining has been demonstrated to be the preferential mechanism to repair double strand breaks which can often result in genomic rearrangements (Povirk, 2006). The *KCNQ1* introns contain several blocks of repetitive sequence and Alu type repeat elements. These repetitive elements are the most numerous family of repetitive elements (1 every 4kb) and when double strand breaks occur next to identical Alu elements, translocations occur at high frequencies (Elliott et al., 2005). The location of Alu elements in *KCNQ1* is more consistent with the location of balanced maternally transmitted translocations and inversions. Regions with high GC content, like Alu repeat sequences, near B-Z DNA transitions provide a much more likely explanation as to the mechanism of formation of translocation and inversion associated with BWS (Gajecka et al., 2006). To resolve this question, however, would require determining the exact sequence at each of the breakpoints. Therefore, although a further refinement of the breakpoint mechanism would be very interesting in determining the mechanisms involved in recurrent breakpoints in this region associated with BWS the hypothesis that microdeletions and microduplications are causative for BWS in translocation and inversion patients is unlikely. Since balanced rearrangements can be carried on the paternal allele without apparent phenotypic consequence it lends further support to the hypothesis that upon maternal transmission of a balanced rearrangement an epigenetic alteration on the derivative chromosomes is taking place.

Maternal transmission of all the identified balanced translocations and inversions is required for disease in the cases studied (Hoovers et al., 1995; Norman et al., 1992; Sait et al., 1994; Squire et

al., 2000; Weksberg et al., 1993b). Although reports in the literature also describe unbalanced translocations and inversions associated with BWS, such samples were intentionally excluded here as the gains or losses of paternal or maternal chromosomal material would clearly alter the balanced contribution of maternal and paternal gene expression. Subjects without an apparent imbalance of parental material were of highest interest to look for disruption of imprinting regulation. In the case of balanced translocations and inversions the pathogenesis of BWS could be one of two distinct possibilities. The first possibility was that the translocation or inversion with disruption of the *KCNQ1* gene separated enhancers and chromatin regulatory elements that are crucial for the correct expression of maternally expressed genes in IC2. This hypothesis is supported by decreased expression of *CDKN1C* seen in translocation and inversion patients with BWS for whom we had fibroblast tissue and were able to test. Since the translocation on the paternal chromosome would not disrupt the expression of the maternally expressed imprinted genes in most tissues it would have a silent phenotype unless the breakpoint on the partner chromosome of the translocated or inverted 11 disrupted another gene or regulatory sequence. This would cause phenotypes or a syndrome other than Beckwith-Wiedemann.

The second possible mechanism is that translocations and inversions cause a long-range position-effect altering the chromatin conformation on the maternal allele in Domain 2 and downregulating the expression of *CDKN1C*. This mechanism is supported by data published by Diaz-Meyer and colleagues showing that some cases of BWS had a closed chromatin conformation at *CDKN1C* independently repressing the expression of this gene without any other detectable genetic or epigenetic alteration (Diaz-Meyer et al., 2005). Since the majority of imprinted genes on 11p15.5 are maternally expressed, the maternal chromosome may exhibit a

more open chromatin conformation relative to the paternal chromosome. When a translocation or inversion occurs and is then passed through the maternal germline the position effect induced by a rearrangement could silence the normally active maternal alleles of imprinted genes an effect that may spread along the chromosome *in cis* and may be comparable to the observations seen with translocations involving the inactive X and autosomal chromosomes where the increased DNA methylation and compacted chromatin associated with the inactive X spread into the autosome thereby inactivating genes and changing the local chromatin conformation.

Differential packaging of genetic information into chromatin defines the accessibility of DNA for transcription. This is dependent on many factors including DNA methylation, various histone modifications, nucleosome remodeling and features imposed by non-coding RNA molecules (Costa, 2008; Ebert et al., 2006). These epigenetic processes therefore are mechanisms that control the context of gene expression in many situations including normal development, tissue differentiation and also disease states.

Position-effect variegation (PEV) has been well documented in Drosophila and genetic dissection of PEV has allowed the identification of basic molecular mechanisms associated with the establishment of heterochromatic chromatin domains. A well documented case of PEV in Drosophila involves the inversion on the X chromosome that juxtaposes the white gene near the heterochromatin distal to the nucleolus organizer region (Howe et al., 1995; Wallrath and Elgin, 1995). Clonal transcriptional repression produces a variegated white eye phenotype.

When genomic rearrangements occur in barley plants, large-scale DNA methylation remodeling of the chromosomes occurs (Ruffini Castiglione et al., 2008) similar to the results we found in translocation and inversion patients with BWS. Specific translocations in barley that disrupt nucleolar organizer regions have been demonstrated to repress gene expression (Georgiev et al., 2001). Thus, if euchromatic regions are juxtaposed adjacent to the constitutive heterochromatin by a chromosomal rearrangement, spreading of the heterochromatic chromatin state into the euchromatic region can result in gene silencing. This may result from either a disruption of normal boundary elements that regulate chromatin domains or, perhaps, as a consequence of maintaining functional chromatin structure.

We demonstrate that translocations and inversions disrupting imprinted domains can result in regional changes in DNA methylation and dysregulation of imprinted gene transcription in a parent-of-origin specific manner resulting in disease. This illustrates that rearrangements of DNA, including translocations and inversions may alter chromatin packaging causing human disease. This finding is also especially relevant in light of recent findings with copy number variations that may change genomic structure, DNA methylation or chromatin context over large distances.

Chapter 5: Future Directions

5.1 Genomic Imprinting and Epigenetics

During the last several years, interest in the study of epigenetics has grown tremendously. New technologies that have increased both capacity and speed of data generation in this area will soon allow many questions previously unfathomable in complexity to be addressed. Studying the epigenome in living organisms is complicated by the fact that, unlike DNA, the epigenome can change its signature in different cell types, in response to developmental signals, but also to environmental exposure and in disease processes. Unravelling the complexity and coordination of the factors that are involved in epigenetic processes has the potential to benefit our understanding of disease processes and the development of targeted treatments for epigenetic signals.

5.1.1 Imprinting Regulation on 11p15.5

A great deal of progress has been made in identifying key regulatory elements of imprinting on chromosome band 11p15.5. Despite this progress, however, a clear model for the regulation of IC2 is still required. Even for IC1, where the enhancer blocking model involving CTCF has been demonstrated, not all observations can be rationalized. For example, there are still BWS cases that have changes in *IGF2* expression or imprint status without a concomitant change in methylation at IC1 (see Figure 1-5). From mouse studies, it has been demonstrated that *Kcnq1ot1, Cdkn1c, Kcnq1, Slc22a18,* and *Phlda2* are imprinted in both embryo and placenta whereas genes located further from IC2 are imprinted only in placenta (Lewis et al., 2004). The factors involved in mediating the temporal and spatial aspects of gene imprinting are only beginning to be investigated. Regional control of gene expression over large distances is known to involve chromatin structure and the 3-dimensional positioning of chromosomes in the nucleus. Chromosomes have been recently demonstrated to occupy specific chromosome territories and

even to pair routinely with heterologous chromosomes (Brianna Caddle et al., 2007). Therefore the molecular basis of chromosome pairings and their functional consequences when disrupted by chromosomal rearrangement is an interesting area of current research. The clinical implications of cytogenetically detectable alterations of chromosomes cannot always be predicted based on knowledge of the rearrangement. Discordant phenotypes may arise in family members who appear to have the same rearrangement. Further, understanding the clinical implications of smaller rearrangements and variations of genomic structure will require a great deal more research, not just at the level of DNA, but clearly also at levels of epigenetic changes and gene expression levels. Therefore, a multifaceted approach using animal model systems as well as human samples to dissect the roles of genomic imprinting and epigenetics will continue to enhance our understanding of chromosome structure and function.

5.1.2 **Translocations and Inversions in BWS**

Significant advances in the understanding of biological mechanisms (such as X-inactivation) have been made possible by the study of rare patient samples with cytogenetic abnormalities. Maternally transmitted translocations and inversions that have breakpoints within the *KCNQ1* gene are a rare cause of Beckwith-Wiedemann syndrome. Despite their rarity, they provide a unique opportunity to ask questions and examine hypotheses about epigenetics and imprinting. Continued investigation is not only important in the context of elucidating mechanisms involved in imprinting and epigenetics but also in a more general context our understanding about how genome rearrangement may have consequences that extend well beyond the breakpoints. It is important to think about all genome rearrangements not only including translocations and inversions but many others (such as CNVs) and their impact on the epigenetic regulation of

genome stability and gene function. As such, several interesting areas for further research are immediately evident based upon the data generated in Chapter 4 which are described below.

5.1.3 **Nucleotide Level Sequencing of Breakpoints and Mechanism(s)**

In order to continue to study the regulation of the 11p15.5 imprinted cluster in the BWS associated translocations and inversions, a further refinement of the breakpoint regions would be very important. Further refinement of the breakpoints in these cases could be accomplished by arrays using two techniques. Firstly, chromosomes labeled with Hoescht and chromomycin could be flow sorted based on size and then the normal and derivative chromosomes could be differentially labeled with Cy3 and Cy5 and hybridized to microarrays for fine mapping of breakpoints. This technique, used in Gribble et al (Gribble et al., 2005), is technically demanding and requires specialized FACS apparatus. It would also be complicated in our case due to the fact that chromosome 11 is a mid-sized chromosome which is generally not easily discriminated from chromosomes 9, 10, 12, and 13. Alternatively, isolating the normal and derivative chromosome 11s could be accomplished using monochromosomal hybrids constructed in rodent cell lines which could then be hybridized to microarrays. Although both of these strategies would allow us to refine the breakpoint regions they would be more costly than a more traditional approach (below) and still require sequencing of the breakpoints.

Therefore, the easiest approach would be to continue to refine the breakpoints using BAC or fosmid FISH mapping. Since the breakpoints have all been localized to one BAC clone already, using several overlapping BAC and fosmid clones would further delineate the breakpoint region and make it a more manageable interval in order to proceed with cloning the breakpoints. Then the use of a technique such as long-range inverse PCR or the TOPO Walker kit (Invitrogen)

would enable the breakpoints to be readily amplified. PCR products could then be sequenced by traditional automated sequencing.

Examination of the breakpoints will likely reveal interesting elements regarding the structure of the sequence and the motifs present that mediate rearrangement at this locus. Gajecka et al (Gajecka et al., 2006) published a study of the breakpoints of four patients with translocations involving chromosomes 1 and chromosome 9 - t(1;9)(p36.3;q34). Of note, they reported that the translocations were balanced aside from very small (~5bp) insertions and duplications at the breakpoints. The same insertions and duplications were also found in the unaffected parents. This indicates that non-homologous end joining is the likely mechanism for repair and the two chromosomes were repaired with relatively high fidelity. By completing the breakpoint sequencing on the BWS rearrangements an analysis of the DNA sequence features that flank the breakpoints could be determined to facilitate our understanding of why breakpoints associated with BWS cluster within the gene *KCNQ1*.

To further elucidate what mechanisms predispose to chromosome 11p15.5 rearrangements at this locus and the elements involved in the pathophysiology of BWS, a larger collection of BWS rearrangements could be studied to help expand on the few reports in the literature. Russo and colleagues published two cases identified in a screen of 70 BWS trios. Apparently balanced translocations transmitted from the father resulted in cryptic duplications (i.e. not detectable by standard G-banded karyotype) in the probands (Russo et al., 2006). After identifying the approximate breakpoints by FISH, the authors concluded that the cryptic duplications were mediated by segmental duplications. A more comprehensive study of cryptic paternally derived

rearrangements would be required to validate their hypothesis. Additionally, this may also indicate that cryptic rearrangements are more common than is currently estimated (<1% of BWS cases) and would require a larger sample and more intensive cytogenetic and molecular studies to test for the frequency of such rearrangements. Interestingly, a recent report of a BWS series from Japan suggested that their patients had a much higher rate of chromosomal abnormalities (13% vs. 2% in the North American and European series) and that larger studies of rearrangements associated with BWS may indeed be fruitful (Sasaki et al., 2007). This is important because we may be underestimating the role of inherited rearrangements in BWS and this may alter the risk of recurrence for BWS in subsequent pregnancies.

5.1.4 **Effect of Chromosomal Rearrangements on Gene Expression in BWS**

DNA methylation plays an important role in genome stability and gene expression regulation. Chromosomal rearrangements associated with BWS disrupt DNA methylation over several megabases on chromosome 11. Normal functioning of the imprinted domain requires boundary and insulator sequences that when disrupted by chromosomal rearrangement causes a spreading of DNA methylation and possibly heterochromatinization. It would be of great interest to determine the gene expression profile of all the genes on the p-arm of chromosome 11 to determine if the effect of the observed alterations in DNA methylation also alters the expression of chromosome 11 genes. Studying the pattern of gene expression dysregulation in this context would be valuable in building models of human transcriptional regulation in this domain. The easiest approach would be to use gene expression microarrays to investigate changes in gene expression. It is worthwhile to consider that although DNA methylation patterns are changed over a large region it has been demonstrated that promoter DNA methylation has the most profound influence on gene expression (Weber et al., 2005; Weber et al., 2007). With gene

expression data a comparison of DNA promoter methylation to expression could be performed and would likely show a high correlation between promoter DNA methylation and gene expression. Whether maternally transmitted translocations or inversions associated with BWS significantly alter promoter methylation over large distances and change gene expression is an important question to be resolved. Significant changes to gene expression in regions outside the imprinted cluster would suggest that BWS patients with chromosomal rearrangements might have a more complex phenotype. This, however, does not appear to be the case as the patients presented here have clinical features comparable with BWS patients without chromosomal rearrangements.

5.1.5 **Histone Tail Modifications and Chromosomal Alterations**

My demonstration that maternally transmitted translocations and inversions associated with BWS have regional DNA gain of methylation in the imprinted domain on chromosome 11p15.5 suggest that histone tail modifications may also be altered. It would be of interest therefore to use similar array techniques (as used in Chapter 4) to examine this issue in translocation and inversion patients with BWS using chromatin immunoprecipitation for acetylated histone H3 and H4 and methylated histone H3 lysine 4 and lysine 9. An examination of these histone tail modifications would give an excellent picture of the chromatin conformation in control as well as in translocation and inversion patients. I predict that in patients with translocations and inversions with BWS that they will have decreased histone acetylation, decreased H3 lysine 4 methylation and increased H3 lysine 9 methylation corresponding with regions of increased DNA methylation.

In the above mentioned experiments close examination of the histone tail modifications at IC1 and IC2 would help shed additional light on the regulatory mechanisms at work normally in these regions as well as their dysregulation in BWS patients with chromosomal rearragements. In most translocation and inversion patients with BWS the methylation at these imprinting centres is unchanged indicating that the establishment and maintenance of DNA methylation is not affected by the chromosome rearrangement. However, chromatin modification can occur in the absence of changes of DNA methylation at imprinting centres in patients with BWS (Diaz-Meyer et al., 2005). This then could answer an important question about the mechanism of disease in these patients. If DNA methylation at the ICs is unchanged but histone modifications are changed it indicates that although these two systems often cooperate they can be uncoupled, as was discovered by Diaz-Meyer and colleagues. The downregulation of *CDKN1C* seen in translocation and inversion BWS cases could be achieved by changes in chromatin conformation without alteration in DNA methylation at IC2. If, however, histone tail modifications are also unchanged at this locus, downregulation of *CDKN1C* must occur by another mechanism, such as the disruption of a promoter-enhancer interaction secondary to the translocation or inversion breakpoint. This would demonstrate in the human what has only been demonstrated in mouse to date, that the regulation of *CDKN1C* is in part controlled by distant elements likely in the 5' region of *KCNQ1*.

5.1.6 **Intra- and Inter-chromosomal Conformation**

Regional chromatin modifications seen on human chromosome 11p15.5 in BWS associated translocations and inversions is evidence that the structure/function of the genome responds dynamically to rearrangements in the chromosomes. What is less clear at the present time is the

intra- and inter-chromosomal interactions that can occur between different regions. Recent publications indicate that chromosomal loci can have multiple interactions in *cis* and *trans* with a variety of chromosomal regions in a tissue-specific manner (Simonis et al., 2006). Studying translocations and inversions that cause disease and how these disrupt the interactions with other chromosomal regions will give significant insights into nuclear architecture and the dynamics that may be disrupted by rearranging material in the nucleus.

IC2 has been shown to have CTCF binding sites (Fitzpatrick et al., 2007), silencers and enhancer sequences within the IC itself (Du et al., 2003). However, experiments in mice have illustrated that distant elements are also required for the correct expression of imprinted genes in mice (John et al., 2001). A combination of approaches will be necessary to expand our understanding of the regulation of this region and the biological mechanisms that are at work. Identification of shared elements, such as enhancers, may be accomplished in part by computational approaches that can then be validated with in vitro or in vivo experiments. Further regulatory elements may be identified using chromatin conformational capture techniques using the *KCNQ1OT1* promoter or other imprinted gene promoters as bait sequences to find out how the 11p15.5 imprinted cluster interacts in the 3-dimensional domain of the nucleus. These experiments are complicated by the lack of a human model system that can represent the entire imprinted cluster to help functionally validate these results. Dr. Andrea Riccio has been working on a yeast artificial chromosome system to do just this kind of validation. However, problems with stability of this system have caused him to abandon this approach (personal communication). Still, individual elements can be validated using smaller more stable systems and also model organisms, such as

mouse, could be used. Therefore, the use of unique BWS clinical samples will provide natural model systems that can drive the development of hypotheses about the regulation of this region.

5.1.7 **Other Chromosomal Rearrangements**

The examination of diseases other than BWS that occur in conjunction with chromosomal rearrangements should also prove to be quite interesting. It is likely that many such rearrangements cause large scale changes in epigenetic marks. For some conditions and syndromes this may shed light on the variability of the phenotypic presentation or identify genes that impact phenotype and therefore must be part of the "critical" breakpoint region. This can be accomplished by breakpoint mapping and confirmation of long-range position-effects or epigenetic modifications that impact gene expression.

5.2 Conclusions

In diseases like cancer where genomic rearrangements are frequent and teasing out the mechanisms can be tedious, work on single chromosomal rearrangements (like those presented here) and their genomic consequences can help our understanding of the sequence elements and various pathways that lead to disease. The future study of epigenetics in the context of chromosomal rearrangements could have many applications to our understanding of genome regulation and disease.

Chapter 6: References

Aideyan, U.O., and Kao, S.C. (1998). Case report: Urinary bladder rhabdomyosarcoma associated with Beckwith-Wiedemann syndrome. Clin Radiol *53*, 457-459.

Aleck, K.A., and Hadro, T.A. (1989). Dominant inheritance of Wiedemann-Beckwith syndrome: further evidence for transmission of "unstable premutation" through carrier women. Am J Med Genet *33*, 155-160.

Anderson, J., Gordon, A., McManus, A., Shipley, J., and Pritchard-Jones, K. (1999). Disruption of imprinted genes at chromosome region 11p15.5 in paediatric rhabdomyosarcoma. Neoplasia *1*, 340-348.

Antequera, F. (2003). Structure, function and evolution of CpG island promoters. Cell Mol Life Sci *60*, 1647-1658.

Barlow, D.P. (1997). Competition--a common motif for the imprinting mechanism? EMBO Journal *16*, 6899-6905.

Barr, F.G. (1999). The role of chimeric paired box transcription factors in the pathogenesis of pediatric rhabdomysarcoma. Cancer Res *59*, 1711s-1715s.

Barr, F.G., Chatten, J., D'Cruz, C.M., Wilson, A.E., Nauta, L.E., Nycum, L.M., Biegel, J.A., and Womer, R.B. (1995). Molecular assays for chromosomal translocations in the diagnosis of pediatric soft tissue sarcomas. Jama *273*, 553-557.

Barreto, G., Schafer, A., Marhold, J., Stach, D., Swaminathan, S.K., Handa, V., Doderlein, G., Maltry, N., Wu, W., Lyko, F.*, et al.* (2007). Gadd45a promotes epigenetic gene activation by repair-mediated DNA demethylation. Nature *445*, 671-675.

Barski, A., Cuddapah, S., Cui, K., Roh, T.Y., Schones, D.E., Wang, Z., Wei, G., Chepelev, I., and Zhao, K. (2007). High-resolution profiling of histone methylations in the human genome. Cell *129*, 823-837.

Bartholdi, D., Krajewska-Walasek, M., Ounap, K., Gaspar, H., Chrzanowska, K.H., Ilyana, H., Kayserili, H., Lurie, I.W., Schinzel, A., and Baumer, A. (2009). Epigenetic mutations of the imprinted IGF2-H19 domain in Silver-Russell syndrome (SRS): results from a large cohort of patients with SRS and SRS-like phenotypes. J Med Genet *46*, 192-197.

Bartolomei, M.S., and Tilghman, S.M. (1997). Genomic imprinting in mammals. Annual Review of Genetics *31*, 493-525.

Beatty, B., Mai, S., and Squire, J. (2002). FISH: a practical approach. (Oxford, New York, Oxford University Press).

Beaudet, A.L., and Jiang, Y.H. (2002). A rheostat model for a rapid and reversible form of imprinting-dependent evolution. Am J Hum Genet *70*, 1389-1397.

Beckwith, J.B. (1963). Extreme cytomegaly of the adrenal fetal cortex, omphalocele, hyperplasia of kidneys and pancreas, and Leydig-cell hyperplasia: Another syndrome? . Abstract, Western Society for Pediatric Research, Los Angeles, November 11.

Bergstrom, R., Whitehead, J., Kurukuti, S., and Ohlsson, R. (2007). CTCF regulates asynchronous replication of the imprinted H19/Igf2 domain. Cell Cycle *6*, 450-454.

Bernstein, B.E., Meissner, A., and Lander, E.S. (2007). The mammalian epigenome. Cell *128*, 669-681.

Best, L.G., and Hoekstra, R.E. (1981). Wiedemann-Beckwith syndrome: autosomal-dominant inheritance in a family. Am J Med Genet *9*, 291-299.

Bhattacharya, S.K., Ramchandani, S., Cervoni, N., and Szyf, M. (1999). A mammalian protein with specific demethylase activity for mCpG DNA. Nature *397*, 579-583.

Bird, A.P. (1986). CpG-rich islands and the function of DNA methylation. Nature *321*, 209-213.

Bix, M., and Locksley, R.M. (1998). Independent and epigenetic regulation of the interleukin-4 alleles in CD4+ T cells. Science *281*, 1352-1354.

Bjornsson, H.T., Brown, L.J., Fallin, M.D., Rongione, M.A., Bibikova, M., Wickham, E., Fan, J.B., and Feinberg, A.P. (2007). Epigenetic specificity of loss of imprinting of the IGF2 gene in Wilms tumors. J Natl Cancer Inst *99*, 1270-1273.

Bliek, J., Gicquel, C., Maas, S., Gaston, V., Le Bouc, Y., and Mannens, M. (2004). Epigenotyping as a tool for the prediction of tumor risk and tumor type in patients with Beckwith-Wiedemann syndrome (BWS). J Pediatr *145*, 796-799.

Bliek, J., Maas, S.M., Ruijter, J.M., Hennekam, R.C., Alders, M., Westerveld, A., and Mannens, M.M. (2001). Increased tumour risk for BWS patients correlates with aberrant H19 and not

KCNQ1OT1 methylation: occurrence of KCNQ1OT1 hypomethylation in familial cases of BWS. Hum Mol Genet *10*, 467-476.

Bliek, J., Terhal, P., van den Bogaard, M.J., Maas, S., Hamel, B., Salieb-Beugelaar, G., Simon, M., Letteboer, T., van der Smagt, J., Kroes, H.*, et al.* (2006). Hypomethylation of the H19 gene causes not only Silver-Russell syndrome (SRS) but also isolated asymmetry or an SRS-like phenotype. Am J Hum Genet *78*, 604-614.

Böhringer, S., Gödde, R., Böhringer, D., Schulte, T., and Epplen, J.T. (2002). A software package for drawing ideograms automatically. Onl J Bioinform *1*, 51–61.

Bose, B., Wilkie, R.A., Madlom, M., Forsyth, J.S., and Faed, M.J. (1985). Wiedemann-Beckwith syndrome in one of monozygotic twins. Arch Dis Child *60*, 1191-1192.

Bourc'his, D., Xu, G.L., Lin, C.S., Bollman, B., and Bestor, T.H. (2001). Dnmt3L and the establishment of maternal genomic imprints. Science *294*, 2536-2539.

Brianna Caddle, L., Grant, J.L., Szatkiewicz, J., van Hase, J., Shirley, B.J., Bewersdorf, J., Cremer, C., Arneodo, A., Khalil, A., and Mills, K.D. (2007). Chromosome neighborhood composition determines translocation outcomes after exposure to high-dose radiation in primary cells. Chromosome Res *15*, 1061-1073.

Briggs, S.D., and Strahl, B.D. (2002). Unraveling heterochromatin. Nat Genet *30*, 241-242.

Brown, C.J., and Greally, J.M. (2003). A stain upon the silence: genes escaping X inactivation. Trends Genet *19*, 432-438.

Brown, K.W., Villar, A.J., Bickmore, W., Clayton-Smith, J., Catchpoole, D., Maher, E.R., and Reik, W. (1996). Imprinting mutation in the Beckwith-Wiedemann syndrome leads to biallelic IGF2 expression through an H19-independent pathway. Hum Mol Genet *5*, 2027-2032.

Brown, S. (1986). Wiedemann-Beckwith syndrome in one of monozygotic twins. Arch Dis Child *61*, 717.

Bruce, S., Hannula-Jouppi, K., Peltonen, J., Kere, J., and Lipsanen-Nyman, M. (2009). Clinically distinct epigenetic subgroups in Silver-Russell syndrome: the degree of H19 hypomethylation associates with phenotype severity and genital and skeletal anomalies. J Clin Endocrinol Metab *94*, 579-587.

Buiting, K., Saitoh, S., Gross, S., Dittrich, B., Schwartz, S., Nicholls, R.D., and Horsthemke, B. (1995). Inherited microdeletions in the Angelman and Prader-Willi syndromes define an imprinting centre on human chromosome 15 [published erratum appears in Nat Genet 1995 Jun;10(2):249]. Nature Genetics *9*, 395-400.

Bulger, M. (2005). Hyperacetylated chromatin domains: Lessons from heterochromatin. J Biol Chem *280*, 21689-21692.

Cai, X., and Cullen, B.R. (2007). The imprinted H19 noncoding RNA is a primary microRNA precursor. Rna *13*, 313-316.

Carrel, L., and Willard, H.F. (2005). X-inactivation profile reveals extensive variability in X-linked gene expression in females. Nature *434*, 400-404.

Caspary, T., Cleary, M.A., Baker, C.C., Guan, X.J., and Tilghman, S.M. (1998). Multiple mechanisms regulate imprinting of the mouse distal chromosome 7 gene cluster. Mol Cell Biol *18*, 3466-3474.

Caspary, T., Cleary, M.A., Perlman, E.J., Zhang, P., Elledge, S.J., and Tilghman, S.M. (1999). Oppositely imprinted genes p57(Kip2) and Igf2 interact in a mouse model for Beckwith-Wiedemann syndrome. Genes Dev *13*, 3115-3124.

Chen, T., and Li, E. (2004). Structure and function of eukaryotic DNA methyltransferases. Curr Top Dev Biol *60*, 55-89.

Chien, C.H., Lee, J.S., Tsai, W.Y., and Wang, T.R. (1990). Wiedemann-Beckwith syndrome with congenital central hypothyroidism in one of monozygotic twins. J Formos Med Assoc *89*, 132-136.

Chuang, J.C., and Jones, P.A. (2007). Epigenetics and microRNAs. Pediatr Res *61*, 24R-29R.

Clayton-Smith, J., Read, A.P., and Donnai, D. (1992). Monozygotic twinning and Wiedemann-Beckwith syndrome. Am J Med Genet *42*, 633-637.

Cleary, M.A., van Raamsdonk, C.D., Levorse, J., Zheng, B., Bradley, A., and Tilghman, S.M. (2001). Disruption of an imprinted gene cluster by a targeted chromosomal translocation in mice. Nat Genet *29*, 78-82.

Coan, P.M., Burton, G.J., and Ferguson-Smith, A.C. (2005). Imprinted genes in the placenta--a review. Placenta *26 Suppl A*, S10-20.

Cohen, M.M., Jr. (2005). Beckwith-Wiedemann syndrome: historical, clinicopathological, and etiopathogenetic perspectives. Pediatr Dev Pathol *8*, 287-304.

Constancia, M., Dean, W., Lopes, S., Moore, T., Kelsey, G., and Reik, W. (2000). Deletion of a silencer element in Igf2 results in loss of imprinting independent of H19. Nat Genet *26*, 203-206.

Cooper, W.N., Curley, R., Macdonald, F., and Maher, E.R. (2007). Mitotic recombination and uniparental disomy in Beckwith-Wiedemann syndrome. Genomics *89*, 613-617.

Cooper, W.N., Luharia, A., Evans, G.A., Raza, H., Haire, A.C., Grundy, R., Bowdin, S.C., Riccio, A., Sebastio, G., Bliek, J.*, et al.* (2005). Molecular subtypes and phenotypic expression of Beckwith-Wiedemann syndrome. Eur J Hum Genet *13*, 1025-1032.

Costa, F.F. (2008). Non-coding RNAs, epigenetics and complexity. Gene *410*, 9-17.

DeBaun, M.R., Niemitz, E.L., McNeil, D.E., Brandenburg, S.A., Lee, M.P., and Feinberg, A.P. (2002). Epigenetic alterations of H19 and LIT1 distinguish patients with Beckwith-Wiedemann syndrome with cancer and birth defects. Am J Hum Genet *70*, 604-611.

DeBaun, M.R., and Tucker, M.A. (1998). Risk of cancer during the first four years of life in children from The Beckwith-Wiedemann Syndrome Registry. J Pediatr *132*, 398-400.

Delicado, A., Lapunzina, P., Palomares, M., Molina, M.A., Galan, E., and Lopez Pajares, I. (2005). Beckwith-Wiedemann syndrome due to 11p15.5 paternal duplication associated with Klinefelter syndrome and a "de novo" pericentric inversion of chromosome Y. Eur J Med Genet *48*, 159-166.

Denisova, O.V., Chernov, A.V., Koledachkina, T.Y., and Matvienko, N.I. (2007). A tag-based approach for high-throughput analysis of CCWGG methylation. Anal Biochem *369*, 154-160.

Diaz-Meyer, N., Day, C.D., Khatod, K., Maher, E.R., Cooper, W., Reik, W., Junien, C., Graham, G., Algar, E., Der Kaloustian, V.M.*, et al.* (2003). Silencing of CDKN1C (p57KIP2) is associated with hypomethylation at KvDMR1 in Beckwith-Wiedemann syndrome. J Med Genet *40*, 797-801.

Diaz-Meyer, N., Yang, Y., Sait, S.N., Maher, E.R., and Higgins, M.J. (2005). Alternative mechanisms associated with silencing of CDKN1C in Beckwith-Wiedemann syndrome. J Med Genet *42*, 648-655.

Diller, L. (1992). Rhabdomyosarcoma and other soft tissue sarcomas of childhood. Curr Opin Oncol *4*, 689-695.

Douc-Rasy, S., Barrois, M., Fogel, S., Ahomadegbe, J.C., Stehelin, D., Coll, J., and Riou, G. (1996). High incidence of loss of heterozygosity and abnormal imprinting of H19 and IGF2 genes in invasive cervical carcinomas. Uncoupling of H19 and IGF2 expression and biallelic hypomethylation of H19. Oncogene *12*, 423-430.

Dracopoli, N.C. (1994). Current protocols in human genetics (New York, NY, Wiley), pp. 2 v. (looseleaf).

Drewell, R.A., Brenton, J.D., Ainscough, J.F., Barton, S.C., Hilton, K.J., Arney, K.L., Dandolo, L., and Surani, M.A. (2000). Deletion of a silencer element disrupts H19 imprinting independently of a DNA methylation epigenetic switch. Development *127*, 3419-3428.

Du, M., Beatty, L.G., Zhou, W., Lew, J., Schoenherr, C., Weksberg, R., and Sadowski, P.D. (2003). Insulator and silencer sequences in the imprinted region of human chromosome 11p15.5. Hum Mol Genet *12*, 1927-1939.

Du, M., Zhou, W., Beatty, L.G., Weksberg, R., and Sadowski, P.D. (2004). The KCNQ1OT1 promoter, a key regulator of genomic imprinting in human chromosome 11p15.5. Genomics *84*, 288-300.

Ebert, A., Lein, S., Schotta, G., and Reuter, G. (2006). Histone modification and the control of heterochromatic gene silencing in Drosophila. Chromosome Res *14*, 377-392.

Edwards, C.A., Rens, W., Clarke, O., Mungall, A.J., Hore, T., Graves, J.A., Dunham, I., Ferguson-Smith, A.C., and Ferguson-Smith, M.A. (2007). The evolution of imprinting: chromosomal mapping of orthologues of mammalian imprinted domains in monotreme and marsupial mammals. BMC Evol Biol *7*, 157.

Eggenschwiler, J., Ludwig, T., Fisher, P., Leighton, P.A., Tilghman, S.M., and Efstratiadis, A. (1997). Mouse mutant embryos overexpressing IGF-II exhibit phenotypic features of the Beckwith-Wiedemann and Simpson-Golabi-Behmel syndromes. Genes Dev *11*, 3128-3142.

Elliott, B., Richardson, C., and Jasin, M. (2005). Chromosomal translocation mechanisms at intronic alu elements in mammalian cells. Mol Cell *17*, 885-894.

Elliott, M., Bayly, R., Cole, T., Temple, I.K., and Maher, E.R. (1994). Clinical features and natural history of Beckwith-Wiedemann syndrome: presentation of 74 new cases. Clin Genet *46*, 168-174.

Engel, J.R., Smallwood, A., Harper, A., Higgins, M.J., Oshimura, M., Reik, W., Schofield, P.N., and Maher, E.R. (2000). Epigenotype-phenotype correlations in Beckwith-Wiedemann syndrome. J Med Genet *37*, 921-926.

Fert-Ferrer, S., Guichet, A., Tantau, J., Delezoide, A.L., Ozilou, C., Romana, S.P., Gosset, P., Viot, G., Loison, S., Moraine, C.*, et al.* (2000). Subtle familial unbalanced translocation t(8;11)(p23.2;p15.5) in two fetuses with Beckwith-Wiedemann features. Prenat Diagn *20*, 511-515.

Fitzpatrick, G.V., Pugacheva, E.M., Shin, J.Y., Abdullaev, Z., Yang, Y., Khatod, K., Lobanenkov, V.V., and Higgins, M.J. (2007). Allele-specific binding of CTCF to the multipartite imprinting control region KvDMR1. Mol Cell Biol *27*, 2636-2647.

Fitzpatrick, G.V., Soloway, P.D., and Higgins, M.J. (2002). Regional loss of imprinting and growth deficiency in mice with a targeted deletion of KvDMR1. Nat Genet.

Franceschini, P., Guala, A., Vardeu, M.P., and Franceschini, D. (1993). Monozygotic twinning and Wiedemann-Beckwith syndrome. Am J Med Genet *46*, 353-354.

Gajecka, M., Pavlicek, A., Glotzbach, C.D., Ballif, B.C., Jarmuz, M., Jurka, J., and Shaffer, L.G. (2006). Identification of sequence motifs at the breakpoint junctions in three t(1;9)(p36.3;q34) and delineation of mechanisms involved in generating balanced translocations. Hum Genet *120*, 519-526.

Gardiner-Garden, M., and Frommer, M. (1987). CpG islands in vertebrate genomes. J Mol Biol *196*, 261-282.

Gaston, V., Le Bouc, Y., Soupre, V., Burglen, L., Donadieu, J., Oro, H., Audry, G., Vazquez, M.P., and Gicquel, C. (2001). Analysis of the methylation status of the KCNQ1OT and H19 genes in leukocyte DNA for the diagnosis and prognosis of Beckwith-Wiedemann syndrome. Eur J Hum Genet *9*, 409-418.

Georgiev, S., Papazova, N., and Gecheff, K. (2001). Transcriptional activity of an inversion split NOR in barley (Hordeum vulgare L.). Chromosome Res *9*, 507-514.

Gimelbrant, A., Hutchinson, J.N., Thompson, B.R., and Chess, A. (2007). Widespread monoallelic expression on human autosomes. Science *318*, 1136-1140.

Gribble, S.M., Prigmore, E., Burford, D.C., Porter, K.M., Ng, B.L., Douglas, E.J., Fiegler, H., Carr, P., Kalaitzopoulos, D., Clegg, S.*, et al.* (2005). The complex nature of constitutional de novo apparently balanced translocations in patients presenting with abnormal phenotypes. J Med Genet *42*, 8-16.

Gribnau, J., Hochedlinger, K., Hata, K., Li, E., and Jaenisch, R. (2003). Asynchronous replication timing of imprinted loci is independent of DNA methylation, but consistent with differential subnuclear localization. Genes Dev *17*, 759-773.

Grundy, R.G., Aledo, R., and Cowell, J.K. (1998). Characterization of the breakpoints in unbalanced t(5;11)(p15;p15) constitutional chromosome translocations in two patients with beckwith-wiedemann syndrome using fluorescence in situ hybridisation. Int J Mol Med *1*, 801-808.

Guo, L., Choufani, S., Ferreira, J., Smith, A., Chitayat, D., Shuman, C., Uxa, R., Keating, S., Kingdom, J., and Weksberg, R. (2008). Altered gene expression and methylation of the human

chromosome 11 imprinted region in small for gestational age (SGA) placentae. Dev Biol *320*, 79-91.

Haig, D. (1993). Genetic conflicts in human pregnancy. Q Rev Biol *68*, 495-532.

Haig, D., and Westoby, M. (1989). Parent-specific gene expression and the triploid endosperm. Am Nat *134*, 147-155.

Hall, J.G., and Lopez-Rangel, E. (1996). Embryologic development and monozygotic twinning. Acta Genet Med Gemellol (Roma) *45*, 53-57.

Han, J.Y., Shin, J.H., Han, M.S., Je, G.H., and Shaffer, L.G. (2006). Microarray detection of a de novo der(X)t(X;11)(q28;p13) in a girl with premature ovarian failure and features of Beckwith-Wiedemann syndrome. J Hum Genet *51*, 641-643.

Hark, A.T., Schoenherr, C.J., Katz, D.J., Ingram, R.S., Levorse, J.M., and Tilghman, S.M. (2000). CTCF mediates methylation-sensitive enhancer-blocking activity at the H19/Igf2 locus. Nature *405*, 486-489.

Hatada, I., Ohashi, H., Fukushima, Y., Kaneko, Y., Inoue, M., Komoto, Y., Okada, A., Ohishi, S., Nabetani, A., Morisaki, H*., et al.* (1996). An imprinted gene p57KIP2 is mutated in Beckwith-Wiedemann syndrome. Nat Genet *14*, 171-173.

Hollander, G.A., Zuklys, S., Morel, C., Mizoguchi, E., Mobisson, K., Simpson, S., Terhorst, C., Wishart, W., Golan, D.E., Bhan, A.K*., et al.* (1998). Monoallelic expression of the interleukin-2 locus. Science *279*, 2118-2121.

Hoovers, J.M., Kalikin, L.M., Johnson, L.A., Alders, M., Redeker, B., Law, D.J., Bliek, J., Steenman, M., Benedict, M., Wiegant, J.*, et al.* (1995). Multiple genetic loci within 11p15 defined by Beckwith-Wiedemann syndrome rearrangement breakpoints and subchromosomal transferable fragments. Proc Natl Acad Sci U S A *92*, 12456-12460.

Horike, S., Mitsuya, K., Meguro, M., Kotobuki, N., Kashiwagi, A., Notsu, T., Schulz, T.C., Shirayoshi, Y., and Oshimura, M. (2000). Targeted disruption of the human LIT1 locus defines a putative imprinting control element playing an essential role in Beckwith-Wiedemann syndrome. Hum Mol Genet *9*, 2075-2083.

Howe, M., Dimitri, P., Berloco, M., and Wakimoto, B.T. (1995). Cis-effects of heterochromatin on heterochromatic and euchromatic gene activity in Drosophila melanogaster. Genetics *140*, 1033-1045.

Howell, C.Y., Bestor, T.H., Ding, F., Latham, K.E., Mertineit, C., Trasler, J.M., and Chaillet, J.R. (2001). Genomic imprinting disrupted by a maternal effect mutation in the Dnmt1 gene. Cell *104*, 829-838.

Jaenisch, R., and Bird, A. (2003). Epigenetic regulation of gene expression: how the genome integrates intrinsic and environmental signals. Nat Genet *33 Suppl*, 245-254.

Jin, R.J., Lho, Y., Wang, Y., Ao, M., Revelo, M.P., Hayward, S.W., Wills, M.L., Logan, S.K., Zhang, P., and Matusik, R.J. (2008a). Down-regulation of p57Kip2 induces prostate cancer in the mouse. Cancer Res *68*, 3601-3608.

Jin, S.G., Guo, C., and Pfeifer, G.P. (2008b). GADD45A does not promote DNA demethylation. PLoS Genet *4*, e1000013.

John, R.M., Ainscough, J.F., Barton, S.C., and Surani, M.A. (2001). Distant cis-elements regulate imprinted expression of the mouse p57(Kip2) (Cdkn1c) gene: implications for the human disorder, Beckwith--Wiedemann syndrome. Hum Mol Genet *10*, 1601-1609.

Jones, B.K., Levorse, J., and Tilghman, S.M. (2001). Deletion of a nuclease-sensitive region between the Igf2 and H19 genes leads to Igf2 misregulation and increased adiposity. Hum Mol Genet *10*, 807-814.

Jones, P.A., and Baylin, S.B. (2002). The fundamental role of epigenetic events in cancer. Nat Rev Genet *3*, 415-428.

Jones, P.A., Rideout, W.M.d., Shen, J.C., Spruck, C.H., and Tsai, Y.C. (1992). Methylation, mutation and cancer. Bioessays *14*, 33-36.

Joyce, J.A., Lam, W.K., Catchpoole, D.J., Jenks, P., Reik, W., Maher, E.R., and Schofield, P.N. (1997). Imprinting of IGF2 and H19: lack of reciprocity in sporadic Beckwith-Wiedemann syndrome. Hum Mol Genet *6*, 1543-1548.

Juan, V., Crain, C., and Wilson, C. (2000). Evidence for evolutionarily conserved secondary structure in the H19 tumor suppressor RNA. Nucleic Acids Res *28*, 1221-1227.

Kanduri, C., Thakur, N., and Pandey, R.R. (2006). The length of the transcript encoded from the Kcnq1ot1 antisense promoter determines the degree of silencing. Embo J *25*, 2096-2106.

Kaneda, M., Sado, T., Hata, K., Okano, M., Tsujimoto, N., Li, E., and Sasaki, H. (2004). Role of de novo DNA methyltransferases in initiation of genomic imprinting and X-chromosome inactivation. Cold Spring Harb Symp Quant Biol *69*, 125-129.

Kangaspeska, S., Stride, B., Metivier, R., Polycarpou-Schwarz, M., Ibberson, D., Carmouche, R.P., Benes, V., Gannon, F., and Reid, G. (2008). Transient cyclical methylation of promoter DNA. Nature *452*, 112-115.

Karnes, P.S., Tran, T.N., Cui, M.Y., Bogenmann, E., Shimada, H., and Ying, K.L. (1991). Establishment of a rhabdoid tumor cell line with a specific chromosomal abnormality, 46,XY,t(11;22)(p15.5;q11.23). Cancer Genet Cytogenet *56*, 31-38.

Kawame, H., Gartler, S.M., and Hansen, R.S. (1995). Allele-specific replication timing in imprinted domains: absence of asynchrony at several loci. Hum Mol Genet *4*, 2287-2293.

Keshet, I., Lieman-Hurwitz, J., and Cedar, H. (1986). DNA methylation affects the formation of active chromatin. Cell *44*, 535-543.

Khan, J., Bittner, M.L., Saal, L.H., Teichmann, U., Azorsa, D.O., Gooden, G.C., Pavan, W.J., Trent, J.M., and Meltzer, P.S. (1999). cDNA microarrays detect activation of a myogenic transcription program by the PAX3-FKHR fusion oncogene. Proc Natl Acad Sci U S A *96*, 13264-13269.

Khulan, B., Thompson, R.F., Ye, K., Fazzari, M.J., Suzuki, M., Stasiek, E., Figueroa, M.E., Glass, J.L., Chen, Q., Montagna, C.*, et al.* (2006). Comparative isoschizomer profiling of cytosine methylation: the HELP assay. Genome Res *16*, 1046-1055.

Killian, J.K., Byrd, J.C., Jirtle, J.V., Munday, B.L., Stoskopf, M.K., MacDonald, R.G., and Jirtle, R.L. (2000). M6P/IGF2R imprinting evolution in mammals. Mol Cell *5*, 707-716.

Killian, J.K., Nolan, C.M., Stewart, N., Munday, B.L., Andersen, N.A., Nicol, S., and Jirtle, R.L. (2001). Monotreme IGF2 expression and ancestral origin of genomic imprinting. J Exp Zool *291*, 205-212.

Kim, P.M., Lam, H.Y., Urban, A.E., Korbel, J.O., Affourtit, J., Grubert, F., Chen, X., Weissman, S., Snyder, M., and Gerstein, M.B. (2008). Analysis of copy number variants and segmental duplications in the human genome: Evidence for a change in the process of formation in recent evolutionary history. Genome Res *18*, 1865-1874.

Kishore, S., and Stamm, S. (2006). The snoRNA HBII-52 regulates alternative splicing of the serotonin receptor 2C. Science *311*, 230-232.

Ko, Y.G., Nishino, K., Hattori, N., Arai, Y., Tanaka, S., and Shiota, K. (2005). Stage-by-stage change in DNA methylation status of Dnmt1 locus during mouse early development. J Biol Chem *280*, 9627-9634.

Kohda, M., Hoshiya, H., Katoh, M., Tanaka, I., Masuda, R., Takemura, T., Fujiwara, M., and Oshimura, M. (2001). Frequent loss of imprinting of IGF2 and MEST in lung adenocarcinoma. Mol Carcinog *31*, 184-191.

Kono, T., Obata, Y., Wu, Q., Niwa, K., Ono, Y., Yamamoto, Y., Park, E.S., Seo, J.S., and Ogawa, H. (2004). Birth of parthenogenetic mice that can develop to adulthood. Nature *428*, 860-864.

Koufos, A., Grundy, P., Morgan, K., Aleck, K.A., Hadro, T., Lampkin, B.C., Kalbakji, A., and Cavenee, W.K. (1989). Familial Wiedemann-Beckwith syndrome and a second Wilms tumor locus both map to 11p15.5. Am J Hum Genet *44*, 711-719.

Koufos, A., Hansen, M.F., Copeland, N.G., Jenkins, N.A., Lampkin, B.C., and Cavenee, W.K. (1985). Loss of heterozygosity in three embryonal tumours suggests a common pathogenetic mechanism. Nature *316*, 330-334.

Krajewska-Walasek, M., Gutkowska, A., Mospinek-Krasnopolska, M., and Chrzanowska, K. (1996). A new case of Beckwith-Wiedemann syndrome with an 11p15 duplication of paternal origin [46,XY,-21,+der(21), t(11;21)(p15.2;q22.3)pat]. Acta Genet Med Gemellol (Roma) *45*, 245-250.

Lam, W.W., Hatada, I., Ohishi, S., Mukai, T., Joyce, J.A., Cole, T.R., Donnai, D., Reik, W., Schofield, P.N., and Maher, E.R. (1999). Analysis of germline CDKN1C (p57KIP2) mutations in familial and sporadic Beckwith-Wiedemann syndrome (BWS) provides a novel genotype-phenotype correlation. J Med Genet *36*, 518-523.

Larson, P.S., Schlechter, B.L., King, C.L., Yang, Q., Glass, C.N., Mack, C., Pistey, R., de Las Morenas, A., and Rosenberg, C.L. (2008). CDKN1C/p57kip2 is a candidate tumor suppressor gene in human breast cancer. BMC Cancer *8*, 68.

Lawton, B.R., Sevigny, L., Obergfell, C., Reznick, D., O'Neill R, J., and O'Neill M, J. (2005). Allelic expression of IGF2 in live-bearing, matrotrophic fishes. Dev Genes Evol *215*, 207-212.

Lee, M.P., DeBaun, M.R., Mitsuya, K., Galonek, H.L., Brandenburg, S., Oshimura, M., and Feinberg, A.P. (1999). Loss of imprinting of a paternally expressed transcript, with antisense orientation to KVLQT1, occurs frequently in Beckwith-Wiedemann syndrome and is independent of insulin-like growth factor II imprinting. Proc Natl Acad Sci U S A *96*, 5203-5208.

Lee, M.P., Hu, R.J., Johnson, L.A., and Feinberg, A.P. (1997). Human KVLQT1 gene shows tissue-specific imprinting and encompasses Beckwith-Wiedemann syndrome chromosomal rearrangements. Nat Genet *15*, 181-185.

Leonard, N.J., Bernier, F.P., Rudd, N., Machin, G.A., Bamforth, F., Bamforth, S., Grundy, P., and Johnson, C. (1996). Two pairs of male monozygotic twins discordant for Wiedemann-Beckwith syndrome. Am J Med Genet *61*, 253-257.

Lewis, A., Mitsuya, K., Umlauf, D., Smith, P., Dean, W., Walter, J., Higgins, M., Feil, R., and Reik, W. (2004). Imprinting on distal chromosome 7 in the placenta involves repressive histone methylation independent of DNA methylation. Nat Genet *36*, 1291-1295.

Li, M., Squire, J., Shuman, C., Fei, Y.L., Atkin, J., Pauli, R., Smith, A., Nishikawa, J., Chitayat, D., and Weksberg, R. (2001). Imprinting status of 11p15 genes in Beckwith-Wiedemann syndrome patients with CDKN1C mutations. Genomics *74*, 370-376.

Li, M., Squire, J.A., and Weksberg, R. (1997). Molecular genetics of Beckwith-Wiedemann syndrome. Curr Opin Pediatr *9*, 623-629.

Litz, C.E., Taylor, K.A., Qiu, J.S., Pescovitz, O.H., and de Martinville, B. (1988). Absence of detectable chromosomal and molecular abnormalities in monozygotic twins discordant for the Wiedemann-Beckwith syndrome. Am J Med Genet *30*, 821-833.

Lubinsky, M.S., and Hall, J.G. (1991). Genomic imprinting, monozygous twinning, and X inactivation. Lancet *337*, 1288.

Machin, G.A. (1996). Some causes of genotypic and phenotypic discordance in monozygotic twin pairs. Am J Med Genet *61*, 216-228.

Mager, J., Montgomery, N.D., de Villena, F.P., and Magnuson, T. (2003). Genome imprinting regulated by the mouse Polycomb group protein Eed. Nat Genet *33*, 502-507.

Maher, E.R., and Reik, W. (2000). Beckwith-Wiedemann syndrome: imprinting in clusters revisited. J Clin Invest *105*, 247-252.

Mancini-Dinardo, D., Steele, S.J., Levorse, J.M., Ingram, R.S., and Tilghman, S.M. (2006). Elongation of the Kcnq1ot1 transcript is required for genomic imprinting of neighboring genes. Genes Dev *20*, 1268-1282.

Mannens, M., Hoovers, J.M., Redeker, E., Verjaal, M., Feinberg, A.P., Little, P., Boavida, M., Coad, N., Steenman, M., Bliek, J.*, et al.* (1994). Parental imprinting of human chromosome region 11p15.3-pter involved in the Beckwith-Wiedemann syndrome and various human neoplasia. Eur J Hum Genet *2*, 3-23.

Marcus-Soekarman, D., Hamers, G., Velzeboer, S., Nijhuis, J., Loneus, W.H., Herbergs, J., de Die-Smulders, C., Schrander-Stumpel, C., and Engelen, J. (2004). Mosaic trisomy 11p in monozygotic twins with discordant clinical phenotypes. Am J Med Genet A *124A*, 288-291.

Masui, O., and Heard, E. (2006). RNA and protein actors in X-chromosome inactivation. Cold Spring Harb Symp Quant Biol *71*, 419-428.

Matsumoto, T., Kinoshita, E., Maeda, H., Niikawa, N., Kurosaki, N., Harada, N., Yun, K., Sawai, T., Aoki, S., Kondoh, T.*, et al.* (1994). Molecular analysis of a patient with Beckwith-

Wiedemann syndrome, rhabdomyosarcoma and renal cell carcinoma. Jpn J Hum Genet *39*, 225-234.

Matsuoka, S., Edwards, M.C., Bai, C., Parker, S., Zhang, P., Baldini, A., Harper, J.W., and Elledge, S.J. (1995). p57kip2, a structurally distinct member of the p21cip1 Cdk inhibitor family, is a candidate tumor suppressor gene. Genes & Development *9*, 650-662.

Maurer, H., Ruyamann, F., and Pochedly, C. (1991). Rhabdomyosarcoma and Related Tumors in Children and Adolescents. (Boca Raton, FL., CRC Press).

McGrath, J., and Solter, D. (1984). Completion of mouse embryogenesis requires both the maternal and paternal genomes. Cell *37*, 179-183.

Metivier, R., Gallais, R., Tiffoche, C., Le Peron, C., Jurkowska, R.Z., Carmouche, R.P., Ibberson, D., Barath, P., Demay, F., Reid, G.*, et al.* (2008). Cyclical DNA methylation of a transcriptionally active promoter. Nature *452*, 45-50.

Mikhail, F.M., Sathienkijkanchai, A., Robin, N.H., Prucka, S., Biggerstaff, J.S., Komorowski, J., Andersson, R., Bruder, C.E., Piotrowski, A., de Stahl, T.D.*, et al.* (2007). Overlapping phenotype of Wolf-Hirschhorn and Beckwith-Wiedemann syndromes in a girl with der(4)t(4;11)(pter;pter). Am J Med Genet A *143*, 1760-1766.

Milani, L., Lundmark, A., Nordlund, J., Kiialainen, A., Flaegstad, T., Jonmundsson, G., Kanerva, J., Schmiegelow, K., Gunderson, K.L., Lonnerholm, G.*, et al.* (2008). Allele-specific gene expression patterns in primary leukemic cells reveal regulation of gene expression by CpG site methylation. Genome Res.

Mitsuya, K., Meguro, M., Lee, M.P., Katoh, M., Schulz, T.C., Kugoh, H., Yoshida, M.A., Niikawa, N., Feinberg, A.P., and Oshimura, M. (1999). LIT1, an imprinted antisense RNA in the human KvLQT1 locus identified by screening for differentially expressed transcripts using monochromosomal hybrids. Hum Mol Genet *8*, 1209-1217.

Morison, I.M., Ramsay, J.P., and Spencer, H.G. (2005). A census of mammalian imprinting. Trends Genet *21*, 457-465.

Moulton, T., Chung, W.Y., Yuan, L., Hensle, T., Waber, P., Nisen, P., and Tycko, B. (1996). Genomic imprinting and Wilms' tumor. Med Pediatr Oncol *27*, 476-483.

Muller, S., van den Boom, D., Zirkel, D., Koster, H., Berthold, F., Schwab, M., Westphal, M., and Zumkeller, W. (2000). Retention of imprinting of the human apoptosis-related gene TSSC3 in human brain tumors. Hum Mol Genet *9*, 757-763.

Murakami, K., Oshimura, M., and Kugoh, H. (2007). Suggestive evidence for chromosomal localization of non-coding RNA from imprinted LIT1. J Hum Genet *52*, 926-933.

Murrell, A., Ito, Y., Verde, G., Huddleston, J., Woodfine, K., Silengo, M.C., Spreafico, F., Perotti, D., De Crescenzo, A., Sparago, A.*, et al.* (2008). Distinct methylation changes at the IGF2-H19 locus in congenital growth disorders and cancer. PLoS ONE *3*, e1849.

Nakabayashi, K., Bentley, L., Hitchins, M.P., Mitsuya, K., Meguro, M., Minagawa, S., Bamforth, J.S., Stanier, P., Preece, M., Weksberg, R.*, et al.* (2002). Identification and characterization of an imprinted antisense RNA (MESTIT1) in the human MEST locus on chromosome 7q32. Hum Mol Genet *11*, 1743-1756.

Nakano, S., Murakami, K., Meguro, M., Soejima, H., Higashimoto, K., Urano, T., Kugoh, H., Mukai, T., Ikeguchi, M., and Oshimura, M. (2006). Expression profile of LIT1/KCNQ1OT1 and epigenetic status at the KvDMR1 in colorectal cancers. Cancer Sci *97*, 1147-1154.

Newsham, I., Kindler-Rohrborn, A., Daub, D., and Cavenee, W. (1995). A constitutional BWS-related t(11;16) chromosome translocation occurring in the same region of chromosome 16 implicated in Wilms' tumors. Genes Chromosomes Cancer *12*, 1-7.

Newton, W.A., Jr., Gehan, E.A., Webber, B.L., Marsden, H.B., van Unnik, A.J., Hamoudi, A.B., Tsokos, M.G., Shimada, H., Harms, D., Schmidt, D.*, et al.* (1995). Classification of rhabdomyosarcomas and related sarcomas. Pathologic aspects and proposal for a new classification--an Intergroup Rhabdomyosarcoma Study. Cancer *76*, 1073-1085.

Neyroud, N., Tesson, F., Denjoy, I., Leibovici, M., Donger, C., Barhanin, J., Faure, S., Gary, F., Coumel, P., Petit, C.*, et al.* (1997). A novel mutation in the potassium channel gene KVLQT1 causes the Jervell and Lange-Nielsen cardioauditory syndrome. Nat Genet *15*, 186-189.

Nicholls, R.D. (2000). The impact of genomic imprinting for neurobehavioral and developmental disorders. J Clin Invest *105*, 413-418.

Nicholls, R.D., Saitoh, S., and Horsthemke, B. (1998). Imprinting in Prader-Willi and Angelman syndromes. Trends in Genetics *14*, 194-200.

Niemitz, E.L., DeBaun, M.R., Fallon, J., Murakami, K., Kugoh, H., Oshimura, M., and Feinberg, A.P. (2004). Microdeletion of LIT1 in familial Beckwith-Wiedemann syndrome. Am J Hum Genet *75*, 844-849.

Nolan, C.M., Killian, J.K., Petitte, J.N., and Jirtle, R.L. (2001). Imprint status of M6P/IGF2R and IGF2 in chickens. Dev Genes Evol *211*, 179-183.

Norman, A.M., Read, A.P., Clayton-Smith, J., Andrews, T., and Donnai, D. (1992). Recurrent Wiedemann-Beckwith syndrome with inversion of chromosome (11)(p11.2p15.5). Am J Med Genet *42*, 638-641.

Nuwaysir, E.F., Huang, W., Albert, T.J., Singh, J., Nuwaysir, K., Pitas, A., Richmond, T., Gorski, T., Berg, J.P., Ballin, J.*, et al.* (2002). Gene expression analysis using oligonucleotide arrays produced by maskless photolithography. Genome Res *12*, 1749-1755.

Ogur, G., Hayez, F., Herinckx, A., Van Regemorter, N., and Vamos, E. (1988). Familial trisomy 11p resulting from a balanced paternal translocation: 3 new cases including first trimester diagnosis. J Genet Hum *36*, 323-329.

Ohlsson, R., Tycko, B., and Sapienza, C. (1998). Monoallelic expression: 'there can only be one'. Trends Genet *14*, 435-438.

Pandey, R.R., Mondal, T., Mohammad, F., Enroth, S., Redrup, L., Komorowski, J., Nagano, T., Mancini-Dinardo, D., and Kanduri, C. (2008). Kcnq1ot1 antisense noncoding RNA mediates lineage-specific transcriptional silencing through chromatin-level regulation. Mol Cell *32*, 232-246.

Pandita, A., Zielenska, M., Thorner, P., Bayani, J., Godbout, R., Greenberg, M., and Squire, J.A. (1999). Application of comparative genomic hybridization, spectral karyotyping, and microarray analysis in the identification of subtype-specific patterns of genomic changes in rhabdomyosarcoma. Neoplasia *1*, 262-275.

Pant, P.V., Tao, H., Beilharz, E.J., Ballinger, D.G., Cox, D.R., and Frazer, K.A. (2006). Analysis of allelic differential expression in human white blood cells. Genome Res *16*, 331-339.

Pedone, P.V., Tirabosco, R., Cavazzana, A.O., Ungaro, P., Basso, G., Luksch, R., Carli, M., Bruni, C.B., Frunzio, R., and Riccio, A. (1994). Mono- and bi-allelic expression of insulin-like growth factor II gene in human muscle tumors. Hum Mol Genet *3*, 1117-1121.

Pettenati, M.J., Haines, J.L., Higgins, R.R., Wappner, R.S., Palmer, C.G., and Weaver, D.D. (1986). Wiedemann-Beckwith syndrome: presentation of clinical and cytogenetic data on 22 new cases and review of the literature. Hum Genet *74*, 143-154.

Ping, A.J., Reeve, A.E., Law, D.J., Young, M.R., Boehnke, M., and Feinberg, A.P. (1989). Genetic linkage of Beckwith-Wiedemann syndrome to 11p15. Am J Hum Genet *44*, 720-723.

Povirk, L.F. (2006). Biochemical mechanisms of chromosomal translocations resulting from DNA double-strand breaks. DNA Repair (Amst) *5*, 1199-1212.

Pradhan, S., Bacolla, A., Wells, R.D., and Roberts, R.J. (1999). Recombinant human DNA (cytosine-5) methyltransferase. I. Expression, purification, and comparison of de novo and maintenance methylation. J Biol Chem *274*, 33002-33010.

Pradhan, S., Talbot, D., Sha, M., Benner, J., Hornstra, L., Li, E., Jaenisch, R., and Roberts, R.J. (1997). Baculovirus-mediated expression and characterization of the full-length murine DNA methyltransferase. Nucleic Acids Research *25*, 4666-4673.

Qualman, S.J., Coffin, C.M., Newton, W.A., Hojo, H., Triche, T.J., Parham, D.M., and Crist, W.M. (1998). Intergroup Rhabdomyosarcoma Study: update for pathologists. Pediatr Dev Pathol *1*, 550-561.

Rainier, S., Dobry, C.J., and Feinberg, A.P. (1995). Loss of imprinting in hepatoblastoma. Cancer Res *55*, 1836-1838.

Reeve, A.E. (1996). Role of genomic imprinting in Wilms' tumour and overgrowth disorders. Med Pediatr Oncol *27*, 470-475.

Reik, W., Dean, W., and Walter, J. (2001). Epigenetic reprogramming in mammalian development. Science *293*, 1089-1093.

Robertson, K.D. (2005). DNA methylation and human disease. Nat Rev Genet *6*, 597-610.

Robinson, L. (1997). General Principles of the Epidemiology of Childhood Cancer. In Principles and practice of pediatric oncology, P.A. Pizzo, and D.G. Poplack, eds. (Philadelphia, Lippincott-Raven), p. 1522

Rougier, N., Bourc'his, D., Gomes, D.M., Niveleau, A., Plachot, M., Paldi, A., and Viegas-Pequignot, E. (1998). Chromosome methylation patterns during mammalian preimplantation development. Genes Dev *12*, 2108-2113.

Rouhi, A., Mager, D.L., Humphries, R.K., and Kuchenbauer, F. (2008). MiRNAs, epigenetics, and cancer. Mamm Genome *19*, 517-525.

Royo, H., and Cavaille, J. (2008). Non-coding RNAs in imprinted gene clusters. Biol Cell *100*, 149-166.

Royo, J.L., Hidalgo, M., and Ruiz, A. (2007). Pyrosequencing protocol using a universal biotinylated primer for mutation detection and SNP genotyping. Nat Protoc *2*, 1734-1739.

Royo, J.L., Pascual, M.H., Salinas, A., Tello, F.J., Rivero Mdel, C., Herrero, E.F., Real, L.M., and Ruiz, A. (2006). Pyrosequencing protocol requiring a unique biotinylated primer. Clin Chem Lab Med *44*, 435-441.

Ruffini Castiglione, M., Venora, G., Ravalli, C., Stoilov, L., Gecheff, K., and Cremonini, R. (2008). DNA methylation and chromosomal rearrangements in reconstructed karyotypes of Hordeum vulgare L. Protoplasma *232*:215-222.

Rump, P., Zeegers, M.P., and van Essen, A.J. (2005). Tumor risk in Beckwith-Wiedemann syndrome: A review and meta-analysis. Am J Med Genet A *136*, 95-104.

Russo, S., Finelli, P., Recalcati, M.P., Ferraiuolo, S., Cogliati, F., Dalla Bernardina, B., Tibiletti, M.G., Agosti, M., Sala, M., Bonati, M.T.*, et al.* (2006). Molecular and genomic characterisation of cryptic chromosomal alterations leading to paternal duplication of the 11p15.5 Beckwith-Wiedemann region. J Med Genet *43*, e39.

Rutledge, R.G., and Cote, C. (2003). Mathematics of quantitative kinetic PCR and the application of standard curves. Nucleic Acids Res *31*, e93.

Sait, S.N., Nowak, N.J., Singh-Kahlon, P., Weksberg, R., Squire, J., Shows, T.B., and Higgins, M.J. (1994). Localization of Beckwith-Wiedemann and rhabdoid tumor chromosome rearrangements to a defined interval in chromosome band 11p15.5. Genes Chromosomes Cancer *11*, 97-105.

Sakatani, T., Wei, M., Katoh, M., Okita, C., Wada, D., Mitsuya, K., Meguro, M., Ikeguchi, M., Ito, H., Tycko, B.*, et al.* (2001). Epigenetic heterogeneity at imprinted loci in normal populations. Biochem Biophys Res Commun *283*, 1124-1130.

Salas, M., John, R.M., Saxena, A., Barton, S., Frank, D., Fitzpatrick, G.V., Higgins, M.J., and Tycko, B. (2004). Placental growth retardation due to loss of imprinting of Phlda2. Mechanisms of Development *121*, 1199-1210.

Sanders, V.M. (2006). Epigenetic regulation of Th1 and Th2 cell development. Brain Behav Immun *20*, 317-324.

Santos, F., Hendrich, B., Reik, W., and Dean, W. (2002). Dynamic reprogramming of DNA methylation in the early mouse embryo. Dev Biol *241*, 172-182.

Sasaki, K., Soejima, H., Higashimoto, K., Yatsuki, H., Ohashi, H., Yakabe, S., Joh, K., Niikawa, N., and Mukai, T. (2007). Japanese and North American/European patients with Beckwith-Wiedemann syndrome have different frequencies of some epigenetic and genetic alterations. Eur J Hum Genet *15*, 1205-1210.

Schier, F., Sauerbrey, A., and Kosmehl, H. (2000). A Meckel's diverticulum containing pancreatic tissue and nesidioblastosis in a patient with Beckwith-Wiedemann syndrome. Pediatr Surg Int *16*, 124-127.

Schofield, P.N., Joyce, J.A., Lam, W.K., Grandjean, V., Ferguson-Smith, A., Reik, W., and Maher, E.R. (2001). Genomic imprinting and cancer; new paradigms in the genetics of neoplasia. Toxicol Lett *120*, 151-160.

Schwienbacher, C., Sabbioni, S., Campi, M., Veronese, A., Bernardi, G., Menegatti, A., Hatada, I., Mukai, T., Ohashi, H., Barbanti-Brodano, G.*, et al.* (1998). Transcriptional map of 170-kb region at chromosome 11p15.5: identification and mutational analysis of the BWR1A gene reveals the presence of mutations in tumor samples. Proc Natl Acad Sci U S A *95*, 3873-3878.

Scrable, H., Cavenee, W., Ghavimi, F., Lovell, M., Morgan, K., and Sapienza, C. (1989a). A model for embryonal rhabdomyosarcoma tumorigenesis that involves genome imprinting. Proc Natl Acad Sci U S A *86*, 7480-7484.

Scrable, H., Witte, D., Shimada, H., Seemayer, T., Sheng, W.W., Soukup, S., Koufos, A., Houghton, P., Lampkin, B., and Cavenee, W. (1989b). Molecular differential pathology of rhabdomyosarcoma. Genes Chromosomes Cancer *1*, 23-35.

Scrable, H.J., Witte, D.P., Lampkin, B.C., and Cavenee, W.K. (1987). Chromosomal localization of the human rhabdomyosarcoma locus by mitotic recombination mapping. Nature *329*, 645-647.

Serre, D., Gurd, S., Ge, B., Sladek, R., Sinnett, D., Harmsen, E., Bibikova, M., Chudin, E., Barker, D.L., Dickinson, T.*, et al.* (2008). Differential allelic expression in the human genome: a robust approach to identify genetic and epigenetic cis-acting mechanisms regulating gene expression. PLoS Genet *4*, e1000006.

Simonis, M., Klous, P., Splinter, E., Moshkin, Y., Willemsen, R., de Wit, E., van Steensel, B., and de Laat, W. (2006). Nuclear organization of active and inactive chromatin domains uncovered by chromosome conformation capture-on-chip (4C). Nat Genet *38*, 1348-1354.

Sismani, C., Kitsiou-Tzeli, S., Ioannides, M., Christodoulou, C., Anastasiadou, V., Stylianidou, G., Papadopoulou, E., Kanavakis, E., Kosmaidou-Aravidou, Z., and Patsalis, P.C. (2008).

Cryptic genomic imbalances in patients with de novo or familial apparently balanced translocations and abnormal phenotype. Mol Cytogenet *1*, 15.

Slavotinek, A., Gaunt, L., and Donnai, D. (1997). Paternally inherited duplications of 11p15.5 and Beckwith-Wiedemann syndrome. J Med Genet *34*, 819-826.

Smilinich, N.J., Day, C.D., Fitzpatrick, G.V., Caldwell, G.M., Lossie, A.C., Cooper, P.R., Smallwood, A.C., Joyce, J.A., Schofield, P.N., Reik, W.*, et al.* (1999). A maternally methylated CpG island in KvLQT1 is associated with an antisense paternal transcript and loss of imprinting in Beckwith-Wiedemann syndrome. Proc Natl Acad Sci U S A *96*, 8064-8069.

Smith, A.C., Choufani, S., Ferreira, J.C., and Weksberg, R. (2007). Growth regulation, imprinted genes, and chromosome 11p15.5. Pediatr Res *61*, 43R-47R.

Sotelo-Avila, C., and Gooch, W.M., 3rd (1976). Neoplasms associated with the Beckwith-Wiedemann syndrome. Perspect Pediatr Pathol *3*, 255-272.

Sparago, A., Cerrato, F., Vernucci, M., Ferrero, G.B., Silengo, M.C., and Riccio, A. (2004). Microdeletions in the human H19 DMR result in loss of IGF2 imprinting and Beckwith-Wiedemann syndrome. Nat Genet *36*, 958-960.

Sparago, A., Russo, S., Cerrato, F., Ferraiuolo, S., Castorina, P., Selicorni, A., Schwienbacher, C., Negrini, M., Battista Ferrero, G., Cirillo Silengo, M.*, et al.* (2006). Mechanisms causing Imprinting Defects in Familial Beckwith-Wiedemann Syndrome with Wilms' Tumour. Hum Mol Genet. 16:254-264

Squire, J.A., Li, M., Perlikowski, S., Fei, Y.L., Bayani, J., Zhang, Z.M., and Weksberg, R. (2000). Alterations of H19 imprinting and IGF2 replication timing are infrequent in Beckwith-Wiedemann syndrome. Genomics *65*, 234-242.

Steenman, M.J., Rainier, S., Dobry, C.J., Grundy, P., Horon, I.L., and Feinberg, A.P. (1994). Loss of imprinting of IGF2 is linked to reduced expression and abnormal methylation of H19 in Wilms' tumour. Nat Genet *7*, 433-439.

Sun, F.L., Dean, W.L., Kelsey, G., Allen, N.D., and Reik, W. (1997). Transactivation of Igf2 in a mouse model of Beckwith-Wiedemann syndrome [see comments]. Nature *389*, 809-815.

Surani, M.A., Barton, S.C., and Norris, M.L. (1984). Development of reconstituted mouse eggs suggests imprinting of the genome during gametogenesis. Nature *308*, 548-550.

Takai, D., and Jones, P.A. (2002). Comprehensive analysis of CpG islands in human chromosomes 21 and 22. Proc Natl Acad Sci U S A *99*, 3740-3745.

Tanaka, K., Shiota, G., Meguro, M., Mitsuya, K., Oshimura, M., and Kawasaki, H. (2001). Loss of imprinting of long QT intronic transcript 1 in colorectal cancer. Oncology *60*, 268-273.

Thorburn, M.J., Wright, E.S., Miller, C.G., and Smith-Read, E.H. (1970). Exomphalos-macroglossia-gigantism syndrome in Jamaican infants. Am J Dis Child *119*, 316-321.

Tsugu, A., Sakai, K., Dirks, P.B., Jung, S., Weksberg, R., Fei, Y.L., Mondal, S., Ivanchuk, S., Ackerley, C., Hamel, P.A.*, et al.* (2000). Expression of p57(KIP2) potently blocks the growth of human astrocytomas and induces cell senescence. Am J Pathol *157*, 919-932.

Turleau, C., de Grouchy, J., Chavin-Colin, F., Martelli, H., Voyer, M., and Charlas, R. (1984). Trisomy 11p15 and Beckwith-Wiedemann syndrome. A report of two cases. Hum Genet *67*, 219-221.

Tycko, B. (2000). Epigenetic gene silencing in cancer. J Clin Invest *105*, 401-407.

Tycko, B. (2006). Imprinted genes in placental growth and obstetric disorders. Cytogenet Genome Res 113:271-8.

Umlauf, D., Goto, Y., Cao, R., Cerqueira, F., Wagschal, A., Zhang, Y., and Feil, R. (2004). Imprinting along the Kcnq1 domain on mouse chromosome 7 involves repressive histone methylation and recruitment of Polycomb group complexes. Nat Genet *36*, 1296-1300.

Vandesompele, J., De Preter, K., Pattyn, F., Poppe, B., Van Roy, N., De Paepe, A., and Speleman, F. (2002). Accurate normalization of real-time quantitative RT-PCR data by geometric averaging of multiple internal control genes. Genome Biol *3*, RESEARCH0034.

Varmuza, S., and Mann, M. (1994). Genomic imprinting--defusing the ovarian time bomb. Trends Genet *10*, 118-123.

Varrault, A., Gueydan, C., Delalbre, A., Bellmann, A., Houssami, S., Aknin, C., Severac, D., Chotard, L., Kahli, M., Le Digarcher, A.*, et al.* (2006). Zac1 regulates an imprinted gene network critically involved in the control of embryonic growth. Dev Cell *11*, 711-722.

Vaughan, W.G., Sanders, D.W., Grosfeld, J.L., Plumley, D.A., Rescorla, F.J., Scherer, L.R., 3rd, West, K.W., and Breitfeld, P.P. (1995). Favorable outcome in children with Beckwith-

Wiedemann syndrome and intraabdominal malignant tumors. J Pediatr Surg *30*, 1042-1044; discussion 1044-1045.

Verona, R.I., Mann, M.R., and Bartolomei, M.S. (2003). Genomic imprinting: intricacies of epigenetic regulation in clusters. Annu Rev Cell Dev Biol *19*, 237-259.

Vu, T.H., and Hoffman, A.R. (1994). Promoter-specific imprinting of the human insulin-like growth factor-II gene. Nature *371*, 714-717.

Wallrath, L.L., and Elgin, S.C. (1995). Position effect variegation in Drosophila is associated with an altered chromatin structure. Genes Dev *9*, 1263-1277.

Wang, Q., Curran, M.E., Splawski, I., Burn, T.C., Millholland, J.M., VanRaay, T.J., Shen, J., Timothy, K.W., Vincent, G.M., de Jager, T.*, et al.* (1996). Positional cloning of a novel potassium channel gene: KVLQT1 mutations cause cardiac arrhythmias. Nat Genet *12*, 17-23.

Weber, M., Davies, J.J., Wittig, D., Oakeley, E.J., Haase, M., Lam, W.L., and Schubeler, D. (2005). Chromosome-wide and promoter-specific analyses identify sites of differential DNA methylation in normal and transformed human cells. Nat Genet *37*, 853-862.

Weber, M., Hellmann, I., Stadler, M.B., Ramos, L., Paabo, S., Rebhan, M., and Schubeler, D. (2007). Distribution, silencing potential and evolutionary impact of promoter DNA methylation in the human genome. Nat Genet *39*, 457-466.

Weisenberger, D.J., Campan, M., Long, T.I., Kim, M., Woods, C., Fiala, E., Ehrlich, M., and Laird, P.W. (2005). Analysis of repetitive element DNA methylation by MethyLight. Nucleic Acids Res *33*, 6823-6836.

Weksberg, R., Glaves, M., Teshima, I., Waziri, M., Patil, S., and Williams, B.R. (1990). Molecular characterization of Beckwith-Wiedemann syndrome (BWS) patients with partial duplication of chromosome 11p excludes the gene MYOD1 from the BWS region. Genomics *8*, 693-698.

Weksberg, R., Nishikawa, J., Caluseriu, O., Fei, Y.L., Shuman, C., Wei, C., Steele, L., Cameron, J., Smith, A., Ambus, I.*, et al.* (2001). Tumor development in the Beckwith-Wiedemann syndrome is associated with a variety of constitutional molecular 11p15 alterations including imprinting defects of KCNQ1OT1. Hum Mol Genet *10*, 2989-3000.

Weksberg, R., Sadowski, P., Smith, A.C., and Tycko, B. (2007). Epigenetics. In Emery and Rimoin's principles and practice of medical genetics (Philadelphia, Churchill Livingstone), p. 81-100.

Weksberg, R., Shen, D.R., Fei, Y.L., Song, Q.L., and Squire, J. (1993a). Disruption of insulin-like growth factor 2 imprinting in Beckwith-Wiedemann syndrome. Nat Genet *5*, 143-150.

Weksberg, R., Shuman, C., Caluseriu, O., Smith, A.C., Fei, Y.L., Nishikawa, J., Stockley, T.L., Best, L., Chitayat, D., Olney, A.*, et al.* (2002). Discordant KCNQ1OT1 imprinting in sets of monozygotic twins discordant for Beckwith-Wiedemann syndrome. Hum Mol Genet *11*, 1317-1325.

Weksberg, R., Shuman, C., and Smith, A.C. (2005). Beckwith-Wiedemann syndrome. Am J Med Genet C Semin Med Genet *137*, 12-23.

Weksberg, R., Smith, A.C., Squire, J., and Sadowski, P. (2003). Beckwith-Wiedemann syndrome demonstrates a role for epigenetic control of normal development. Hum Mol Genet *12 Spec No 1*, R61-68.

Weksberg, R., Teshima, I., Williams, B.R., Greenberg, C.R., Pueschel, S.M., Chernos, J.E., Fowlow, S.B., Hoyme, E., Anderson, I.J., Whiteman, D.A.*, et al.* (1993b). Molecular characterization of cytogenetic alterations associated with the Beckwith-Wiedemann syndrome (BWS) phenotype refines the localization and suggests the gene for BWS is imprinted. Hum Mol Genet *2*, 549-556.

Weng, E.Y., Moeschler, J.B., and Graham, J.M., Jr. (1995a). Longitudinal observations on 15 children with Wiedemann-Beckwith syndrome. Am J Med Genet *56*, 366-373.

Weng, E.Y., Mortier, G.R., and Graham, J.M., Jr. (1995b). Beckwith-Wiedemann syndrome. An update and review for the primary pediatrician. Clin Pediatr (Phila) *34*, 317-326.

Wiedemann, H.R. (1964). [Familial Malformation Complex with Umbilical Hernia and Macroglossia--a "New Syndrome"?]. J Genet Hum *13*, 223-232.

Wiedemann, H.R. (1983). Tumours and hemihypertrophy associated with Wiedemann-Beckwith syndrome. Eur J Paediatr *141*, 129.

Wilkins, J.F., and Haig, D. (2003). What good is genomic imprinting: the function of parent-specific gene expression. Nat Rev Genet *4*, 359-368.

Wolffe, A.P., and Matzke, M.A. (1999). Epigenetics: regulation through repression. Science *286*, 481-486.

Workman, C., Jensen, L.J., Jarmer, H., Berka, R., Gautier, L., Nielser, H.B., Saxild, H.H., Nielsen, C., Brunak, S., and Knudsen, S. (2002). A new non-linear normalization method for reducing variability in DNA microarray experiments. Genome Biol *3*, research0048.

Yamazawa, K., Kagami, M., Fukami, M., Matsubara, K., and Ogata, T. (2008). Monozygotic female twins discordant for Silver-Russell syndrome and hypomethylation of the H19-DMR. J Hum Genet *53*, 950-955.

Yan, H., Yuan, W., Velculescu, V.E., Vogelstein, B., and Kinzler, K.W. (2002). Allelic variation in human gene expression. Science *297*, 1143.

Yoder, J.A., Walsh, C.P., and Bestor, T.H. (1997). Cytosine methylation and the ecology of intragenomic parasites. Trends Genet *13*, 335-340.

Zeschnigk, M., Albrecht, B., Buiting, K., Kanber, D., Eggermann, T., Binder, G., Gromoll, J., Prott, E.C., Seland, S., and Horsthemke, B. (2008). IGF2/H19 hypomethylation in Silver-Russell syndrome and isolated hemihypoplasia. Eur J Hum Genet *16*, 328-334.

Zhan, S., Shapiro, D.N., and Helman, L.J. (1994). Activation of an imprinted allele of the insulin-like growth factor II gene implicated in rhabdomyosarcoma. J Clin Invest *94*, 445-448.

Zhang, P., Liegeois, N.J., Wong, C., Finegold, M., Hou, H., Thompson, J.C., Silverman, A., Harper, J.W., DePinho, R.A., and Elledge, S.J. (1997). Altered cell differentiation and proliferation in mice lacking p57KIP2 indicates a role in Beckwith-Wiedemann syndrome. Nature *387*, 151-158.

Zhao, Z., Tavoosidana, G., Sjolinder, M., Gondor, A., Mariano, P., Wang, S., Kanduri, C., Lezcano, M., Sandhu, K.S., Singh, U.*, et al.* (2006). Circular chromosome conformation capture (4C) uncovers extensive networks of epigenetically regulated intra- and interchromosomal interactions. Nat Genet *38*, 1341-1347.